CHARACTERIZATION OF CD62L AS A MARKER OF HEMATOPOIETIC DIFFERENTIATION IN ADULT MICE

by

Hyung Jin (Scott) Cho

A dissertation submitted to the faculty of
The University of Utah
in partial fulfillment of the requirements for the degree of

Doctor of Philosophy

in

Experimental Pathology

Department of Pathology

The University of Utah

December 2010

The University of Utah Graduate School

STATEMENT OF DISSERTATION APPROVAL

The dissertation of **Hyung Jin (Scott) Cho**

has been approved by the following supervisory committee members:

Gerald Spangrude	, Chair	**10/26/2010** Date Approved
Lorise Gahring	, Member	**10/26/2010** Date Approved
John Phillips	, Member	**10/26/2010** Date Approved
Janis Weis	, Member	**10/26/2010** Date Approved
John Weis	, Member	**10/26/2010** Date Approved

and by **Peter Jensen** , Chair of the Department of **Pathology**

and by Charles A. Wight, Dean of The Graduate School.

ABSTRACT

The progression of early hematopoietic differentiation remains a topic of controversy. Topics of ongoing debate include the identification of a pure hematopoietic stem cell population and bifurcation of the lymphoid and myeloid lineages following commitment by multipotent progenitors. This dissertation contributes to the current knowledge of early hematopoietic differentiation and enhances the understanding of hematopoietic stem cell and progenitor biology by characterizing CD62L as a novel marker of early hematopoietic differentiation. Transplant studies revealed in vivo evidence for the existence of stem cell-containing CD62L– fraction and multipotent progenitor-containing CD62L+ fraction within the traditionally defined hematopoietic stem cell population. Sca-1 fractionation of the hematopoietic stem cell compartment demonstrated that cells of the Sca-1^{HIGH} subset were almost homogeneous in their lack of CD62L expression. In contrast, the Sca-1^{LOW} subset contained a heterogeneous mixture of CD62L+ and CD62L– cells. Engraftment analysis of the Sca-1^{LOW} and Sca-1^{HIGH} fractions demonstrated that the CD62L– cells of both Sca-1 fractions contained hematopoietic stem cells, with a higher frequency of stem cells within the Sca-1^{HIGH} CD62L– fraction. Within the traditionally defined multipotent progenitor population, CD62L segregated a CD62L+ lymphoid-biased multipotent progenitor and a CD62L– multipotent progenitor with robust multipotency. Flow cytometric analysis of CD62L expression pattern within the multipotent progenitor population demonstrated that CD62L-based separation of progenitors was achieved independently of Flt3 expression. Lastly, the concomitant expression of CD62L and Flt3 revealed a rare population of

multipotent progenitors and a possible B cell/erythroid bipotent precursor within the previously demonstrated myeloid compartment. Simultaneous loss of CD62L and Flt3 was observed in the myeloid lineage-specific population. Together, these data demonstrate the expression of CD62L within the context of early hematopoietic differentiation and establish CD62L as a useful tool in the study of early hematopoiesis.

For my grandfather

The one who instilled in me the value of scholarship

…there comes a point where you'll find something out,
where you'll see something,
or where something will suddenly come together,
and you'll realize that you know something that
no one else in the world knows yet.
Just you.
No one else.

Christopher Moore
Fluke: Or, I Know Why the Winged Whale Sings

TABLE OF CONTENTS

LIST OF FIGURES

ACKNOWLEDGEMENTS

When a graduate student completes his degree, it is an accomplishment, not just for himself, but also for the laboratory that has trained him and for the department that has supported him. For it is not the efforts of the student alone, but also the efforts of all those around him that make this great journey possible. I would like to express my gratitude toward all those who contributed to the completion of my journey.

My foremost thanks go to Dr. Jerry Spangrude. Aside from providing material support for my research, he has been a much appreciated teacher and a comrade-in-science during my years in his laboratory. His demonstration of profound scientific insights and encyclopedic knowledge has been a source of both information and inspiration. His generosity has granted me greater freedom than I have deserved in the pursuit of my research goals and personal interests. His passion for science has set high standards for me as I sought the profession of a scientist.

I would also like to thank the other members of the Spangrude lab. Jeanne Pierce has been a vital member of the lab handling the day-to-day operations and maintenance of the lab itself. Without her the efficacy of the lab and the quality of my experiments would have suffered. She has also taught me various techniques that were vital to my project. Former graduate students, Hongfang Wang and Xiosong Huang have taught me through their examples how to manage the travails of graduate studies and appreciate this

unique opportunity. I would also like to thank a former postdoctoral fellow, Dr. Jaeyong Kwak for his assistance with my project and his friendship.

I would be remiss if I did not thank the faculty of the Pathology Department for their feedbacks over the years. My thesis committee members, Dr. Lorise Gahring, Dr. John Phillips, Dr. Janis Weis and Dr. John Weis have been incredibly helpful in the progression of my project with constructive criticisms. Their inputs have granted me greater insights into my own work and allowed me to appreciate the value of outside sources for aid.

I would like to thank the American taxpayers for funding my research and the Molecular Biology program at the University of Utah. Without their collective sacrifice, the astonishing advancement of science and the training of scientists would not be possible.

Finally I would like to thank my family for their unconditionally support. My parents have supported me with constant encouragements, assurances and consolations, especially during times of stress. My brother Daniel has been my most trusted confidante and a source of both intellectual and emotional support. I would like to express my deepest appreciation to my mother and my wife for supporting me during the last several weeks of my writing phase. Without them, I would have never completed this journey.

CHAPTER 1

INTRODUCTION

Hematopoietic stem cells

The source of all blood cells in the body is the hematopoietic stem cell (HSC). Residing primarily in the bone marrow throughout the entire life of the animal, HSC amazingly replenish the blood supply by generating billions of cells while maintaining the stem cell pool (reviewed in Ogawa, 1993). The various functions of mature progenies of HSC are essential for preservation of the life of the animal and are specific to the specialized progenies. The progenies and some of their specialized functions are: red blood cells (RBC) serve as transports of oxygen throughout the body, platelets induce blood clotting in the event of an injury, and white blood cells (WBC; lymphocytes, granulocytes and macrophages) function as protectors against pathogens (reviewed in Sigvardsson, 2009). These facts demonstrate the importance of HSC and target HSC as a subject of intense research.

The first experimental demonstration of HSC function was published in 1951 when a transplant experiment demonstrated that bone marrow cells could rescue irradiated mice and guinea-pigs (Lorenz et al., 1951). In the 1960s, several studies demonstrated that a population of bone marrow cells was capable of generating RBC in the spleen, and upon transplantation into lethally irradiated hosts, provided radioprotection (Till and McCulloch, 1961; Becker et al., 1963; Wu et al., 1968). With the advent of fluorescence activated cell sorter technology, several groups were able to successfully concentrate bone marrow fractions containing HSC (Visser et al., 1984; Muller-Sieburg et al., 1986). However, it was not until 1988 that a highly enriched population of HSC was identified through targeting a subset of bone marrow cells using

the surface expression pattern of Lin–Sca-1+Thy1.1^{LOW} for FACS sorting (Spangrude et al., 1988).

Since then, an array of new markers has been identified in an attempt to isolate the purest HSC population possible. A currently widely used marker is C-kit, which has been demonstrated to enrich HSC in the brightest fraction of C-kit-labeled bone marrow cells (C-kit^{BRIGHT}) and has become part of a regular protocol for isolating HSC (Besmer, 1991; Ikuta and Weissman, 1992; Morrison et al., 1997; Rawls et al., 2001). Gene expression studies have identified three members of the SLAM (Signaling Lymphocytic Activation Molecules family surface receptor molecules) for isolating HSC (CD150+, CD48–, CD244–; Kiel et al., 2005; Papathanasiou, 2009). Another widely used marker for HSC purification is CD34, a ligand for CD62L. While human HSC express CD34, experiments in mouse models have demonstrated that HSC reside in the CD34– fraction. (Osawa et al., 1996; Yang et al., 2005). The DNA-binding supravital dye Hoechst 33342 has been demonstrated to be efficiently effluxed by a bone marrow population (side population or SP) that has been identified to be enriched for HSC (Goodell et al., 1996). Labeling the bone marrow with the vital mitochondrial dye rhodamine-123 has also resolved a side population that contains HSC (Spangrude and Johnson, 1990; Okada et al., 1993; Li and Johnson, 1995). Despite the availability of abundant markers for HSC isolation, no group has made the claim of isolating an absolutely pure HSC population, indicating that a comprehensive marker set for HSC isolation is not yet complete.

The estimation for the frequency of HSC in the whole bone marrow is quite broad. Currently it is estimated that 1 in 10^4 to 1 in 10^5 cells in the bone marrow represent the HSC frequency (Chao et al., 2008; Luc et al., 2008; Orkin and Zon, 2008). An accurate

calculation of HSC in vivo has proven to a challenge. When a population of cells, containing an unknown number of HSC, is transplanted into lethally irradiated hosts, it is unclear what fraction of transplanted HSC contributes to the reconstitution of the hematopoietic system. Furthermore, it is also unclear if contributing HSC generate equal number of progenies. A common way to characterize the degree of hematopoietic reconstitution is the calculation of repopulating units (RU; Harrison, 1980). Transplanting a population of cells containing an unknown number of HSC into lethally irradiated hosts along with competitor whole bone marrow cells establishes an internal standard (100K competitors = 1 RU) to compare the repopulation capacity of the population in question (Harrison et al., 2005; Yuan et al., 2005). Several constraints limit this method, such as the number of recipients used, number of donor cells transplanted, and the engraftment duration of donor cells (Purton and Scadden, 2007). While the RU calculation does not determine the absolute number of HSC in a given population, it is useful for calculating a relative number of HSC among different populations. In vitro approaches to the determination of HSC frequency suffer from the fact that the observed multipotency output does not necessarily represent HSC as multipotent progenitors also exhibit significant output of progenies into all lineages, and the long term persistence observed in vitro may be an unintended artifact. Regardless, an in vitro based estimation has been made at 2.8 ± 1.06 HSC per 10^5 bone marrow cells (Sieburg et al., 2002). Taken together, a conservative estimation of HSC frequency appears to be approximately 1 HSC per 10^5 whole bone marrow cells.

The key to isolating the absolutely pure HSC and calculating an accurate HSC frequency is to identify the appropriate set of markers. Knowing the actual HSC markers

will assure the isolation of pure, live HSC, and facilitate future studies seeking greater understanding of stem cell biology.

Early hematopoietic differentiation

The traditional model of hematopoiesis identifies the hematopoietic stem cell compartment of the bone marrow as the site of early hematopoietic differentiation. The hematopoietic stem cell compartment is identified by a shared expression pattern of stem cell-associated surface markers, Sca-1 and C-kit (Spangrude et al., 1988; Ikuta and Weissman, 1992). These cells also lack an array of mature cell surface markers collectively known as lineage (Lin). Therefore, the hematopoietic stem cell compartment is also commonly referred to as KLS for C-kit+Lin–Sca-1+. Within the KLS population, three early hematopoietic populations have been identified according to Flt3 and Thy1.1 expression levels: Thy1.1+ Flt3– long-term HSC (LT-HSC), Thy1.1+ Flt3+ short-term HSC (ST-HSC), and Thy1.1– Flt3+ multipotent progenitors (MPP) (Spangrude et al., 1988; Morrison et al., 1997; Adolfsson et al., 2001; Christensen and Weissman, 2001). LT-HSC is the true HSC, and represents the origin of hematopoietic differentiation. As LT-HSC enters the differentiation state, its capacity for self-renewal becomes limited and is accompanied by the expression of Flt3. While LT-HSC can self-renew for the life of the animal, ST-HSC can persist for only 6-12 weeks (Morrison and Weissman, 1994; Christensen and Weissman, 2001). Further maturation is characterized by the loss of self-renewal capacity and Thy1.1 expression. Multipotency is still preserved, therefore, the cells of this stage are known as MPP. These cells represent the end subpopulation within the KLS population. Outside KLS, the progenitors are bifurcated into lymphoid

and myeloid lineage committed progenitors through the establishment of common lymphoid progenitors (CLP) (Kondo et al., 1997) and common myeloid progenitors (CMP) (Akashi et al., 2000).

This traditional model of early hematopoietic differentiation has been the subject of much controversy. Adolffson et al. have demonstrated that the top 25% of KLS cells for Flt3 expression rapidly lost the potential to generate platelets and RBC (Meg/E potential) and that this population was mostly lymphoid-biased. Based on these observations, they proposed a new name for this population, LMPP for lymphoid-primed multipotent progenitors (Adolfsson et al., 2005). The laboratory responsible for the establishment of the traditional hematopoietic tree, the Weissman group at Stanford University, released a rebuttal study demonstrating that there is a detectable amount of Meg/E activity from the newly proposed LMPP population, however, they conceded that the Meg/E activity was reduced compared to the Meg/E activity expected from the MPP population (Forsberg et al., 2006). These studies demonstrate that the MPP population of KLS is not a homogeneous population. Another example of heterogeneity within MPP came from the Kondo laboratory. They have demonstrated that by using the vascular cell adhesion molecule-1 (VCAM-1), it was possible to subfractionate the MPP population into a VCAM-1– LMPP-like population and a VCAM-1+ traditional MPP (Lai et al., 2005; Lai and Kondo, 2006). Interestingly the cells of VCAM-1– LMPP were mostly $Flt3^{HIGH}$ cells; however, VCAM-1+ MPP contained both low and high levels of Flt3. This observation suggests that perhaps the VCAM-1+ MPP is also heterogeneous.

Together, the above findings represent ongoing research efforts to complete the identification of all members of the hematopoietic tree. One of the ways that will

expedite this process is to identify novel markers that will aid in the identification of subsets that are currently unknown.

CD62L and hematopoietic differentiation

CD62L (also known as L-Selectin) is a member of the Selectin family of cell surface adhesion molecules that is constitutively expressed on many WBC (Griffin et al., 1990; Tedder et al., 1990). Three glycoprotein ligands for CD62L have been reported: GlyCam-1 (Laskey et al., 1992), CD34 (Baumhueter et al., 1993), and MAdCAM-1 (Briskin et al., 1993). Two isoforms of CD62L have been described to be expressed due to posttranslational modifications: a 74 kDa-sized isoform on lymphocytes and a 100 kDa-sized isoform on neutrophils (Lewinsohn et al., 1987). Unlike the other two members of the Selectin family, E-selectin and P-selectin, CD62L contains an extracellular cleavage site near the plasma membrane (Ivetic and Ridley, 2004). Following an activation stimulus, the extracellular domain of CD62L is autoproteolysed and releases soluble fragments of CD62L, 62 kDa-sized fragments from lymphocytes and 75-100 kDa-sized fragments from neutrophils (Schleiffenbaum et al., 1992).

CD62L has been described to play an important role in lymphocyte migration into peripheral lymph nodes and sites of inflammation (Arbones et al., 1994). It has also been suggested that the loss of CD62L might be required for CD62L+ cells to migrate across endothelium (Kishimoto et al., 1989). Knockout experiments in mice have demonstrated that the complete loss of CD62L resulted in impaired lymphocyte migration to peripheral lymph nodes, impaired neutrophil migration to peritoneum and defects in leukocyte rolling (Arbones et al., 1994). While intracellular signaling induced by CD62L has not

been well characterized, in vitro stimulation of CD62L, using monoclonal antibodies against Jurkat cells, has resulted in the induction of $p56^{lck}$, Grb2/Sos, Ras, and Rac2 to peroxide anion production signaling cascade (Brenner et al., 1996). Interestingly, a measurable amount of CD62L suppression has also been observed in the blood serum samples of human patients with hereditary hemochromatosis (Norris et al., 2010).

Characterization of CD62L in the context of hematopoietic differentiation has been limited. One of the ligands for CD62L listed above is CD34, a marker of HSC (Baumhueter et al., 1993; Osawa et al., 1996; Yang et al., 2005). However, the relationship between CD62L and HSC has not been ascertained.

Previously our laboratory has reported the subfractionation of the Thy1.1– fraction of KLS (KLST–) using CD62L (Perry et al., 2004). It was reported that the majority of KLST– cells expressed CD62L. When the CD62L– fraction of KLST– were transplanted into lethally irradiated recipients, the donor cells generated significant engraftment in B cell, T cell, granulocyte and monocyte lineages, indicative of an MPP population. Interestingly, when the CD62L+ fraction of KLST– were transplanted, the donor cells generated robust T cell activity with lesser amounts of B cell, granulocytes and monocytes. These findings indicated that CD62L expression marked a bone marrow population similar to an early T-lineage progenitor (ETP; Allman et al., 2003). These observations led our laboratory to suspect a greater capacity of CD62L to identify stages in early hematopoietic differentiation than previously realized.

Transplant experiment design

The primary tool used in this dissertation was bone marrow transplantation for in vivo analysis of target cells. The general schematic for the experimental procedure is shown in Figure 1.1. Four strains of mice were used. For donor mice, green fluorescent protein (GFP) transgenic mice derived by microinjection of C57B/6 oocytes were used. These mice were kindly provided by Dr. Masaru Okabe (Osaka University, Osaka, Japan) (Spangrude et al., 2006). These mice express GFP in all blood lineages except the RBC lineage. They also express the Thy1.2 allele. This is problematic for the study of KLS cells, since only the Thy1.1 allele marks HSC (Spangrude and Brooks, 1992). Therefore, these mice were bred with GFP– Thy1.1+ mice that were bred in our laboratory to produce GFP+Thy1.1+ litters.

When transplanted into GFP– recipient mice, GFP+ donor cells generate GFP+ progenies that can be tracked using flow cytometry. However, the lack of GFP expression in the erythroid lineage prevents the tracking of RBC generation. Therefore, we have developed a novel HPLC protocol to discriminate the donor-derived RBC from the recipient RBC using allelic variants of hemoglobin beta chain (Hbb). The GFP+Thy1.1+ mice used in our experiments express the Hbb^S variant, while the GFP– Thy1.2+ mice express the Hbb^D variant. This system is explained in greater detail in Appendix A.

Whole bone marrow cells were harvested from the GFP+Thy1.1+Hbb^S mice. The cells were incubated with a cocktail of rat antibodies directed against mature cell surface markers (Lin: B220, CD2, CD3, CD5, CD8, CD19, Ly-6G, Mac1 and Ter119). The labeled mature cells were incubated secondarily with anti-rat antibodies coupled with

magnetic beads. Finally the labeled mature cells were removed using a magnetic column. When the Lin-depleted cells were obtained, they were stained for fluorochrome-conjugated antibodies to FACS purify specific populations. Following a successful FACS sort, the purified target cells were retro-orbitally injected into lethally irradiated GFP–Thy1.2+Hbb^D mice (12~13 Gy).

Following the transplantation, periodically the peripheral blood samples were drawn retro-orbitally using heparinized capillary tubes. The blood samples were counted, processed for flow cytometry analysis for the detection of WBC and platelet engraftment, or HPLC analysis for RBC engraftment through Hbb^S versus Hbb^D quantification.

Scope of the study

Flow cytometric analysis of CD62L expression has revealed heterogeneity among the previously defined LT-HSC, ST-HSC and MPP populations. Using transplant studies, the work described in this dissertation characterized the constituents of KLS at a greater resolution. The techniques used here allow for the identification and quantification of the engraftment potential of transplanted cells in all lineages. The data represent examination of lineage potential among various subpopulations identified through CD62L expression pattern and provides opportunities for refining the traditionally defined hematopoietic tree. While the findings are based on differential CD62L expression patterns among early hematopoietic cells, they do not indicate any direct relationship between CD62L and HSC/progenitor function. The application of CD62L as presented justifies the use of CD62L for identifying subpopulations that were not possible previously. The engraftment data of CD62L subfractionated populations provide in vivo

evidence for gradual change in lineage potential, in contrast to the widely described stage-by-stage developmental model with abrupt lineage commitments. The transplant studies using competitor whole bone marrow cells in the context of lethally irradiated recipients allowed for the RU calculation to determine the relevant population for HSC enrichment and created future opportunities for such analysis in other compartments of early hematopoietic progenitors.

Significance

One of the primary goals of studying hematopoiesis is to clearly identify the hematopoietic tree that accurately portrays the developmental events occurring in vivo. The initially established model of LT-HSC→ ST-HSC → MPP→ CLP or CMP (Morrison et al., 1997; Kondo et al., 1997; Akashi et al., 2000; Adolfsson et al., 2001; Christensen and Weissman, 2001) has been proven to be oversimplified and inaccurate (Adolfsson et al., 2005; Forsberg et al., 2006). Ongoing studies searching for more markers and missing populations in the hematopoietic tree indicates that more data is required to completely understand the developmental events of hematopoiesis. The data presented in this dissertation contributes to that effort. Using antibodies against CD62L, we demonstrate heterogeneity within the early populations of hematopoiesis. In vivo evidence points to CD62L as a potential substitute for currently used markers for efficient HSC enrichment as well as its concomitant use with the other markers to isolate purer HSC population.

In addition, the data support the idea that lineage commitment occurs gradually, accompanied by the gradual changes in the expression patterns of surface markers.

Currently, it is widely perceived that the progression of hematopoietic development occurs in a stage-by-stage manner with instant changes in the expression profiles of surface markers. While some surface markers' expressions may change quickly and lineage potential lost abruptly with such changes, we and others have observed that there are other markers that behave differently. Therefore, it is important that more evidence be gathered to present a more accurate view of hematopoietic development.

References

Adolfsson, J., Borge, O.J., Bryder, D., Theilgaard-Monch, K., Astrand-Grundstrom, I., Sitnicka, E., Sasaki, Y., and Jacobsen, S.E. (2001). Upregulation of Flt3 expression within the bone marrow Lin(–)Sca1(+)c-kit(+) stem cell compartment is accompanied by loss of self-renewal capacity. Immunity *15*, 659-669.

Adolfsson, J., Mansson, R., Buza-Vidas, N., Hultquist, A., Liuba, K., Jensen, C.T., Bryder, D., Yang, L., Borge, O.J., Thoren, L.A., Anderson, K., Sitnicka, E., Sasaki, Y., Sigvardsson, M., and Jacobsen, S.E. (2005). Identification of Flt3+ lympho-myeloid stem cells lacking erythro-megakaryocytic potential: a new road map for blood lineage commitment. Cell *121*, 295-306.

Akashi, K., Traver, D., Miyamoto, T., and Weissman, I.L. (2000). A clonogenic common myeloid progenitor that gives rise to all myeloid lineages. Nature *404*, 193-197.

Allman, D., Sambandam, A., Kim S., Miller, J.P., Pagan, A., Well, D., Meraz, A., and Bhandoola, A. (2003) Thymopoiesis independent of common lymphoid progenitors. Nat Immunol. *4*, 168-174.

Arbones, M.L., Ord, D.C., Ley, K., Ratech, H., Maynard-Curry, C., Otten, G., Capon, D.J., and Tedder, T.F. (1994) Lymphocyte homing and leukocyte rolling and mirgration are impaired in L-selectin-deficient mice. Immunigy *4*, 247-260.

Baumhueter, S., Singer, M.S., Henzel, W., Hemmerich, S., Renz, M., Rosen, S.D., and Lasky, L.A. (1993) Binding of L-Selectin to the vascular sialomucin CD34. Science *262*, 436-438.

Becker, A., McCulloch, E., and Till, J. (1963). Cytological demonstrating of the clonal nature of spleen colonies derived from transplanted mouse marrow cells. Nature *197*, 452-454.

Besmer, P. (1991) The kit ligand encoded at the murine Steel locus: a pleiotropic growth and differentiation factor. Curr Opin Cell Biol *3*:939-946.

Brenner, B., Gulbin, E., Scholottmnn, K., Koppenhoefer, U., Busch, G.L., Walzog, B., Steinhausen, M., Coggeshall, K.M., Linderkamp, O., and Lang, F. (1996). L-selectin activates the ras pathway via the tyrosine kinase p56lck. PNAS. 93, 15376-15381.

Brisken, M.J., McEvoy, L.M., and Butcher, E.C. (1993). MAdCAM-1 has homology to immunoglobulin and mucin-like adhesion receptors and to IgA1. Nature 363, 461-464.

Chao, M.P., Seita, J., and Weissman, I.L. (2008). Establishment of a normal hematopoietic and leukemia stem cell hierarchy. Cld Spring Harb. Symp. Quant. Biol. *73*, 439-449.

Christensen, J.L., and Weissman, I.L. (2001). Flk2 is a marker in hematopoietic stem cell differentiation: a simple method to isolate long-term stem cells. Proc. Natl. Acad. Sci. USA *98*, 14541-14546.

Forsberg, E.C., Prohaska, S.S., Katzman, S., Heffner, G.C., Stuart, J.M., and Weissman, I.L. (2005). Differential expression of novel potential regulators in hematopoietic stem cells. PLoS Genetics *1*, e28.10.1371/journal.pgen.0010028.

Goodell, M.A., Brose, K., Paradis, G., Conner, A.S., Mulligan, R.C. (1996). Isolation and functional properties of murine hematopoietic stem cells that are replicating in vivo. J. Exp. Med. *183*, 1797-1806.

Griffin, J.D., Spertini, O., Ernst, T.J., Belvin, M.P., Levine, H.B., Kanakura, Y., and Tedder, T.F. (1990) Graunolcyte-macrophage colony-stimulating factor and other cytokines regulate surface expression of the leukocyte adhesion molecule-1 on human neutrophils, monocytes, and their precursors. J. Immunol. *145*, 576-584.

Harrison, D.E. (1980). Competitive repopulation: a new assay for long-term stem cell functional capacity. Blood *55*, 77-81.

Harrison, D.E., Jordan, C.T., Zhong, R.K., and Astle, C.M. (1993). Primitive hemopoietic stem cells: direct assay of most productive populations by competitive repopulation with simple binomial, correlation and covariance calculations. Exp. Hematol. *21*, 206-219.

Ikuta, K., and Weissman, I.L. (1992). Evidence that hematopoietic stem cells express mouse c-kit but do not depend on steel factor for their generation. Proc. Natl. Acad. Sci. USA *89*, 1502-1506.

Ivetic, A., and Ridley, A.J. (2004). The telling tail of L-selectin. Biochemical Society Transactions 32, 1118-1121.

Kiel, M.J., Yilmaz, O.H., Iwashita, T., Yilmaz, O.H., Terhorst, C., and Morrison, s.J. (2005). SLAM family receptors distinguish hematopoietic stem and progenitor cells and reveal endothelial niches for stem cells. Cell *121*, 1109-1121.

Kishimoto, T.K., Jutila, M.A., Berg, E.L., and Butcher, E.C. (1989). Neutrophil Mac-1 and Mel-14 adhesion proteins inversely regulated by chemotactic factors. Science *245*, 1238-1241.

Kondo, M., Weissman, I.L., and Akashi, K. (1997). Identification of clonogenic common lymphoid progenitors in mouse bone marrow. Cell *91*, 661-672.

Laskey, L.A., Singer, M.S., Dowbenko, D., Imai, Y., Henzel, W.J., Grimley, C., Fennie, C., Gillett, N., Watson, S.R., and Rosen, S.D. (1992). An endothelial ligand for L-selectin is a novel-mucin-like molecule. Cell 69, 927-938.

Lewinsohn, D.M., Bargatze, R.F., and Butcher, E.C. (1987). Leukocyte-endothelial cell recognition: evidence of a common molecular mechanism shared by neutrophils, lymphocytes, and other leukocytes. J. Immunol. 138, 4313-4321.

Li, C.L., and Johnson, G.R. Murine hematopoietic stem and progenitor cells: I. enrichment and biologic characterization. Blood *85*, 1472-1479.

Lorenz, E., Uphoff, D., Reid, T.R., Shelton, E. (1951). Modification of irradiation injury in mice and guinea pigs by bone marrow injections. J. Natl. Cancer. Inst. *12*, 197-210.

Luc, S., Buza-Vidas, N., and Jacobsen, S.E. (2008) Delineating the cellular pathways of hematopoietic lineage commitment. Semin. Immunol. *20*, 213-220.

Muller-Sieburg, C.E., Whitlock, C.A., and Weissman, I.L. (1986). Isolation of two early lymphocyte progenitors from mouse marrow: a committed pre-pre-B cell and a clonogenic Thy-1^{LO} hematopoietic stem cell. Cell *44*, 653-662.

Morrison, S.J., Wandycz, A.M., Hemmatic, H.D., Wright, D.E., and Weissman, I.L. (1997). Identification of a lineage of multipotent hematopoietic progenitors. Development *124*, 1929-1939.

Norris, S., White, M., Mankan, A.K., and Lawless, M.W. (2010). Highly sensitivity adhesion molecules detection in hereditary haemochromatosis patients reveals altered expression. International Journal of Immunogenetics 36, 125-133.

Okada, S., Nagayoshi, K., Nakuchi, H., Nishikawa, S.I., Miura, Y., and Suda, T. (1993) Sequential analysis of hematopoietic reconstitution achieved by transplantation of hematopoietic stem cells. Blood *81*, 1720-1725.

Ogawa, M. (1993). Differentiation and proliferation of hematopoietic stem cells. Blood 81, 2844-2853.

Orkin, S.H., and Zon, L.I. (2008). Hematopoiesis: an evolving paradigm for stem cell biology. Cell *132*, 631-644.

Osawa, M., Hanada, K., Hamada, H., and Nakauchi, H. (1996). Long-term lymphohematopoietic reconstitution by a single CD34-low/negative hematopoietic stem cell. Science *273*, 242-245.

Papathanasiou, P., Attema, J.L., Karsunky, H., Xu, J., Smale, S.T., Weissman, I.L. (2009). Evaluation of the long-term reconstituting subset of hematopoietic stem cells with CD150. Stem Cells *27*, 2498-2508.

Purton, L.E., and Scadden, D.T. (2007). Limiting factors in murine hematopoietic stem cell assays. Cell Stem Cell *1*, 263-270.

Rawls, J.F., Mellgren, E.M., and Johnson, S.L. (2001) How the zebrafish gets its stripes. Developmental Biology *240*, 301-314.

Schleiffenbaum, B., Spertini, O., and Tedder, T.F. (1992). Soluble L-selectin is present in human plasma at high levels and retains functional activity. J. Cell. Biol. 119, 229-238.

Sieburg, H.B., Cho, R.H., and Muller-Sieburg, C.E. (2002). Limiting dilution analysis for estimating the frequency of hematopoietic stem cells: uncertainty and significance. Exp Hematol. *30*, 1436-1443.

Sigvardsson, M. (2009). New light on the biology and developmental potential of haematopoietic stem cells and progenitor cells. J. Intern. Med. *266*, 311-324.

Spangrude, G.J., and Brooks, D.M. (1992). Phenotypic analysis of mouse hematopoietic stem cells show a Thy-1-negative subset. Blood *80*, 1957-1964.

Spangrude, G.J., Heimfeld, S., and Weissman, I.L. (1988). Purification and characterization of mouse hematopoietic stem cells. Science *241*, 58-62.

Spangurde, G.J., and Johnson, G.R. (1990) Resting and activated subsets of mouse multipotent hematopoietic stem cells. Proc. Natl. Acad. Sci. USA. *87*, 7433-7437.

Spangrude, G.J., Cho, S., Guedelhoefer, O., VanWoerkom, R.C., and Fleming, W.H. (2006) Mouse models of hematopoietic engraftment: limitations of transgenic green fluorescent protein strains and a HPLC approach to analysis of erythroid chimerism. Stem Cells *24*, 2045-2051.

Tedder, T.F., Penta, A.C., Levine, H.B., and Freedman, A.S. (1990) Expression of the human leukocyte adhesion molecule, LAM1. Identity with the TQ1 and Leu-8 differentiation antigens. J. Immunol. *1440*, 532-540.

Till, J.E., and McCulloch, E.A. (1961). A direct measurement of the radiation sensitivity of normal mouse bone marrow cells. Radiat. Res. *14*, 1419-1430.

Wu, A., Till, J., Siminovitch, L., and McCulloch, E. (1968). Cytological evidence for a relationship between normal hematopoietic colony-forming cells and cells of the lymphoid system. J. Exp. Med. *127*, 455-467.

Visser, J.W.M., Gauman, J.G.J., Mulder, A.H., Eliason, J.F., and de Leeuw, A.W. (1984). Isolation of murine pluripotent hemopoietic stem cells. J. Exp. Med. *59*, 1576-1590.

Yang, L., Bryder, D., Adolfsson, J., Nygren, J., Mansson, R., Sigvardsson, M., and Jacobsen, S.E. (2005). Identification of Lin(-)Sca1(+)-kit(+)CD34(+)Flt3-short-term hematopoietic stem cells capable of rapidly reconstituting and rescuing myeloablated transplant recipients. Blood *105*, 2717-2723.

Yuan, R., Astle, C.M., Chen, J., and Harrison, D.E. (2005). Genetic regulation of hematopoietic stem cell exhaustion during development and growth. Exp. Hematol. *33*, 243-250.

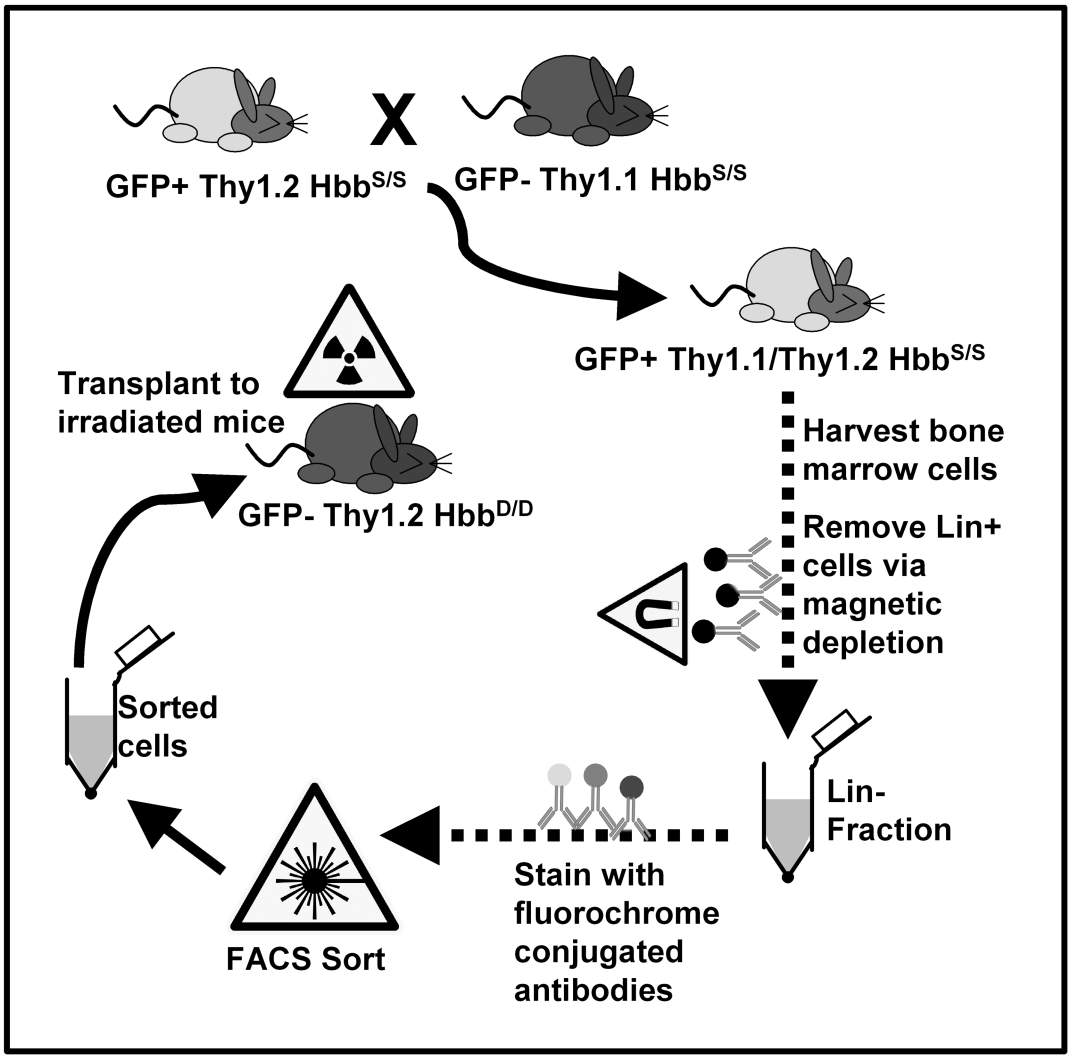

Figure 1.1 Transplant experiment schematic

CHAPTER 2

ENRICHMENT OF HEMATOPOIETIC STEM CELLS BASED ON CD62L EXPRESSION

Abstract

The source of adult hematopoiesis is a population of hematopoietic stem cells (HSC) that replenishes itself and generates the entire blood system throughout the life of the animal. While a set of known markers for identifying a population containing HSC has been defined, a pure population of HSC has been unobtainable. In this report we present an additional marker previously not reported for an effective enrichment of HSC. We observed that in vivo transplant studies using CD62L to fractionate the hematopoietic stem cell compartment led to a multipotent progenitor-enriched CD62L+ fraction and a HSC-enriched CD62L– fraction. We also observed that the use of CD62L in addition to Flt3, a commonly used marker for HSC-enrichment, uncovered a CD62L–Flt3– population that is the primary source of HSC. These data provide direct evidence for the application of CD62L in combination with other markers for isolating a more highly enriched population of HSC. Furthermore, the data establish CD62L as an effective substitute for the widely used Flt3 for an efficient and reproducible method of HSC enrichment.

Introduction

In adult mammals, all blood cells originate from a pool of hematopoietic stem cells (HSC) residing in the bone marrow. These adult stem cells possess the prototypical stem cell characteristics: the ability to self-renew through mitosis and the capacity to generate cells of all hematopoietic lineages (reviewed in Weissman, 2000). As HSC mature and differentiate into progeny cells, their self-renewal ability becomes limited and their multipotency lost through lineage commitment. The early events of hematopoietic

differentiation have been described to occur within a subset of immature cells in the bone marrow identified by a shared expression pattern of surface markers: co-expression of stem cell-associated markers C-kit and Sca-1 and the lack mature cell markers collectively known as Lineage (Lin) (Spangrude et al, 1988; Ikuta and Weissman, 1992). This subset of hematopoietic progenitors have been named the hematopoietic stem cell compartment or KLS (C-kit+Lin–Sca-1+).

Within the KLS population reside three distinct subpopulations that delineate the early hematopoietic differentiation events. According to expression patterns of Flt3 and Thy1.1 surface markers, the three subpopulations are designated as Thy1.1+ Flt3– long-term HSC (LT-HSC), Thy1.1+ Flt3+ short-term HSC (ST-HSC), and Thy1.1– Flt3+ MPP (Spangrude et al., 1988; Morrison et al., 1997; Adolfsson et al., 2001; Christensen and Weissman, 2001). The labels reflect each subpopulation's hematopoietic potential. LT-HSC contains the true HSC that initiates hematopoiesis. As LT-HSC enters differentiation, it upregulates Flt3 and is labeled ST-HSC, due to its limited capacity for self-renewal. ST-HSC when transplanted has been shown to reconstitute the hematopoietic system of recipients for approximately 6~12 weeks, and therefore, is not a true HSC (Morrison and Weissman, 1994; Christensen and Weissman, 2001). Finally, the last stage within the KLS population is the MPP stage that has lost self-renewal capability, accompanied by the loss of Thy1.1, but maintains multipotency. The heterogeneity within this subpopulation has been the focus of recent discussions (Chapter 3; Adolfsson et al., 2005; Akashi et al., 2005; Lai et al., 2005; Lai and Kondo, 2006; Forsberg et al., 2006).

As the source of hematopoiesis, the isolation of pure HSC has been the target of much research. A major breakthrough in HSC purification came in 1988 when Spangrude et al. demonstrated that a highly enriched HSC population can be obtained through the application of fluorescence-activated cell sorter (FACS) using the surface expression pattern of Lin–Sca-1+Thy1.1^{LOW} (Spangrude et al., 1998). Subsequent studies have added an extensive array of markers in order to obtain the purest HSC sample possible. C-kit, a receptor for stem cell factor, has been identified as a significant marker that contains the HSC in its C-kit^{BRIGHT} fraction (C-kit+ hereafter) and is currently a part of regular regimen for HSC and progenitor isolation studies (Besmer, 1991; Ikuta and Weissman, 1992; Morrison et al., 1997; Rawls et al., 2001). Gene expression studies have identified a set of surface receptors of the SLAM family (Signaling Lymphocytic Activation Molecules) for isolating HSC (Kiel et al., 2005). Another widely used marker for HSC purification is CD34, a ligand for CD62L (Osawa et al., 1996; Yang et al., 2005).

Previously our laboratory has reported that the CD62L adhesion molecule can be used to fractionate the Thy1.1– portion of KLS to identify a T cell-biased CD62L+ MPP and a CD62L– MPP with more generally distributed multipotency (Perry et al., 2004). These findings have led us to hypothesize that CD62L is an early marker of hematopoietic development. To test this hypothesis, we have examined in vivo engraftment potential of CD62L– and CD62L+ fractions of KLS through transplant experiments.

In this report we establish CD62L as a novel marker for HSC purification. Our data demonstrate that in a transplant setting, the CD62L– fraction of KLS contains highly

enriched HSC, while the CD62L+ fraction contains MPP with a limited duration of output. Furthermore, we present that the CD62L– fraction contains HSC in both Sca-1^{HIGH} as well as Sca-1^{LOW} fractions of KLS, albeit less HSC in Sca-1^{LOW}, indicating a gradual population shift as Sca-1 is downregulated. Lastly we present evidence that the primary source of HSC resides in the CD62L– fraction of the now widely accepted Flt3– Thy1.1^{LOW} HSC population. These data indicate that CD62L is an effective marker for isolating an enriched population of HSC.

Results

CD62L expression pattern in KLS is analogous to Flt3 expression pattern

In order to test the hypothesis that CD62L is a marker of early hematopoietic differentiation, KLS, the pool of early hematopoietic progenitors, was analyzed for CD62L expression along with Thy1.1 (Figure 2.1A). The expression pattern revealed a distribution of CD62L expression between the Thy1.1– to Thy1.1^{LOW} (Thy1.1+ hereafter) populations. Visual examination of the data indicated a clear discrimination of three distinct populations: CD62L–Thy1.1+, CD62L+Thy1.1+, and CD62L+Thy1.1–. The three population pattern is analogous to the traditionally defined LT-HSC, ST-HSC and MPP indicted by Flt3 and Thy1.1 levels (Figure 2.1B). The frequency of cells belonging to each distinct population in figure 2.1A is similar to the frequency of cells belonging to each population in Figure 2.1B. Moreover, co-staining of CD62L and Flt3 in KLS revealed a high degree of co-expression, while a significant number of cells were mutually exclusive for CD62L or Flt3 expression (data not shown; Chapter 3).

To examine the erythroid potential of each of the populations in Figure 2.1A, in vitro methylcellulose culture was performed. FACS sorted cells from the four quadrants were plated independently in an erythroid inducing environment with SCF, IL-2 and EPO supplements. Erythroid colonies were detected with benzidine staining. The results indicated that the cells from all four populations produced a significant number of erythroid colonies early during the culture period. However, only the CD62L–Thy1.1+ population maintained a persistent number of erythroid colonies for the duration of the observation period, while the other three populations showed reduced numbers of erythroid colonies as days progressed (Figure 2.1C). The presence of strong and persistent erythroid colonies from CD62L–Thy1.1+ population indicated that it had greater erythroid progenitors than the other three populations and suggested that it may contain HSC.

CD62L– fraction of KLS contains the HSC population

In order to investigate the presence of HSC in the CD62L+ and CD62L– fractions in vivo, we performed a transplant experiment. GFP+Hbb^S mice were used as donors to allow for the tracking of platelets and white blood cells (WBC) produced from the transplanted populations via flow cytometric analysis. Red blood cells (RBC) were tracked via hemoglobin variant Hbb^S via HPLC analysis. 1000 donor KLS cells were sorted according to CD62L expression (Figure 2.2A and 2.2B). The donor cells were transplanted into lethally irradiated GFP–Hbb^D recipient mice with 100K cells of recipient type as competitors.

The transplant data showed that CD62L– cells reconstituted the hematopoietic system of the recipient mice strongly and persistently (Figure 2.1C~E). In contrast, CD62L+ cells failed to engraft persistently. They did generate cells of all lineages, however, the donor-derived cells diminished significantly during the weeks posttransplant. More specifically, platelets were undetectable shortly after the transplant, RBC level was stronger but did completely disappear by week 13, while WBC diminished to a very low level after the initial burst, but persisted throughout the entire observation period. When transplanted, HSC would be expected to generate progenies for the life of the recipient, since HSC has the capacity to self-renew. It is also expected that it will produce progenies in all lineages. MPP, on the other hand, while expected to produce cells of all lineages, is not expected to produce them for the life of the animal with their limited capacity for self-renewal. In addition, their progeny output is expected to be less than that of HSC. One aspect of MPP that is expected to surpass HSC in a transplant setting is the temporal kinetics of progeny production. Considering the fact that MPP is a more mature population than HSC, it is logical that MPP would differentiate into progeny cells quicker than HSC, which must pass through the MPP stage first. In agreement with this concept, the data showed that RBC level peaked prior to week 3 for CD62L+ cells, however, CD62L– cells did not peak in RBC production until week 5 (Figure 2.2D). Together, the data suggest that the CD62L– population contained HSC, while the CD62L+ population contained MPP.

To confirm that the CD62L– population contains HSC, the bone marrow cells of the recipient mice were examined following the termination of transplant observation. Harvested bone marrow cells of CD62L+ recipients were stained with C-kit and Sca-1 to

analyze the KLS compartment for GFP+ donor cells (Figure 2.3A). Only a trace amount of GFP+ cells were found (<0.1%, Figure 2.3B). In contrast, the bone marrow cells of the CD62L– recipients showed a significant level of GFP+ cells (Figure 2.3C and 2.3D). On average, 45% of KLS cells in these animals were donor-derived cells. The GFP+ KLS cells were then isolated by FACS sorting and transplanted into another set of lethally irradiated hosts. Since CD62L+ recipients generated only trace amounts of GFP+ cells in their KLS fractions, all GFP+ cells were pooled into one injection and given to one recipient. Five weeks later, the hosts' peripheral blood samples were analyzed for donor-derived cells. Only mice receiving CD62L– donor-derived GFP+ cells produced GFP+ progenies (Figure 2.3E). The mouse receiving CD62L+ donor-derived GFP+ cells did not produce any detectable amount of cells in any lineages. These results confirm that CD62L– fraction contained HSC and CD62L+ fraction contained MPP. In addition, the data indicate that the long term tracking of peripheral blood is sufficient for the determination of donor HSC or MPP identities.

The CD62L– fraction is enriched for HSC, while the CD62L+ fraction is enriched for MPP

In the primary transplant of the preceding experiment, an equal number of 1000 cells was transplanted for both CD62L– and CD62L+ fractions. Therefore, a reasonable follow up question was to inquire if there are different frequencies of HSC present in CD62L– and CD62L+. If CD62L+ contained a rare population of HSC, then it may not have been detectable at 1000 donor cells. Therefore we repeated the above experiments using different numbers of donor cells. The CD62L– fraction was given to the transplant

recipients at 100 cells per recipient, while the CD62L+ fraction was given to the recipients at 10,000 cells per recipient. All other parameters remained the same as above.

The analysis of RBC confirmed our previous findings. The CD62L– fraction, despite the few donor cells injected, produced a strong and persistent output of RBC, while the CD62L+ fraction, despite the overwhelming number of progenitors injected, produced RBC that diminished over time until they became undetectable (Figure 2.4A). Consistent with the large number of cells injected, the CD62L+ population did produce more RBC than did the CD62L– fraction early in the time course. Similarly to figure 2.2D, the CD62L+ progenitors also peaked in RBC production earlier than the CD62L– HSC. WBC analysis showed results similar to the previous experiment, confirming the identities of the CD62L– and CD62L+ populations as HSC and MPP, respectively (Figure 2.4B).

To investigate if both populations of cells conferred radioprotection, the transplant recipient mice were lethally irradiated. 500 cells per CD62L fraction were injected into the mice without any competitors. The results showed that donor cells of both fractions successfully rescued all mice treated with progenies detectable in the peripheral blood, subsequently, with similar kinetics as observed above (Figure 2.4C and 2.4D).

Different frequencies of HSC are observed in CD62L– fractions within Sca-1 subsets

While the above data indicated convincingly that CD62L– fraction of KLS contained HSC, a concern arose if CD62L– HSC can be obtained by gating on Sca-1^{HIGH} fraction without the actual use of CD62L. As discussed previously, Sca-1 is a marker of

stem cells. Therefore it was possible that HSC undergoing differentiation may express CD62L after Sca-1 is downregulated. While this scenario would support the hypothesis that CD62L is a marker of hematopoietic differentiation, it would also limit the value of CD62L as a marker for HSC purification. Hence, the KLS population was subfractionated into Sca-1^{HIGH} and Sca-1^{LOW} subsets for transplantation (Figure 2.5A). No obvious differences in Flt3 and Thy1.1 expression patterns were observed for the two Sca-1 subsets (Figure 2.5B and 2.5C). The known HSC-containing population, Flt3– Thy1.1+, was gated and analyzed for CD62L in both Sca-1^{HIGH} and Sca-1^{LOW} subsets (Figure 2.5D and 2.5E). As one might expect, the Sca-1^{HIGH} fraction of HSC contained very few CD62L+ cells, approximately 6% (Figure 2.5D). The Sca-1^{LOW} fraction of HSC, however, contained a significant number of CD62L+ cells, approximately 38% (Figure 2.5E). The CD62L– cells of Sca-1^{HIGH} fraction (S^{HIGH}) and CD62L– cells of Sca-1^{LOW} fraction (S^{LOW}) cells were sorted and transplanted into lethally irradiated mice at 1000 cells per donor fraction with 100K competitor cells, as previously performed.

Subsequent peripheral blood analysis for RBC and WBC production indicated that both populations contained significant amounts of HSC (Figure 2.5F and 2.5G). RBC production was strong from both populations, and toward the end of observation period at week 16, there was no statistically significant difference observed between the outputs of RBC (Figure 2.5F). Interestingly, a significant difference was observed in WBC engraftment during the late term. While almost all WBC found in S^{HIGH} recipients were of donor origin, approximately 90%, only about 20% of WBC found in S^{LOW} recipients were of donor origin (Figure 2.5G). From these results, it is unclear exactly how different the stem cell frequencies are between S^{HIGH} and S^{LOW} populations. It is a

conservative claim, however, that S^{HIGH} is likely to contain a higher frequency of HSC than S^{LOW}. The data also suggest that the S^{LOW} population is biased for erythroid lineage engraftment. Clonal analysis would be required to confirm these interpretations.

The CD62L– fraction of KLSF– is the primary site of HSC enrichment

Flt3 is a widely used marker for FACS-sorting of HSC. The well established three early hematopoietic populations of KLS, LT-HSC, ST-HSC and MPP are based on the expression pattern of Flt3 and Thy1.1 (Morrison et al., 1997; Adolfsson et al., 2001; Christensen and Weissman, 2001). Therefore, if CD62L is to be established as a marker useful for purifying HSC, it must be tested in the context of Flt3. To examine the efficacy of CD62L in purifying HSC within the Flt3-defined parameter, CD62L– and CD62L+ fractions of Flt3– fraction of KLS (KLSF–) were sorted (Figure 2.6A and 2.6B). The CD62L profile of the KLSF– population indicated a significant portion of CD62L+ cells, approximately 28% (Figure 2.6C). 2000 cells per fraction were transplanted into lethally irradiated recipients with 100K competitor cells.

Peripheral blood analysis for engraftment activity showed strong engraftment in all lineages by the CD62L– fraction, reconstituting approximately 90% across the lineages (Figure 2.6D~F). In contrast, the CD62L+ fraction showed a persistent but weak engraftment. Platelet engraftment diminished to approximately 10% at the end of the analysis period (Figure 2.6D). RBC engraftment was approximately 20% (Figure 2.6E). WBC engraftment was similar to platelet engraftment at approximately 10% (Figure 2.6F). These results indicate that CD62L+ may contain a small number of HSC. The

few HSC activity observed may also be a product of contamination from the neighboring CD62L– population.

To determine how significant the HSC activity in CD62L+ fraction was, repopulating units (RU) was calculated based on the transplant experiment. The RU calculation is a commonly used method to quantify the frequency of repopulating cells in comparison to a known quantity, often competitor cells of whole bone marrow (Harrison, 1980; Purton and Scadden, 2007). The formula for RU calculation is: donor RU = % donor cells * C/(100 - % donor cells), where C = the number of competing RU (Harrison, 1980). 100K whole bone marrow cells are equivalent to 1 competing RU (Harrison et al., 1993; Yuan et al., 2005). It has been our observation that platelet engraftment was most consistent with the presence of HSC among all the transplant experiments; therefore, the platelet data was applied for the calculation. The actual value of platelet engraftment at the end of analysis period was 7.7% (Figure 2.6D). Hence, the formula is: donor RU = 7.7 * 1 / (100 – 7.7). The calculated donor RU for CD62L+ fraction is 0.083. In comparison, the donor RU for CD62L– fraction is 5.7 (85% donor cells, Figure 2.6D). The ratio of CD62L+ RU to CD62L–RU is 1:68.

This is an overestimation of CD62L+ RU in vivo as CD62L+ cells are not present as frequently as CD62L– cells in the KLSF– fraction. As indicated, CD62L+ cells constitute 28% of KLSF–. Adjusting for the actual cell frequency in vivo, the adjusted CD62L+ RU to CD62L– RU comes to 1:175, meaning that for every HSC present in the CD62L+ fraction, there are 175 HSC in the CD62L– fraction. Therefore, approximately 0.57% of the total HSC in the KLSF– population belong in the CD62L+ fraction, while

the rest >99% of HSC belong in the CD62L– fraction. Therefore, we conclude that the CD62L– fraction of the KLSF– population represents the primary source of HSC.

Discussion

In this report, we have presented in vivo evidence for HSC enrichment using CD62L as a marker. While there are numerous markers for HSC isolation already, the quest for the purest form of HSC continues. Current advances in fluorescence-activated cell sorter technology have emphasized the need for expansion of known surface markers of HSC to obtain live samples. The extent of purity we will achieve will depend on the availability and specificity of various markers.

One of the popular methods of HSC enrichment method is the application of Hoechst 33342. It has been demonstrated that a distinct population of bone marrow cells was capable of efficient Hoechst 33342 efflux (Goodell et al., 1996). This population has been called the side population and has been described as HSC enriched population. A recent study, however, demonstrated that CD34–KLS cells contain similar frequencies of HSC in both the side population and in the non-side population, as determined by Hoechst 33342 (Morita et al., 2009).

Flt3 is a widely accepted tool for the isolation of HSC. The expression profile of Flt3 in conjunction with Thy1.1 resolve the three early hematopoietic compartments, LT-HSC, ST-HSC and MPP that has formed the foundation of our current understanding of early hematopoietic events in adult mice (Morrison et al., 1997; Adolfsson et al., 2001; Christensen and Weissman, 2001). Interestingly, a recent report indicated that ST-HSC as defined by the Flt3 and Thy1.1 expression pattern is not entirely limited in its capacity

for self-renewal (Colvin et al., 2009). In fact, it was reported that ST-HSC engrafted for a year when transplanted, and engrafted for as long as three months in secondary transplants.

Thy1.1, while effective for the isolation of HSC within KLS, is limited in the Thy1.1 expressing strains of mice as mice expressing the more common Thy1.2 allele do not express the marker on most HSC (Spangrude and Brooks, 1992).

These findings emphasize the need for ongoing investigation of current markers as well as exploration for new markers to advance our ability to isolate HSC and understand HSC biology. We have presented in vivo evidence for CD62L as an attractive alternative to Flt3 or a supplemental marker to be used in combination with currently known markers for an improved purification of HSC. Our transplant data demonstrated that CD62L fractionation of KLS yields a CD62L– HSC population and a CD62L+ MPP population (Figure 2.2 and 2.3). This is supported by persistent versus transient engraftment observations described above. We have also observed temporal kinetic differences appropriate for transplant experiments using MPP and HSC, as MPP-derived progenies are expected to arrive sooner than HSC-derived progenies (Figure 2.4A and 2.4B).

Additionally our data support the model that the regulation of expression of stem cell markers changes gradually as hematopoietic development progresses gradually. The fractionation of KLS HSC into Sca-1^{LOW} and Sca-1^{HIGH} fraction has shown that the more immature Sca-1^{HIGH} fraction contained a greater frequency of the CD62L– population compared to the Sca-1^{LOW} fraction (Figure 2.5D and 2.5E, respectively), supporting our

claim that CD62L is a marker of hematopoietic differentiation. In vivo engraftment data also supported this model (Figure 2.5F and 2.5G).

In comparison to Flt3, our data show that CD62L fractionation yielded CD62L– and CD62L+ populations within the Flt3– fraction (Figure 2.6C). The identification of heterogeneity within the Flt3– population suggests three conclusions: (1) Flt3– HSC in KLS is not a homogenous population, (2) MPP-containing CD62L+ fraction within the Flt3– fraction can be eliminated to yield a purer HSC population, and (3) as there are Flt3+CD62L– cells that are most likely to lack HSC, concomitant application of Flt3 and CD62L is highly desirable for HSC purification. Our report did not investigate the in vivo potential of Flt3+CD62L– population of KLS. Such an experiment is warranted to confirm the utility of combinations of Flt3 and CD62L antibodies as a tool for dissection of the HSC and MPP compartments.

Experimental procedures

Mice

Mice carrying the Thy1.1 and Ly5.1 alleles on the C57BL background were generated in our animal facility by mating the BKa.AK-Thy1^{a}/Ka and B6.SJL-Ptprc^{a} Pep3b/BoyJ strains and selecting for cosegregation of Thy1.1 and Ly5.1 (GFP– Thy1.1+Hbb^{S} mice). GFP transgenic mice, generated by microinjection of C57BL/6 oocytees, were kindly provided by Dr. Masaru Okabe (Osaka University, Osaka, Japan) (Nakanishi et al., 2002). In these mice, the GFP transgene is driven by the chicken β-actin promoter and is expressed in all lineages except in the erythroid lineage. Hence, hemoglobin variant alleles (Hbb^{S} and Hbb^{D}) were used to track erythroid engraftment

(see below). In order to generate donor mice for transplant studies, we have crossed the GFP transgenic mice with GFP–Thy1.1+Hbb^S mice to generate GFP+Thy1.1+Hbb^S mice. B6.Cg-Gpi1^a Hbb^D H1^b/DehJ mice (Harrison et al., 1988) were kindly provided by Dr. David Harrison (Jackson Laboratory, Bar Harbor, ME, USA). These mice are GFP–Thy1.1–Hbb^D and were used as transplant recipients. All mice were kept in the animal resources center at the University of Utah under the institutional animal care and use committee approved protocols.

Antibodies

Monoclonal antibodies against CD2 (Rm2.2), CD3 (KT3-1.1), CD5 (53-7.3), CD8 (53-6.7), CD11b (M1/70), Ly-6G (RB6-8C5), TER119, B220 (CD45R; RA3-6B2), and CD19 (1D3) were purified from the media of cultured hybridoma cell lines. PE-conjugated Sca-1 monoclonal antibody was purchased from PharMingen (San Diego, CA, USA). C-kit (3C11) monoclonal antibody was purified and conjugated to Alexa Fluor 647 in our laboratory. CD4 and CD8 monoclonal antibodies were purified and conjugated to allophycocyanin (APC). Biotinylated Flt3, CD62L APC-AF750, Thy1.1 PerCP-Cy5.5, Mac-1 PE and Gr-1 PE antibodies were purchased from eBioscience (San Diego, CA, USA).

Isolation of hematopoietic progenitors and stem cells

In order to remove mature cells from the harvested whole bone marrow cells, lineage depletion was performed. The cells were incubated with a cocktail of rat antibodies to mature cell markers (CD2, CD3, CD5, CD8, CD11b, Ly-6G, TER119,

B220 and CD19). Secondary labeling of mature cells was performed by two successive incubations with magnetic beads-coupled sheep anti-rat antibodies (Dynal, Oslo, Norway). Each incubation was followed by a depletion step of the labeled cells using a magnetic column (Dynal, Oslo, Norway). The depleted cells were stained with various fluorochrome-conjugated antibodies as indicated in the figures to electronically visualize and sort using FACS Aria instrument (BD Immunocytometry Systems, San Jose, CA, USA). DAPI was used to discriminate dead cells from live cells.

Bone marrow transplantation

The GFP–Thy1.1–Hbb^{D} recipient mice were lethally irradiated a day prior to the transplant day (^{137}Cs, 13 Gy delivered in a 3 hour-split dose). Isolated GFP+Thy1.1+Hbb^{S} donor cells were injected into the recipients retro-orbitally. The recipient mice were anesthetized with isoflurane using the E-Z Anesthesia system for the injection (Euthanex Corp., Palmer, PA).

Peripheral blood analysis

For the posttransplant analysis, peripheral blood samples were collected from the retro-orbital sinus with heparinized capillary tubes. The mice were anesthetized with isoflurane using the E-Z Anesthesia system (Euthanex Corp., Palmer, PA). Immediately after the collection of blood samples, 10 ul of blood per sample were set aside for platelet analysis. The rest of the samples were mixed with 500ul of 2% Dextran T500 (Amersham Biosciences, Piscataway, NJ) in PBS and incubated at 37 degree C for 30 min for sediment separation of the RBC and WBC fractions. The RBC fraction was

processed for HPLC analysis (see below). WBC were stained with PE-conjugated antibodies against Mac-1 and Gr-1 for myeloid WBC detection, Biotinylated B220 or CD19 antibody with a subsequent labeling with Alexa Fluor 750-conjugated avidin for B cell detection, and CD4 and CD8 conjugated with APC for T cell detection. Platelets and WBC were analyzed by FACScan flow cytometer (BD Biosciences, San Jose, CA; modified by Cytek Development, Fremont, CA). Platelet analysis was performed by increasing forward and side scatter parameters until the platelet population could be gated to exclude contaminants.

HPLC analysis of hemoglobin variants

A HPLC cation exchange protocol was developed in our laboratory to discriminate and quantify Hbb^D and Hbb^S in the peripheral blood samples (Spangrude et al., 2006). A stock solution of 100 mM 5,5'-dithiobis-(2-nitrobenzoic acid) (DTNB) (Sigma-Aldrich, St. Louis, MO) was prepared by dissolving 100 mg of DTNB in 2.5 ml of DMSO and stored at –20 degree C. The RBC fraction was derivatized by adding 5 ul of the RBC fraction into 250ul of 40 mM NaCl and 2 mM DTNB and incubating at room temperature for 30 minutes. Following centrifugation at 12,000 g for 2 minutes, the supernatant were analyzed using a VARIANT hemoglobin testing system (Bio-Rad Laboratories, Hercules, CA) with an optimized β–thalassemia short program.

In vitro erythroid potential assay

To assay clonal erythroid potential, 200 cells per sorted population were plated on 35 mm culture dish in alpha-modified Eagle's medium-based methylcellulose containing

10% fetal calf serum, 10% deionized bovine serum albumen, antibiotics, l-glutamine, and 2-mercaptoethanol. Erythroid development was promoted by supplementing the cultures with stem cell factor (SCF, 100 ng/ml), interleukin-3 (IL-3, 10 ng/ml), and erythropoietin (EPO, 4 U/ml). Periodically, a subset of cultures was stained using benzidine hydrochloride and the erythroid colonies scored.

References

Adolfsson, J., Borge, O.J., Bryder, D., Theilgaard-Monch, K., Astrand-Grundstrom, I., Sitnicka, E., Sasaki, Y., and Jacobsen, S.E. (2001). Upregulation of Flt3 expression within the bone marrow Lin(–)Sca1(+)c-kit(+) stem cell compartment is accompanied by loss of self-renewal capacity. Immunity *15*, 659-669.

Adolfsson, J., Mansson, R., Buza-Vidas, N., Hultquist, A., Liuba, K., Jensen, C.T., Bryder, D., Yang, L., Borge, O.J., Thoren, L.A., Anderson, K., Sitnicka, E., Sasaki, Y., Sigvardsson, M., and Jacobsen, S.E. (2005). Identification of Flt3+ lympho-myeloid stem cells lacking erythro-megakaryocytic potential: a new road map for blood lineage commitment. Cell *121*, 295-306.

Akashi, K., Traver, D., Zon, L.I. (2005). The complex cartography of stem cell commitment. Cell *121*, 160-162.

Besmer, P. (1991) The kit ligand encoded at the murine Steel locus: a pleiotropic growth and differentiation factor. Curr Opin Cell Biol *3*:939-946.

Christensen, J.L., and Weissman, I.L. (2001). Flk2 is a marker in hematopoietic stem cell differentiation: a simple method to isolate long-term stem cells. Proc. Natl. Acad. Sci. USA *98*, 14541-14546.

Colvin, G.A., Berz, D., Quesenberry, P.J., Papa, E., and Liu, L. (2009). ST-HSC have full long-term capacity with sustained but reduced potential compared with LT-HSC. 51ST ASH Annual Meeting and Exposition, Abstract 2550.

Forsberg, E.C., Serwold, T., Kogan, S., Weissman, I.L., and Passegue, E. (2006). New evidence supporting megakaryocyte-erythrocyte potential of Flk2/Flt3+ multipotent hematopoietic progenitors. Cell *126*, 415-426.

Goodell, M.A., Brose, K., Paradis, G., Conner, A.S., Mulligan, R.C. (1996). Isolation and functional properties of murine hematopoietic stem cells that are replicating in vivo. J. Exp. Med. *183*, 1797-1806.

Harrison, D.E. (1980). Competitive repopulation: a new assay for long-term stem cell functional capacity. Blood *55*, 77-81.

Harrison, D.E., Astle, C.M., Lerner, C. (1988) Number and continuous proliferative pattern of transplanted primitive immunohematopoietic stem cells. Proc. Natl. Acad. Sci. USA. *85*, 822-826.

Harrison, D.E., Jordan, C.T., Zhong, R.K., and Astle, C.M. (1993). Primitive hemopoietic stem cells: direct assay of most productive populations by competitive repopulation with simple binomial, correlation and covariance calculations. Exp. Hematol. *21*, 206-219.

Ikuta, K., and Weissman, I.L. (1992). Evidence that hematopoietic stem cells express mouse c-kit but do not depend on steel factor for their generation. Proc. Natl. Acad. Sci. USA *89*, 1502-1506.

Kiel, M.J., Yilmaz, O.H., Iwashita, T., Yilmaz, O.H., Terhorst, C., and Morrison, s.J. (2005). SLAM family receptors distinguish hematopoietic stem and progenitor cells and reveal endothelial niches for stem cells. Cell *121*, 1109-1121.

Lai, A.Y., and Kondo, M. (2006). Asymmetrical lymphoid and myeloid lineage commitment in multipotent hematopoietic progenitors. J. Exp. Med. *203*, 1867-1873.

Lai, A.Y., Simon, M.L., Kondo, M. (2005). Heterogeneity of Flt3-expressing multipotent progenitors in mouse bone marrow. J. Immunol. *175*, 5016-5023.

Morita, Y., Ema, H., Yamazaki, S., and Nakuachi, H. (2009). Non-side population hematopoietic stem cell sin mouse bone marrow. Stem Cells in Hematology *108*, 2850-2856.

Morrison, S.J., and Weissman, I.L. (1994). The long-term repopulating subset of hematopoietic stem cells is deterministic and isolatable by phenotype. Immunity *1*, 661-673.

Morrison, S.J., Wandycz, A.M., Hemmatic, H.D., Wright, D.E., and Weissman, I.L. (1997). Identification of a lineage of multipotent hematopoietic progenitors. Development *124*, 1929-1939.

Nakanishi, T., Kuroiwa, A., Yamada, S., Isotani, A., Yamashita, A., Tairaka, A., Hayashi, T., Takagi, T., Ikawa, M., Matsuda, Y., and Okabe, M. (2002). FISH analysis of 142 EGFP transgene integration sites into the mouse genome. Genomics *80*, 564-574.

Osawa, M., Hanada, K., Hamada, H., and Nakauchi, H. (1996). Long-term lymphohematopoietic reconstitution by a single CD34-low/negative hematopoietic stem cell. Science *273*, 242-245.

Perry, S.S., Wang, H., Pierce, L.J., Yang, A.M., Tsai, S., and Spangrude, G.J. (2004). L-selectin defines a bone marrow analog to the thymic early T-lineage progenitor. Blood *103*, 2990-2996.

Purton, L.E., and Scadden, D.T. (2007). Limiting factors in murine hematopoietic stem cell assays. Cell Stem Cell *1*, 263-270.

Rawls, J.F., Mellgren, E.M., and Johnson, S.L. (2001) How the zebrafish gets its stripes. Developmental Biology *240*, 301-314.

Spangrude, G.J., and Brooks, D.M. (1992). Phenotypic analysis of mouse hematopoietic stem cells show a Thy-1-negative subset. Blood *80*, 1957-1964.

Spangrude, G.J., Cho, S., Guedelhoefer, O., VanWoerkom, R.C., and Fleming, W.H. (2006). Mouse models of hematopoietic engraftment: limitations of transgenic green fluorescent protein strains and a high-performance liquid chromatography approach to analysis of erythroid chimerism. Stem Cells *24*, 2045-2051.

Spangrude, G.J., Heimfeld, S., and Weissman, I.L. (1988). Purification and characterization of mouse hematopoietic stem cells. Science *241*, 58-62.

Weissman, I.L. (2000). Stem cells: units of development, units of regeneration, and units in evolution. Cell *100*, 157-168.

Yang, L., Bryder, D., Adolfsson, J., Nygren, J., Mansson, R., Sigvardsson, M., and Jacobsen, S.E. (2005). Identification of Lin(-)Sca1(+)-kit(+)CD34(+)Flt3-short-term hematopoietic stem cells capable of rapidly reconstituting and rescuing myeloablated transplant recipients. Blood *105*, 2717-2723.

Yuan, R., Astle, C.M., Chen, J., and Harrison, D.E. (2005). Genetic regulation of hematopoietic stem cell exhaustion during development and growth. Exp. Hematol. *33*, 243-250.

Figure 2.1 CD62L expression pattern in early hematopoietic progenitors. Panel A Flow cytometric analysis of the hematopoietic stem cell compartment (KLS) is shown. The KLS cells were labeled with antibodies against CD62L and Thy1.1. The percentages indicate the amount of cells per quadrant. **Panel B** The KLS cells were labeled with antibodies against Flt3 and Thy1.1. The percentages indicate the amount of cells per quadrant. The labels indicate the progenitor identities as previously defined. **Panel C** Fluorescence-activated cell sorting was used to isolate pure cells from each quadrant of panel A for an in vitro experiment. Two-hundred cells per methylcellulose dish were grown with cytokines for erythroid development: SCF, IL-3 and EPO. Periodically a subset of plates was analyzed with benzidine staining for erythroid colonies. The values indicate the percentage of erythroid colonies per plate observed at each time point. The quadrant labels in the legend indicate T+L+ for Thy1.1+CD62L+, T+L– for Thy1.1+CD62L–, T–L+ for Thy1.1–CD62L+ and T–L– for Thy1.1–CD62L–. Error bars indicate SEM.

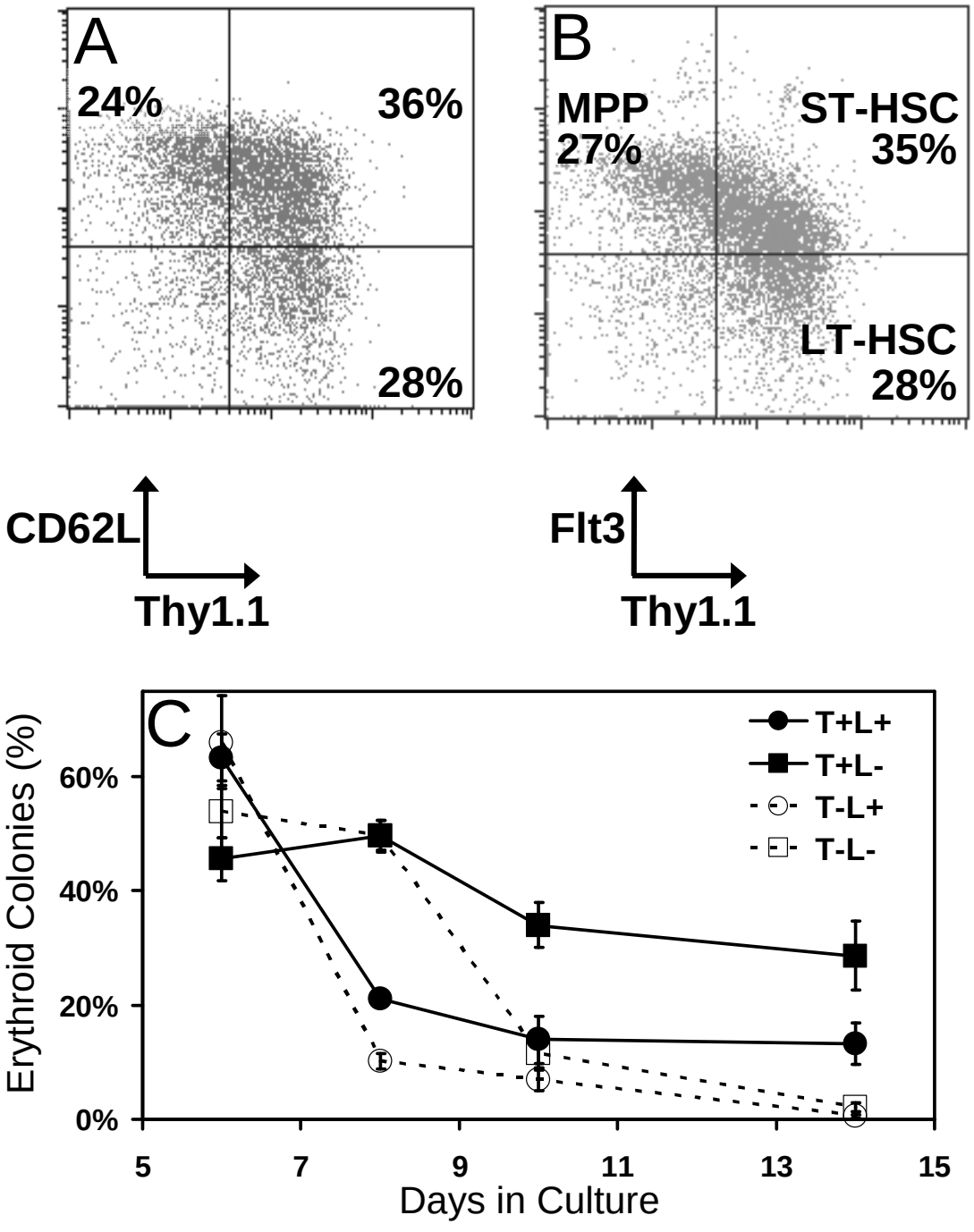
A
24%
36%
28%
CD62L
Thy1.1
B
MPP
27%
ST-HSC
35%
LT-HSC
28%
Flt3
Thy1.1
C
T+L+
T+L-
T-L+
T-L-
Erythroid Colonies (%)
60%
40%
20%
0%
5
7
9
11
13
15
Days in Culture

Figure 2.2 In vivo evidence for HSC in the CD62L– population of KLS. Panel A Mature cell-depleted whole bone marrow was labeled with antibodies against C-kit and Sca-1 to visualize KLS via flow cytometry for sorting. **Panel B** A histogram of CD62L expression within the KLS population as gated in panel A. The percentages indicate the frequency of KLS cells belonging to the CD62L– and CD62L+ fractions. The two fractions were sorted for transplant. For each fraction, 1000 cells were injected into five lethally irradiated recipients with 100K whole bone marrow cells of the recipient type as competitors. The donor-derived cells in peripheral blood were tracked via GFP expression for platelets and white blood cells (WBC) through flow cytometry. Red blood cells were tracked through the hemoglobin variant Hbb^S using HPLC. **Panel C** Platelet output from the injected fractions are shown. CD62L+ cells produced a transient, small but detectable amount of platelets early during the posttransplant analysis period. **Panel D and E** RBC and WBC productions are shown as indicated. CD62L+ cells produced a transient output of RBC as platelets, albeit stronger. WBC production decreased over time but persisted until the end of the analysis period. The CD62L– fraction produced persistent progenies in all lineages as shown in panel C~E. Error bars indicate SEM for panel C~E.

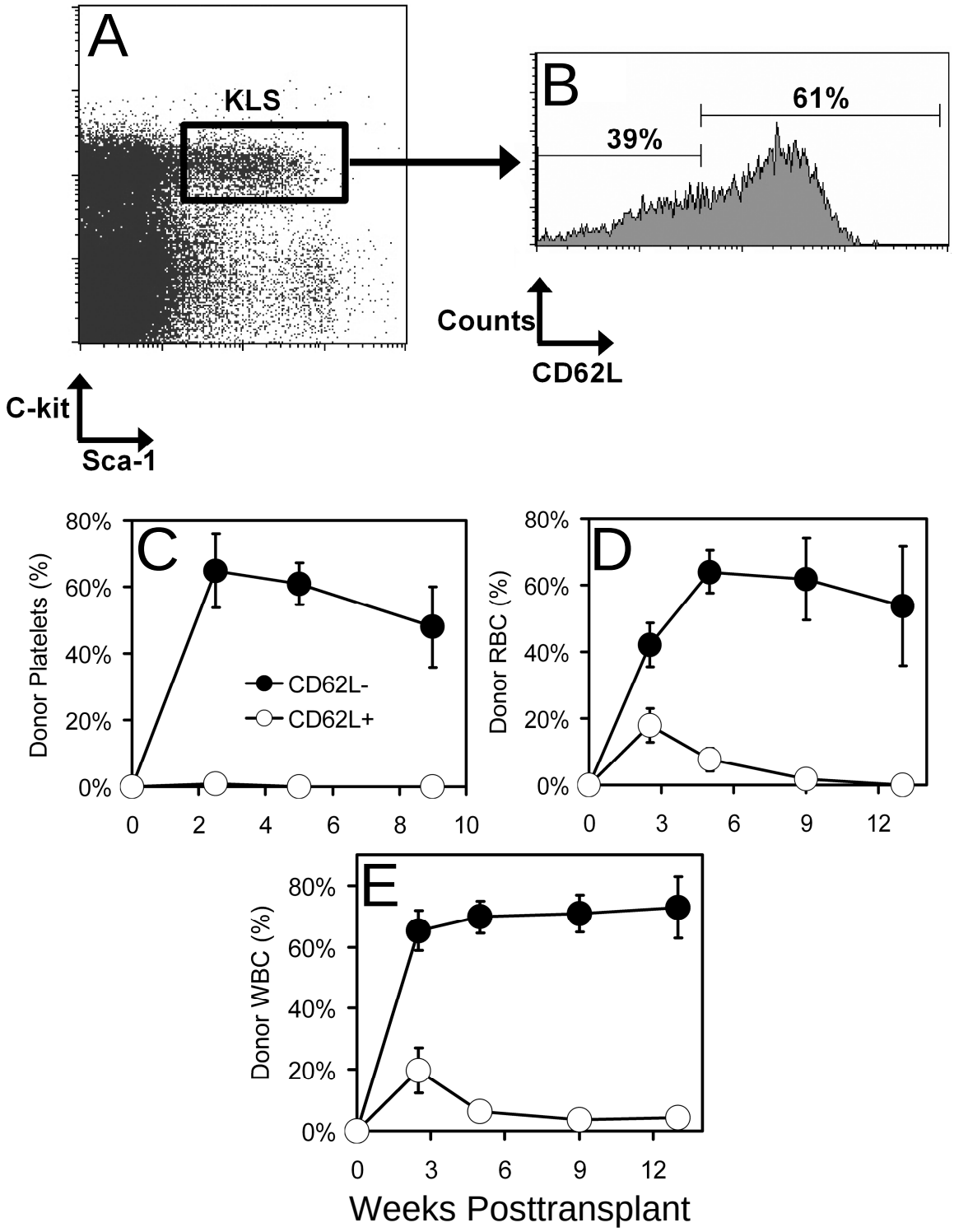
A
KLS
C-kit
Sca-1
B
39%
61%
Counts
CD62L
C
Donor Platelets (%)
80%
60%
40%
20%
0%
0
2
4
6
8
10
CD62L-
CD62L+
D
Donor RBC (%)
0
3
6
9
12
E
Donor WBC (%)
Weeks Posttransplant

Figure 2.3 Confirmation of CD62L– HSC engraftment. Following the last peripheral blood analysis at week 13 of posttransplantation, the transplant recipients shown in Figure 2.1 were sacrificed and their bone marrow cells analyzed for the presence of donor-derived cells in the KLS population. **Panel A** Whole bone marrow flow cytometric analysis of transplant recipients that received the CD62L+ donor fraction. **Panel B** Early hematopoietic stem and progenitor cells of the KLS population as gated in panel A. Only a trace amount of GFP+ donor-derived cells was detected. The percentages indicate the frequency of GFP– competitor-derived cells and GFP+ CD62L+ donor-derived cells. **Panel C** Whole bone marrow analysis of mice that received the CD62L– fraction. **Panel D** Early hematopoietic stem and progenitor cells of the KLS population as gated in panel C. A significant portion of KLS were donor-derived GFP+ cells. The percentages indicate the average percentages found across all recipients of CD62L– fraction. **Panel E** GFP+ KLS cells of CD62L– fraction-transplant recipients were sorted and transplanted into lethally irradiated secondary recipients. The trace amounts of GFP+ KLS cells of CD62L+ fraction-transplant recipients were pooled together and transplanted into one lethally irradiated secondary recipient. Five weeks posttransplant, the peripheral blood analysis was performed. The average amounts of donor-derived cells are shown. "UD" indicates undetectable.

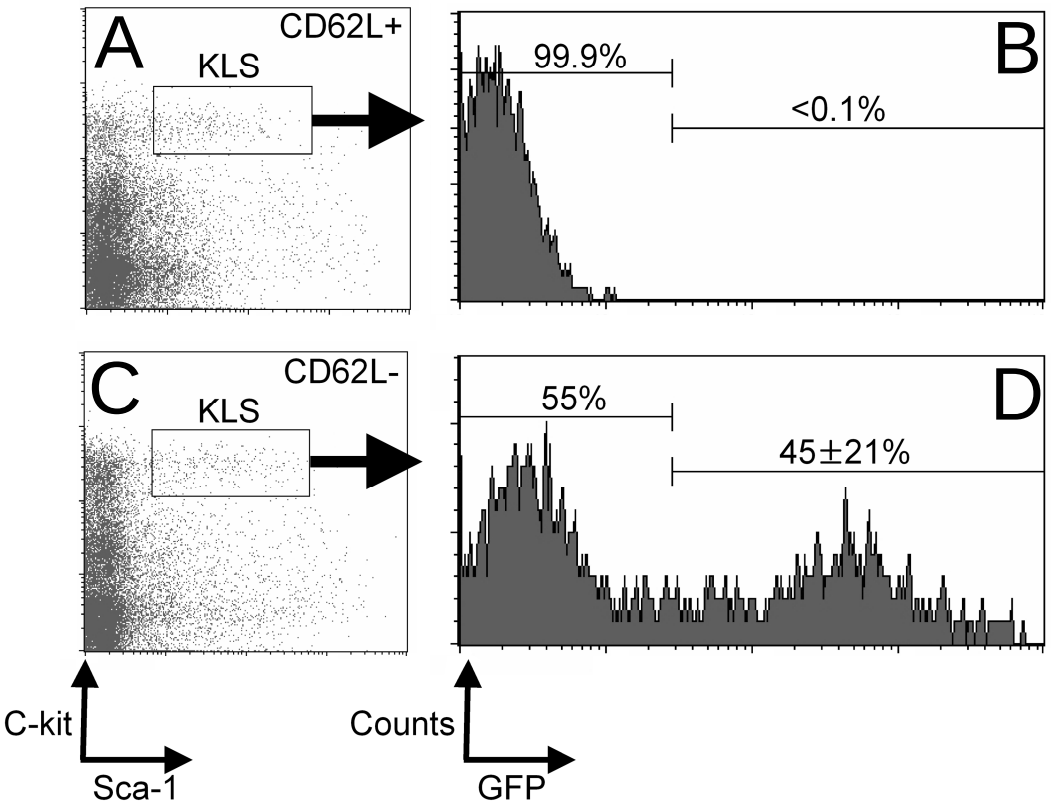
A
CD62L+
KLS
B
99.9%
<0.1%
C
CD62L-
KLS
D
55%
45±21%
C-kit
Sca-1
Counts
GFP

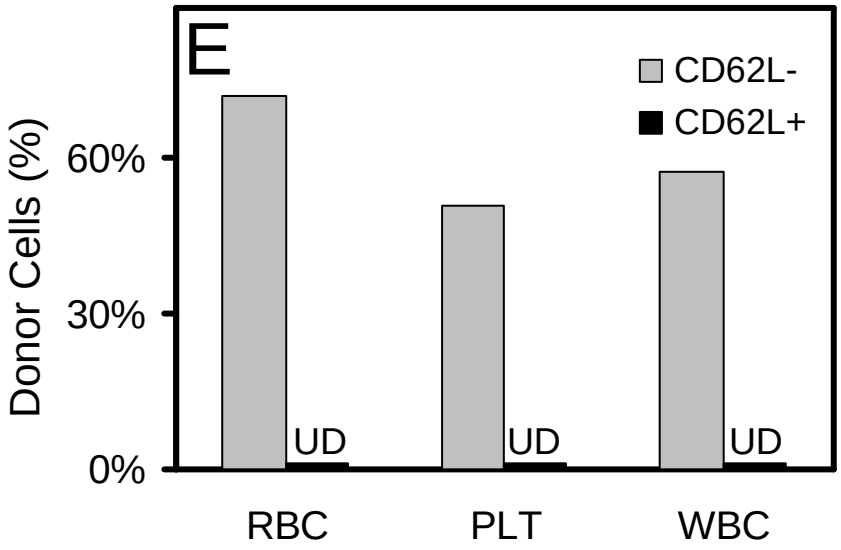
E
CD62L-
CD62L+
Donor Cells (%)
60%
30%
0%
UD
UD
UD
RBC
PLT
WBC

Figure 2.4 In vivo evidence for enrichment of HSC in CD62L– fraction and MPP in CD62L+ fraction of KLS. To further substantiate the CD62L-mediated fractionation of HSC and MPP, two bone marrow transplants were conducted. The first transplant experiment consisted of transplanting 100 cells per CD62L– fraction and 10K cells per CD62L+ fraction with 100K competitor cells as performed previously. Five lethally irradiated recipients per fraction were used. **Panel A** Engraftment was detected via RBC analysis. Both fractions showed strong engraftment early. By the end of analysis at week 16, the CD62L+ fraction failed to maintain RBC production. **Panel B** WBC analysis is shown. Similar results as RBC were observed, however, the CD62L+ fraction maintained a measurable amount of WBC output. The second experiment consisted of transplanting 500 cells per fraction into four lethally irradiated mice per fraction without any competitors to test for each fraction's capability for hematopoietic rescue. **Panel C** All mice from both fractions were successfully rescued from lethal irradiation. RBC analysis showed a similar engraftment pattern seen in panel A. **Panel D** WBC analysis showed a persistent but severely reduced engraftment by the CD62L+ fraction. The CD62L– fraction had nearly completely reconstituted the hematopoietic system of recipient mice (panel C and D). Error bars indicate SEM (all panels).

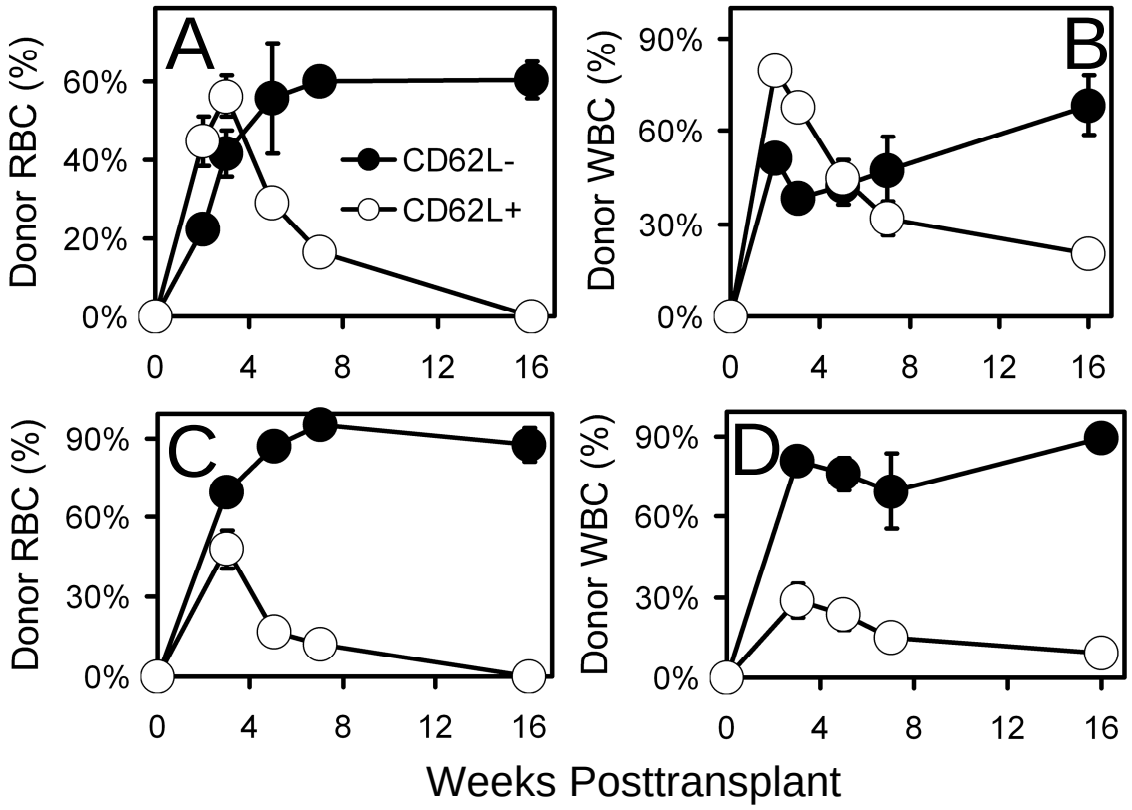
A
B
C
D
Donor RBC (%)
Donor WBC (%)
CD62L-
CD62L+
0%
20%
30%
40%
60%
90%
0
4
8
12
16
Weeks Posttransplant

Figure 2.5 Presence of HSC activity in both Sca-1^{HIGH}and Sca-1^{LOW} fractions of KLS. Panel A In order to determine whether HSC enrichment via CD62L is isolated to immature cells expressing high levels of Sca-1, KLS were subfractionated into Sca-1^{HIGH} and Sca-1^{LOW} as indicated. **Panel B** Flt3 and Thy1.1 expression pattern of KLS was analyzed to gate for Flt3–Thy1.1+ HSC population for Sca-1^{HIGH} fraction. **Panel C** As in panel B, Flt3–Thy1.1+ HSC population is gated for Sca-1^{LOW} fraction. **Panel D** CD62L expression profile of HSC gated in panel B is shown. The percentages indicate the frequencies of CD62L+ and CD62L– cells. CD62L– cells are labeled as S^{HIGH} (Sca-1^{HIGH}HSC population). 1000 S^{HIGH} cells were sorted and transplanted into five lethally irradiated mice with 100K competitors. **Panel E** As in panel D, S^{LOW} (Sca-1^{LOW}HSC population) is indicated for a similar transplant experiment. **Panel F** RBC engraftment data of S^{HIGH} and S^{LOW} transplanted mice are shown. Both groups exhibited persistent RBC engraftment. **Panel G** As in panel E, persistent WBC engraftments from S^{HIGH} and S^{LOW} recipients were observed. In contrast to RBC data, WBC activity by S^{LOW} was significantly lower. Error bars indicate SEM (panel F and G).

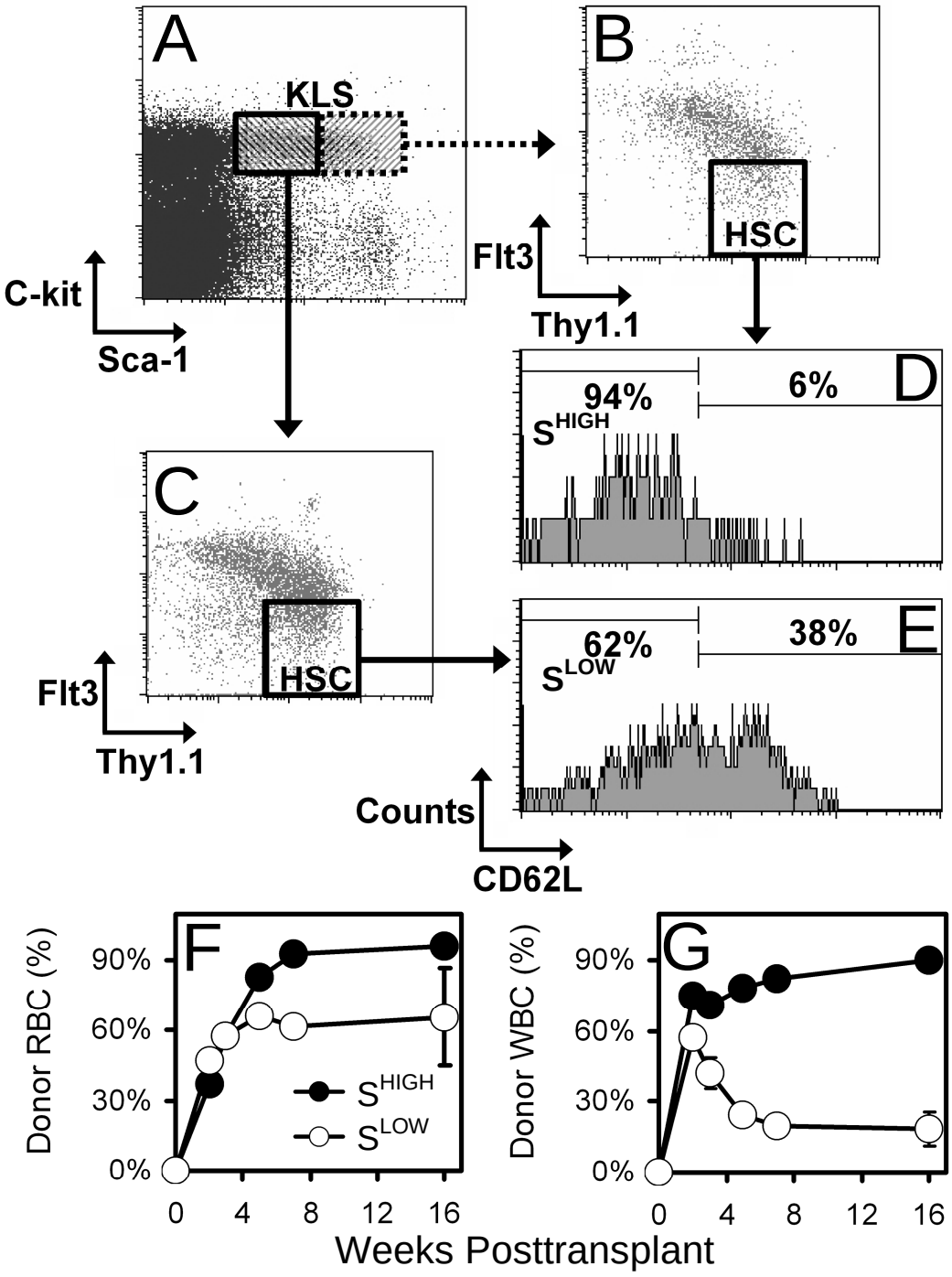
A
KLS
C-kit
Sca-1
B
HSC
Flt3
Thy1.1
C
HSC
Flt3
Thy1.1
D
94%
6%
S^HIGH
E
62%
38%
S^LOW
Counts
CD62L
F
90%
60%
30%
0%
Donor RBC (%)
S^HIGH
S^LOW
0
4
8
12
16
G
90%
60%
30%
0%
Donor WBC (%)
0
4
8
12
16
Weeks Posttransplant

Figure 2.6 HSC activity is primarily enriched in the CD62L–Flt3–Thy1.1+ KLS fraction. Panel A A representative flow cytometric analysis of mature cell-depleted bone marrow is shown with KLS gating. **Panel B** A representative Flt3 Thy1.1 profile of KLS is shown with HSC population gated. **Panel C** CD62L expression of Flt3– population is shown. The percentages indicate the amounts of CD62L– and CD62L+ cells within the Flt3– compartment. The CD62L– and CD62L+ fractions (KLSF–CD62L– and KLSF–CD62L+) as indicated were sorted, and 2000 cells per fraction were transplanted into five lethally irradiated mice with 100K competitor cells. **Panel D** Platelet engraftment by the two fractions are shown. The KLSF–CD62L+ population showed a weak but persistent platelet production. **Panel E** Similarly to platelets, the KLSF–CD62L+ population showed a weak but persistent RBC production. **Panel F** WBC production also showed a weak but persistent output for the KLSF–CD62L+ fraction received cells. The KLSF–CD62L– fraction almost completely reconstituted the recipients' hematopoietic system (panel D~F). Error bars indicate SEM (panel D~F).

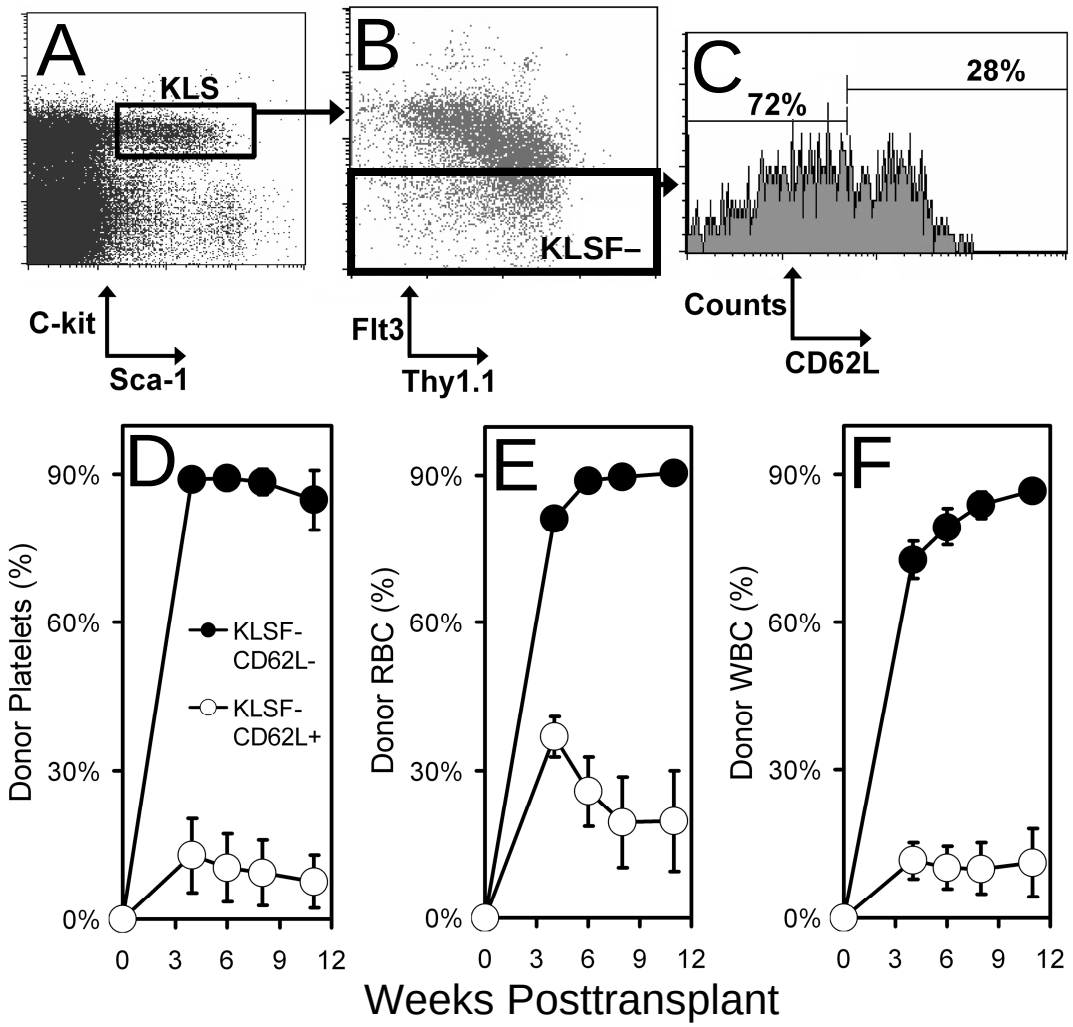
A
KLS
C-kit
Sca-1
B
KLSF–
Flt3
Thy1.1
C
72%
28%
Counts
CD62L
D
E
F
90%
60%
30%
0%
Donor Platelets (%)
Donor RBC (%)
Donor WBC (%)
KLSF-
CD62L-
KLSF-
CD62L+
0 3 6 9 12
Weeks Posttransplant

CHAPTER 3

IN VIVO EVIDENCE FOR HETEROGENIETY AMONG MULTIPOTENT PROGENITORS OF THE HEMATOPOIETIC STEM CELL COMPARTMENT

Abstract

A traditionally described hematopoietic multipotent progenitor is a non-self renewing progenitor that is capable of generating cells of all hematopoietic lineages. This progenitor has been labeled as the most mature population of the hematopoietic stem cell compartment prior to the segregation of lymphoid and myeloid lineages. In this report, we test the hypothesis that the multipotent progenitor population is a heterogeneous population and that CD62L, an adhesion molecule, is a marker of early hematopoietic differentiation that can subfractionate the multipotent progenitor population into functionally distinct subpopulations. We present evidence demonstrating that the multipotent progenitor population contains phenotypically distinct subpopulations according to expression levels of CD62L and Sca-1. In vivo transplant data demonstrate that the multipotent progenitor subpopulations experience significant reduction in erythro-megakaryocyte potential as they upregulate CD62L and downregulate Sca-1. Furthermore, the data show that as multipotent progenitors upregulate CD62L, a greater fraction of their progenies become T cell biased, while maintaining a significant B cell output.

Introduction

In an adult mouse, hematopoiesis originates from a subset of immature cells in the bone marrow. This subset, which includes hematopoietic stem cells (HSC) and multipotent progenitors (MPP), is identified by a shared expression pattern of surface markers: (1) they lack a set of mature hematopoietic cell surface proteins (designated collectively as lineage or Lin), and (2) they express high levels of hematopoietic stem

cell-associated markers c-Kit and Sca-1 (Spangrude et al., 1988; Ikuta and Weissman, 1992). Accordingly, this subset of immature cells is conveniently labeled as the hematopoietic stem cell compartment or KLS for c-Kit+, Lin– and Sca-1+.

The hematopoietic stem cell compartment is further fractionated into three functionally distinct subpopulations based on the expression levels of surface molecules, Thy1.1 and Flt3: Thy1.1+ Flt3– long-term HSC (LT-HSC), Thy1.1+ Flt3+ short-term HSC (ST-HSC), and Thy1.1– Flt3+ MPP (Spangrude et al., 1988; Morrison et al., 1997; Adolfsson et al., 2001; Christensen and Weissman, 2001). Currently, it is widely accepted that only the most primitive LT-HSC maintains the capacity to self-renew for the life of the animal and gives rise to ST-HSC, a more mature population of progenitors with limited capacity for self-renewal. The most mature population of KLS, the MPP, which lacks the capacity to self-renew but still maintains multipotency, is generated last (Spangrude et al., 1988; Morrison et al., 1997; Adolfsson et al., 2001; Christensen and Weissman, 2001).

The three population model of KLS is useful for the purpose of describing the events of early hematopoiesis; however, it is over simplified. As KLS is being studied with increasing scrutiny to delineate the early progression of hematopoiesis, further evidence has emerged that demonstrate the complex heterogeneity within the subpopulations. The traditional description of lineage specification occurs outside KLS with the bifurcation of lymphoid and myeloid lineages through the establishment of common lymphoid progenitors (CLP) (Kondo et al., 1997) and common myeloid progenitors (CMP) (Akashi et al., 2000) in the bone marrow. Emerging data, however,

strongly suggest the loss of and/or bias toward specific hematopoietic lineages occurring within the MPP of KLS, prior to the stages of CLP and CMP.

One example is a study describing the existence of lymphoid-primed multipotent progenitors (LMPP) (Adolfsson et al., 2005). The study identifies LMPP in the hematopoietic stem cell compartment as the population of cells that expresses the highest level of Flt3, constituting a significant fraction of MPP (approximately the top 25% of KLS cells for Flt3 expression). Unlike the MPP cells, which have significant output in all hematopoietic lineages, the LMPP cells generated insignificant numbers of platelets and red blood cells, suggesting the loss of erythro-megakaryocytic lineage (Meg/E) potential prior to cells exiting the hematopoietic stem cell compartment and demonstrating the existence of partially multipotent progenitors within the pool of true multipotent progenitors. A subsequent study by another group showed that while LMPP cells do have a detectable amount of Meg/E activity, it is significantly less than that of MPP, thereby contrasting the previous report's claim of loss of Meg/E activity, while confirming the existence of heterogeneity within the MPP population (Forsberg et al., 2006).

The MPP population has also been subfractionated using the vascular cell adhesion molecule-1 (VCAM-1). In these studies, the MPP population is divided into VCAM-1+ and VCAM-1– populations. Their results show that VCAM-1+ MPP generated cells of all lineages like the traditional MPP cells, however, VCAM-1– MPP failed to generate Meg/E potentially as robustly as the MPP cells or the VCAM-1+ MPP, similar to the above-mentioned LMPP (Lai et al., 2005; Lai and Kondo, 2006).

It should be noted that the investigators also observed that VCAM-1– MPP cells express high levels of Flt3, while VCAM-1+ MPP cells express both low and high levels of Flt3 (Lai and Kondo, 2006). This finding is consistent with the concept of LMPP that within the traditionally described Flt3+ MPP, heterogeneity of multipotency exists based on the actual expression level of Flt3 as demonstrated with the loss of Meg/E potential (Adolfsson et al., 2005). Furthermore, these observations suggest that there are other markers, such as VCAM-1, that may be useful in identifying functionally distinct subpopulations within the MPP (Akashi et al., 2005; Lai and Kondo, 2006)

Our laboratory has previously demonstrated that the Thy1.1– portion of KLS (KLST–) can be divided using CD62L, also known as the cell adhesion molecule CD62L, to produce functionally distinct subpopulations. When so divided, CD62L– KLST– cells behaved as a traditional MPP, generating T cells, B cells, and white blood cells of myeloid lineage (monocytes and granulocytes), while CD62L+ KLST– resembled an early T-lineage progenitor with wavelike thymic seeding kinetics and transient B cell generation and little myeloid potential (Perry et al., 2004). Therefore, CD62L is an effective marker for studying lineage commitment and heterogeneity within early hematopoietic progenitors.

In the following experiments, we expand upon our previous research using CD62L and Sca-1. We have hypothesized that CD62L is a marker of early hematopoietic development and that CD62L can be used to isolate distinct subpopulations within the traditional MPP. To test our hypothesis, the Thy1.1– Flt3+ MPP of the hematopoietic stem cell compartment was subfractionated into CD62L+ and CD62L– fractions. These subpopulations were then further divided according to low and high expression levels of

Sca-1 (Sca-1^{LO} and Sca-1^{HI}). In accordance with our hypothesis, we predicted that the CD62L–Sca-1^{HI} population would be the most primitive progenitor population and that the CD62L+Sca-1^{LO} population would be the most mature progenitor population within the MPP compartment.

Using a novel HPLC protocol for hemoglobin analysis developed in our laboratory and GFP-expressing mice as progenitor donors for transplant, we present in vivo evidence for heterogeneity within the traditional Thy1.1– Flt3+ MPP population. The data presented here demonstrate that each of the subpopulations defined by CD62L represents a functionally distinct hematopoietic progenitor population that signifies a transition stage during early hematopoietic development.

Results

Phenotypically distinct subpopulations suggest heterogeneity within the MPP population

In order to test our hypothesis that CD62L-based subfractionation can demonstrate heterogeneity within the MPP population, we analyzed the hematopoietic stem cell compartment using flow cytometry. Cells of the hematopoietic stem cell compartment, denoted as KLS, was identified as lineage-depleted bone marrow cells gated for c-Kit^{High} and Sca-1+, and were labeled with Flt3 and Thy1.1 antibodies to display the traditional division of KLS into LT-HSC, ST-HSC and MPP (Figure 3.1A). Combined labeling of Flt3 and CD62L revealed a high degree of co-expression, since 26% of cells expressed neither marker and 49% of cells expressed both markers (Figure 3.1B). This high degree of co-expression pattern is particularly interesting considering the previous evidence which demonstrated that variable expression levels of Flt3

correlated with variable capacity for multipotency among Flt3+ MPP (Forsberg et al., 2006; Lai and Kondo, 2006). Also, the presence of cells that are mutually exclusive for the expression of CD62L and Flt3 suggested potential functionally distinct populations that would not be identifiable without the use of CD62L as a marker.

To proceed with the isolation of subpopulations, the Thy1.1– fraction from the KLS were gated to subdivide them into Flt3+ CD62L+ and Flt3+ CD62L- populations (CD62L+ MPP and CD62L– MPP, respectively) (Figure 3.1A and 3.1C). While the majority of these cells were CD62L+ MPP, a significant fraction of cells were detected as CD62L– MPP (approximately 5:1 CD62L+ MPP to CD62L– MPP). Finally the two MPP populations were subfractionated into Sca-1^{LO} and Sca-1^{HI} populations as outlined in Figure 3.1D. These four subpopulations were not flow cytometry artifacts, as after they were sorted, they were reanalyzed to confirm their identity (data not shown).

The receptor for interleukin 7, frequently detected using an antibody raised against its α-chain (IL7Rα), has been reported to be upregulated in more mature lymphoid progenitors (CLP), and has been described as a marker of lymphoid development (Kondo et al., 1997). We were, however, able to detect minute numbers of IL7Rα+ cells within the various subpopulations of KLS. Not surprisingly, the lowest number of IL7Rα+ cells was detected in the least mature LT-HSC population, while the more mature MPP population contained a greater number of IL7Rα+ cells (Figure 3.2). In agreement with our hypothesis that CD62L expression is a marker of hematopoietic development, the CD62L+ cells had the greater number of IL7Rα+ cells than the CD62L– cells (Figure 3.2) when the MPP were subfractionated into CD62L+ and

CD62L– fractions as identified in Figure 3.1C. The IL7Rα data, along with Flt3-CD62L co-expression data, imply the capacity of CD62L to identify distinct MPP subpopulations.

CD62L and Sca-1 subfractionated populations show distinct Meg/E potential in vivo

In order to assess the hematopoietic potential of the four subfractionated MPP populations in vivo (CD62L– Sca-1^{HI}, CD62L– Sca-1^{LO}, CD62L+ Sca-1^{HI}, CD62L+ Sca-1^{LO}), the target populations were isolated via fluorescence-activated cell sorter from GFP+Hbb^{S} donor mice. For each population, 3000 cells were sorted and transplanted via retro-orbital injection into lethally irradiated GFP–Hbb^{D} mice. The donor cells were injected, along with 250k whole bone marrow cells from GFP–Hbb^{D} mice as competitors to comparatively quantify the amounts of engraftment among donor populations. Peripheral blood samples of the transplant recipients were periodically analyzed to identify and quantify progenies of specific lineages. To assess Meg/E potential, megakaryocyte production was identified by the presence of GFP+ donor platelets detected via flow cytometry, and the erythroid potential was identified by the presence of the donor hemoglobin variant Hbb^{S} via HPLC. To assess myeloid potential, GFP+ monocytes and granulocytes were detected via flow cytometry.

Over the course of 9 weeks, the transplanted populations displayed varying amounts Meg/E potential. CD62L–Sca-1^{HI} cells, suspected to include the least mature progenitor population among the four, generated a large spike of platelets detected at week two, while the other three populations generated trace amounts of donor platelets early on (Figure 3.3A). As expected, all four progenitor populations generated platelets only temporarily, dropping to undetectable amounts by week six. The largest amount of

donor-derived RBC was also detected from CD62L–Sca-1^{HI} recipients (Figure 3.3B). The CD62L+Sca-1^{LO} population, suspected to include the most mature progenitors, generated the lowest amount of RBC among the four progenitors. CD62L–Sca-1^{LO} and CD62L+Sca-1^{HI} cells generated moderate amounts of RBC compared to the other two populations, suggesting that they represent transitional populations between the less mature CD62L–Sca-1^{HI} and the more mature CD62L+Sca-1^{LO} populations. The dramatic reduction of Meg/E potential observed as progenitors shifted from CD62L–Sca-1^{HI} to CD62L+Sca-1^{LO} is consistent with the idea that upregulation of this developmental marker is accompanied by loss of capacity for progeny production. This observation parallels other studies that also showed the reduction of Meg/E potential with the changing expression of other developmental antigens (Flt3 and VCAM-1) as discussed above (Adolfsson et al., 2005; Lai and Kondo, 2006). We did not observe any statistically significant difference among the four populations in myeloid potential, suggesting that myeloid potential stands independently from Meg/E potential among these populations (Figure 3.3C).

CD62L subfractionated populations show differential T cell potential bias in vivo

The peripheral blood analysis of the transplant recipients revealed significant differences in the amounts of lymphoid progenies generated from the subfractionated populations of the KLS MPP. All populations generated robust numbers of B cells early on and gradually lost the capacity to replenish. However, as with the Meg/E potential, CD62L–Sca-1^{HI} generated the greatest amount of B cells, while CD62L+Sca-1^{LO} generated the least amount (Figure 3.4A). The other two populations generated

intermediate numbers of B cells. This observation indicates that B cell potential decreases as early hematopoietic progenitors upregulate CD62L and downregulate Sca-1.

Interestingly, T cell potential did not follow the same pattern seen in B cell potential. T cells, having to migrate from bone marrow to thymus before maturation, did not peak in production until after week four. We observed that CD62L–Sca-1^{HI} and CD62L+Sca-1^{HI} populations both generated large amounts of T cells, while CD62L–Sca-1^{LO} and CD62L+Sca-1^{LO} populations generated lesser amounts of T cells (Figure 3.4B). The observation that progenitor populations characterized by the Sca-1^{HI} phenotype generated similarly large amounts of T cells, regardless of CD62L levels, indicates that Sca-1 expression level indicates T cell potential, independently of CD62L. However, based on previous data (Perry et al., 2004), we suspected that a potentially subtle lineage commitment bias detectable by CD62L may have been further diluted by Sca-1 segregation. Therefore, we combined the progeny output data according to CD62L expression to result in CD62L+ and CD62– data only. The ratio of cell numbers generated for each cell type from CD62L+ to CD62L– progenitors was then calculated (Table 3.1A). The analysis confirmed our previous observation that Meg/E potential diminishes with the increased expression of CD62L. For every single platelet and RBC generated by CD62L+ progenitors, approximately two platelets and RBC were generated by CD62L– progenitors as indicated by the average ratio for platelets of 1:2.2 and for RBC of 1:2.0. We also detected a minor bias toward T cell potential. As indicated by the average ratio of 1:0.7, for every T cell generated by CD62L+ progenitors, only 0.7 T cell were generated by CD62L– progenitors.

By analyzing the number of B cells generated per T cell generated, we were able analyze all four CD62L and Sca-1 fractionated populations for T cell bias according to CD62L expression (Table 3.1B). CD62L+Sca-1^{HI} and CD62L+Sca-1^{LO} populations generated 1 T cell per 21 and 20 B cells generated, respectively. CD62L–Sca-1^{HI} and CD62L–Sca-1^{LO} generated 1 T cell per 29 and 33 B cells generated, respectively. Regardless of Sca-1 level, CD62L+ progenitors consistently generated more T cells per B cell than CD62L– progenitors, demonstrating a T cell bias among CD62L-expressing progenitors within their lymphoid capacity. A similar bias toward T cell was also observed when the number of myeloid cells per T cell generated was analyzed.

Comparable frequencies of erythroid progenitors exist among the subpopulations

Despite our efforts to identify specific subpopulations that constitute the heterogeneity of KLS MPP, we recognize that even our subpopulations are likely to be heterogeneous themselves and that not every progenitor cell in any given subpopulation contributes equally to the reconstitution of specific lineages. Therefore, clonal analysis of each subpopulation was conducted by plating 200 progenitors per population in methylcellulose medium and supplementing with erythroid promoting cytokines to determine the frequency of erythroid progenitors. From culture day 5 to 11, every 2 days, colonies of cells, representing single seeder progenitors, were stained with benzidine to identify erythroid colonies. The assay revealed that all four subpopulations generated similar numbers of erythroid colonies, and that the numbers of erythroid colonies diminished over time, disappearing almost completely by the end of the assay at day 11 (Figure 3.5). On the other hand, the positive control population, KLS Thy1.1^{LO} HSC

demonstrated persistent production of erythroid colonies. This result does not reflect the dramatic differences in erythroid potential observed in the transplant experiment shown in Figure 3.3B. The apparent contradiction of the two experiments may indicate that the erythroid progenitors present in the subpopulations may have different capacity for progeny production. That is, while CD62L–Sca-1^{HI} and CD62L+Sca-1^{LO} populations may have similar numbers of erythroid progenitors, CD62L–Sca-1^{HI} may contain more robust erythroid progenitors than CD62L+Sca-1^{LO} and generate more RBC over time.

CD62L subfractionation of KLS MPP
may not be substituted by Flt3

We have demonstrated that subfractionation of KLS MPP using CD62L along with Sca-1 resulted in functionally distinct subpopulations. Our experiments were designed around CD62L, because we have hypothesized it to be a marker of early hematopoiesis like Flt3. In support of this concept, we have demonstrated that CD62L and Flt3 have a substantial degree of co-expression pattern as seen in Figure 3.1B. A relevant follow up question is to inquire whether CD62L adds additional resolution of functional subsets of progenitor cells over those obtained with Flt3. A flow cytometric measurement of Flt3 expression levels by CD62L+ and CD62L– MPP revealed that Flt3 may not substitute CD62L. The mean fluorescence of Flt3 for CD62L+ MPP was 208, and the mean fluorescence of Flt3 for CD62L– MPP was 194, presenting a virtually indistinguishable amount of difference in Flt3 expression (Figure 3.6). Hence, CD62L stands as a unique marker of early hematopoietic differentiation that may be used to identify distinct subpopulations of KLS MPP and provide further evidence for heterogeneity within this traditional MPP population.

Discussion

In this report, we have expanded upon previous findings that described CD62L as an effective marker for dividing the KLST– fraction of the hematopoietic stem cell compartment into a CD62L+ fraction, which resembled an early T-lineage progenitor, and a CD62L– fraction, which resembled the traditional MPP (Perry et al., 2004). The bone marrow transplant results, however, had been restricted to the engraftment of white blood cells only, since the tool used to differentiate the donor-derived hematopoietic cells from the cells of the recipient mice was allele-specific antibody labeling of CD45, a surface marker that is expressed on white blood cells (WBC), but not on platelets or red blood cells (Spangrude et al., 1988; Perry et al., 2004). Therefore, previous studies did not identify Meg/E potential in the two fractions of MPP.

In order to test our hypothesis that CD62L is a marker of hematopoietic differentiation and that CD62L can be used to demonstrate the heterogeneity within the traditionally defined multipotent progenitor population, we have conducted transplant experiments using subfractionated MPP according to CD62L and Sca-1 levels. The use of mouse strains that express GFP along with a variant of the hemoglobin beta-chain (Hbb^S) allows for the tracking of engraftment activity in all hematopoietic lineages: Meg/E lineage, myeloid linage among WBC and lymphoid lineage among WBC.

Our results showed that not only there are subfractions of KLS MPP that are distinguishable by surface expression levels of CD62L and Sca-1, but also that these subpopulations are functionally distinct. Our in vivo transplant experiments have demonstrated that CD62L–Sca-1^{HI} population had the most robust activity in all lineages, while the CD62+Sca-1^{LO} population exhibited significantly less production of T cells, B

cells, platelets and RBC. In fact, platelets and RBC produced by CD62L+Sca-1^{LO} cells were barely detectable and only early on during the weeks following the transplant, even though the production of T cells, B cells, monocytes and granulocytes of myeloid lineage was relatively strong. This is consistent with the other reports demonstrating that there are subpopulations within KLS MPP with significantly less Meg/E activity than the commonly described MPP (Adolfsson et al., 2005; Lai and Kondo, 2006).

We have also demonstrated that with the upregulation of CD62L, the multipotent progenitors develop a relative T cell lineage bias. As described in Table 3.1, all four populations generated more B cells and myeloid WBC than T cells. Only by carefully analyzing the shift in the portions of progenies among different subpopulations of MPP, we were able to identify an increase in the portion of progenies that resulted as T cells and thereby revealing a subtle T cell bias among the CD62L+ subpopulations. This is inconsistent with our previous findings that the CD62L+ fraction constituted a more pronounced T cell bias (Perry et al., 2004). This discrepancy may be due to the different sorting strategy we utilized in this report. The previous study divided the entire KLST– into CD62L+ and CD62L– fractions. We, however, have divided the KLS MPP, that is KLST–Flt3+, into CD62L+ and CD62L–. Therefore, the previous study's CD62L+ and CD62L– fractions included cells of the phenotype KLST–Flt3–. Prior to the execution of the experiments, we have hypothesized that the exclusion of KLST–Flt3– would not make a significant difference, as we have seen. As seen in Figure 3.1A, vast majority of KLST– falls into KLS MPP fraction and only a small fraction resides in the Flt3– fraction. Therefore, we considered the Flt3– portion to be too few to have an impact.

Upon retrospect, the KLST–Flt3– may contain hematopoietic progenitors that may be relevant to the discussion of early hematopoietic development. The Flt3+ compartment of KLS contains almost 1:4 CD62L– to CD62L+ cells (Figure 3.1B). The same figure reveals that the Flt3– compartment contains approximately 2:1 CD62– to CD62L+ cells. If our hypothesis of CD62L being a marker of development is correct, then the Flt3– fraction may represent a pool of significant progenitors that may be upstream of Flt3+ progenitors.

Interestingly there are other markers reported to subfractionate the KLS compartment into distinct subpopulations. A set of mature cell markers that are typically eliminated during the depletion of mature hematopoietic cells, CD4 and Mac-1, have been implicated in the subfractionation of KLS (Morrison and Weissman, 1994). Another set of markers, the Slam family proteins (CD150, CD244 and CD48) have been also reported to be fractionate KLS into HSC and MPP (Kiel et al., 2005; Forsberg et al., 2005). Another interesting marker that has been used to isolate HSC and fractionate KLS is CD34, a ligand for CD62L (Osawa et al., 1996; Yang et al., 2005). The co-expression pattern of these markers with CD62L is unknown. Future investigations into the relationship of CD62L expression with these other markers would be interesting, and may yield new subpopulations that may represent acute transition stages, granting a better understanding of early hematopoietic events at higher resolution.

Surprisingly, our data suggest that the frequencies of erythroid-capable progenitors are similar among the four subpopulations as shown in the in vitro methylcellulose assay. This is in an apparent contradiction with our in vivo transplant data showing that with CD62L upregulation and Sca-1 downregulation, the progenitors

lose dramatic amount of Meg/E potential. One explanation may be that the progenitors lose the extent of Meg/E capability at the level of individual cells, rather than as a population. In that case, the frequency of erythroid progenitors may stay relatively stable as the progenitor population matures; however, the amount of actual RBC produced per progenitor may be reduced. Another possibility is the artificial nature of in vitro cultures. In vitro experiments, which may be informative under the appropriate conditions and necessary in some cases, have been shown to force hematopoietic progenitors to develop into progenies of unnatural lineages under certain conditions (Nutt et al., 1999; Rolink et al., 1999).

Collectively, our data demonstrate that CD62L, despite having an expression pattern that is similar to that of Flt3, is able to identify functionally distinct subpopulations of MPP that would be impossible with the use of Flt3 alone. Furthermore, the data support the model of heterogeneous KLS MPP that sheds Meg/E potential, marked by the upregulation of CD62L, prior to the lymphoid and myeloid lineage separation through CLP and CMP formation.

Experimental procedures

Mice

Mice carrying the Thy1.1 and Ly5.1 alleles on the C57BL background were generated in our animal facility by mating the BKa.AK-Thy1^{a}/Ka and B6.SJL-Ptprc^{a} Pep3b/BoyJ strains and selecting for cosegregation of Thy1.1 and Ly5.1 (GFP– Thy1.1+Hbb^{S} mice). GFP transgenic mice, generated by microinjection of C57BL/6 oocytees, were kindly provided by Dr. Masaru Okabe (Osaka University, Osaka, Japan)

(Nakanishi et al., 2002). In these mice, the GFP transgene is driven by the chicken β-actin promoter and is expressed in all lineages except in the erythroid lineage. Hence, hemoglobin variant alleles (Hbb^S and Hbb^D) were used to track erythroid engraftment (see below). In order to generate donor mice for transplant studies, we have crossed the GFP transgenic mice with GFP–Thy1.1+Hbb^S mice to generate GFP+Thy1.1+Hbb^S mice. B6.Cg-Gpi1^a Hbb^D H1^b/DehJ mice (Harrison et al., 1988) were kindly provided by Dr. David Harrison (Jackson Laboratory, Bar Harbor, ME, USA). These mice are GFP–Thy1.1–Hbb^D and were used as transplant recipients. All mice were kept in the animal resources center at the University of Utah under the institutional animal care and use committee approved protocols.

Antibodies

Monoclonal antibodies against CD2 (Rm2.2), CD3 (KT3-1.1), CD5 (53-7.3), CD8 (53-6.7), CD11b (M1/70), Ly-6G (RB6-8C5), TER119, B220 (CD45R; RA3-6B2), and CD19 (1D3) were purified from the media of cultured hybridoma cell lines. PE-conjugated Sca-1 monoclonal antibody was purchased from PharMingen (San Diego, CA, USA). C-kit (3C11) monoclonal antibody was purified and conjugated to Alexa Fluor 647 in our laboratory. CD4 and CD8 monoclonal antibodies were purified and conjugated to allophycocyanin (APC). Biotinylated Flt3, CD62L APC-AF750, Thy1.1 PerCP-Cy5.5, Mac-1 PE and Gr-1 PE antibodies were purchased from eBioscience (San Diego, CA, USA).

Isolation of hematopoietic progenitors and stem cells

In order to remove mature cells from the harvested whole bone marrow cells, lineage depletion was performed. The cells were incubated with a cocktail of rat antibodies to mature cell markers (CD2, CD3, CD5, CD8, CD11b, Ly-6G, TER119, B220 and CD19). Secondary labeling of mature cells was performed by two successive incubations with magnetic beads-coupled sheep anti-rat antibodies (Dynal, Oslo, Norway). Each incubation was followed by a depletion step of the labeled cells using a magnetic column (Dynal, Oslo, Norway). The depleted cells were stained with various fluorochrome-conjugated antibodies as indicated in the figures to electronically visualize and sort using FACS Aria instrument (BD Immunocytometry Systems, San Jose, CA, USA). DAPI was used to discriminate dead cells from live cells.

Bone marrow transplantation

The GFP–Thy1.1–Hbb^{D} recipient mice were lethally irradiated a day prior to the transplant day (^{137}Cs, 13 Gy delivered in a 3 hour-split dose). Isolated GFP+Thy1.1+Hbb^{S} donor cells were injected into the recipients retro-orbitally. The recipient mice were anesthetized with isoflurane using the E-Z Anesthesia system for the injection (Euthanex Corp., Palmer, PA).

Peripheral blood analysis

For the posttransplant analysis, peripheral blood samples were collected from the retro-orbital sinus with heparinized capillary tubes. The mice were anesthetized with isoflurane using the E-Z Anesthesia system (Euthanex Corp., Palmer, PA). Immediately

after the collection of blood samples, 10 ul of blood per sample were set aside for platelet analysis. The rest of the samples were mixed with 500ul of 2% Dextran T500 (Amersham Biosciences, Piscataway, NJ) in PBS and incubated at 37 degree C for 30 min for sediment separation of the RBC and WBC fractions. The RBC fraction was processed for HPLC analysis (see below). WBC were stained with PE-conjugated antibodies against Mac-1 and Gr-1 for myeloid WBC detection, Biotinylated B220 or CD19 antibody with a subsequent labeling with Alexa Fluor 750-conjugated avidin for B cell detection, and CD4 and CD8 conjugated with APC for T cell detection. Platelets and WBC were analyzed by FACScan flow cytometer (BD Biosciences, San Jose, CA; modified by Cytek Development, Fremont, CA). Platelet analysis was performed by increasing forward and side scatter parameters until the platelet population could be gated to exclude contaminants.

HPLC analysis of hemoglobin variants

A HPLC cation exchange protocol was developed in our laboratory to discriminate and quantify Hbb^D and Hbb^S in the peripheral blood samples (Spangrude et al., 2006). A stock solution of 100 mM 5,5'-dithiobis-(2-nitrobenzoic acid) (DTNB) (Sigma-Aldrich, St. Louis, MO) was prepared by dissolving 100 mg of DTNB in 2.5 ml of DMSO and stored at –20 degree C. The RBC fraction was derivatized by adding 5 ul of the RBC fraction into 250ul of 40 mM NaCl and 2 mM DTNB and incubating at room temperature for 30 minutes. Following centrifugation at 12,000 g for 2 minutes, the supernatant were analyzed using a VARIANT hemoglobin testing system (Bio-Rad Laboratories, Hercules, CA) with an optimized β–thalassemia short program.

In vitro erythroid potential assay

To assay clonal erythroid potential, 200 cells per sorted population were plated on 35 mm culture dish in alpha-modified Eagle's medium-based methylcellulose containing 10% fetal calf serum, 10% deionized bovine serum albumen, antibiotics, l-glutamine, and 2-mercaptoethanol. Erythroid development was promoted by supplementing the cultures with stem cell factor (SCF, 100 ng/ml), interleukin-3 (IL-3, 10 ng/ml), and erythropoietin (EPO, 4 U/ml). Periodically, a subset of cultures was stained using benzidine hydrochloride and the erythroid colonies scored.

References

Adolfsson, J., Borge, O.J., Bryder, D., Theilgaard-Monch, K., Astrand-Grundstrom, I., Sitnicka, E., Sasaki, Y., and Jacobsen, S.E. (2001). Upregulation of Flt3 expression within the bone marrow Lin(–)Sca1(+)c-kit(+) stem cell compartment is accompanied by loss of self-renewal capacity. Immunity *15*, 659-669.

Adolfsson, J., Mansson, R., Buza-Vidas, N., Hultquist, A., Liuba, K., Jensen, C.T., Bryder, D., Yang, L., Borge, O.J., Thoren, L.A., Anderson, K., Sitnicka, E., Sasaki, Y., Sigvardsson, M., and Jacobsen, S.E. (2005). Identification of Flt3+ lympho-myeloid stem cells lacking erythro-megakaryocytic potential: a new road map for blood lineage commitment. Cell *121*, 295-306.

Akashi, K., Traver, D., Miyamoto, T., and Weissman, I.L. (2000). A clonogenic common myeloid progenitor that gives rise to all myeloid lineages. Nature *404*, 193-197.

Akashi, K., Traver, D., Zon, L.I. (2005). The complex cartography of stem cell commitment. Cell *121*, 160-162.

Christensen, J.L., and Weissman, I.L. (2001). Flk2 is a marker in hematopoietic stem cell differentiation: a simple method to isolate long-term stem cells. Proc. Natl. Acad. Sci. USA *98*, 14541-14546.

Forsberg, E.C., Prohaska, S.S., Katzman, S., Heffner, G.C., Stuart, J.M., and Weissman, I.L. (2005). Differential expression of novel potential regulators in hematopoietic stem cells. PLoS Genetics *1*, e28.10.1371/journal.pgen.0010028.

Forsberg, E.C., Serwold, T., Kogan, S., Weissman, I.L., and Passegue, E. (2006). New evidence supporting megakaryocyte-erythrocyte potential of Flk2/Flt3+ multipotent hematopoietic progenitors. Cell *126*, 415-426.

Harrison, D.E., Astle, C.M., Lerner, C. (1988) Number and continuous proliferative pattern of transplanted primitive immunohematopoietic stem cells. Proc. Natl. Acad. Sci. USA. *85*, 822-826.

Ikuta, K., and Weissman, I.L. (1992). Evidence that hematopoietic stem cells express mouse c-kit but do not depend on steel factor for their generation. Proc. Natl. Acad. Sci. USA *89*, 1502-1506.

Kiel, M.J., Yilmaz, O.H., Iwashita, T., Yilmaz, O.H., Terhorst, C., and Morrison, s.J. (2005). SLAM family receptors distinguish hematopoietic stem and progenitor cells and reveal endothelial niches for stem cells. Cell *121*, 1109-1121.

Kondo, M., Weissman, I.L., and Akashi, K. (1997). Identification of clonogenic common lymphoid progenitors in mouse bone marrow. Cell *91*, 661-672.

Kwak, J.Y., Cho, S., and Spangrude, G.J. (2007). Gradients of antigen expression and development potential in hematopoiesis. Ann. N.Y. Acad. Sci. *1106*, 82-88.

Lai, A.Y., and Kondo, M. (2006). Asymmetrical lymphoid and myeloid lineage commitment in multipotent hematopoietic progenitors. J. Exp. Med. *203*, 1867-1873.

Lai, A.Y., Simon, M.L., Kondo, M. (2005). Heterogeneity of Flt3-expressing multipotent progenitors in mouse bone marrow. J. Immunol. *175*, 5016-5023.

Morrison, S.J., and Weissman, I.L. (1994). The long-term repopulating subset of hematopoietic stem cells is deterministic and isolatable by phenotype. Immunity *1*, 661-673.

Morrison, S.J., Wandycz, A.M., Hemmatic, H.D., Wright, D.E., and Weissman, I.L. (1997). Identification of a lineage of multipotent hematopoietic progenitors. Development *124*, 1929-1939.

Nakanishi, T., Kuroiwa, A., Yamada, S., Isotani, A., Yamashita, A., Tairaka, A., Hayashi, T., Takagi, T., Ikawa, M., Matsuda, Y., and Okabe, M. (2002). FISH analysis of 142 EGFP transgene integration sites into the mouse genome. Genomics *80*, 564-574.

Nutt, S.L., Heavy, B., Rolink, A.G., Busslinger, M. (1999). Commitment to the B-lymphoid lineage depends on the transcription factor Pax5. Nature *401*, 556-562.

Osawa, M., Hanada, K., Hamada, H., and Nakauchi, H. (1996). Long-term lymphohematopoietic reconstitution by a single CD34-low/negative hematopoietic stem cell. Science *273*, 242-245.

Perry, S.S., Wang, H., Pierce, L.J., Yang, A.M., Tsai, S., and Spangrude, G.J. (2004). L-selectin defines a bone marrow analog to the thymic early T-lineage progenitor. Blood *103*, 2990-2996.

Rolink, A.G., Nutt, S.L., Melchers, F., Busslinger, M. (1999). Long-term in vivo reconstitution of T-cell development by Pax5-deficient B-cell progenitors. Nature *401*, 603-666.

Spangrude, G.J., Cho, S., Guedelhoefer, O., VanWoerkom, R.C., and Fleming, W.H. (2006). Mouse models of hematopoietic engraftment: limitations of transgenic green fluorescent protein strains and a high-performance liquid chromatography approach to analysis of erythroid chimerism. Stem Cells *24*, 2045-2051.

Spangrude, G.J., Heimfeld, S., and Weissman, I.L. (1988). Purification and characterization of mouse hematopoietic stem cells. Science *241*, 58-62.

Yang, L., Bryder, D., Adolfsson, J., Nygren, J., Mansson, R., Sigvardsson, M., and Jacobsen, S.E. (2005). Identification of Lin(-)Sca1(+)-kit(+)CD34(+)Flt3-short-term hematopoietic stem cells capable of rapidly reconstituting and rescuing myeloablated transplant recipients. Blood *105*, 2717-2723.

Figure 3.1 Flow cytometric subfractionation of the hematopoietic stem cell compartment (KLS). Panel A Representative profile of Flt3 and Thy1.1 expression within the hematopoietic stem cell compartment. The KLS population, identified as lineage-depleted bone marrow cells gated for c-Kit^{High} and Sca-1+, was subfractionated as LT-HSC, ST-HSC and MPP according to the expression levels of Flt3 and Thy1.1. **Panel B** CD62L and Flt3 co-expression profile of KLS. The percentages indicate the portion of cells belonging to each quadrant of KLS. **Panel C** The KLST– population, identified as the Thy1.1– portion of KLS as indicated by the dashed box and arrow from panel A, was analyzed by CD62L and Flt3 expressions and further subfractionated into CD62L+ MPP and CD62L– MPP. **Panel D** Representation of target populations for FACS sorting. CD62L+ MPP and CD62L– MPP were divided into Sca-1^{LO} and Sca-1^{HI}.

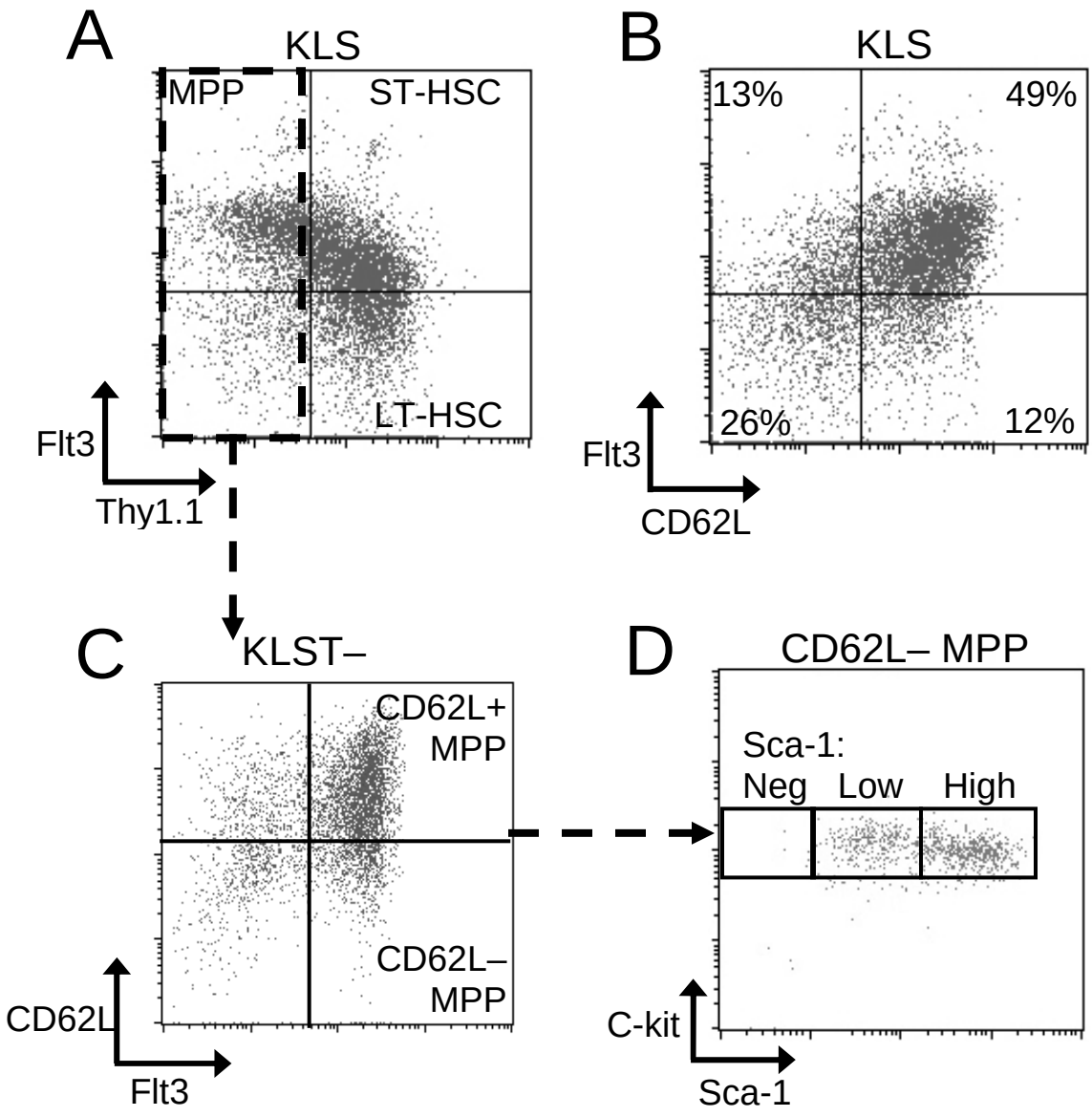
A
KLS
MPP
ST-HSC
LT-HSC
Flt3
Thy1.1
B
KLS
13%
49%
26%
12%
Flt3
CD62L
C
KLST–
CD62L+
MPP
CD62L–
MPP
CD62L
Flt3
D
CD62L– MPP
Sca-1:
Neg
Low
High
C-kit
Sca-1

Figure 3.2 IL7Rα+ cells among hematopoietic stem cells and early hematopoietic progenitors. Traditionally viewed early hematopoietic populations are listed in the order of maturity from LT-HSC to MPP. The amount of IL7Rα+ cells per population was quantified by flow cytometric analysis to demonstrate the degree of lymphoid differentiation per population. CD62L+ MPP (CD62L-neg MPP) and CD62L– MPP (CD62L-pos MPP) are subfractionated populations of MPP via CD62L expression. The common lymphoid progenitor (CLP) represents the most mature population and is the only population outside the hematopoietic stem cell compartment in the array.

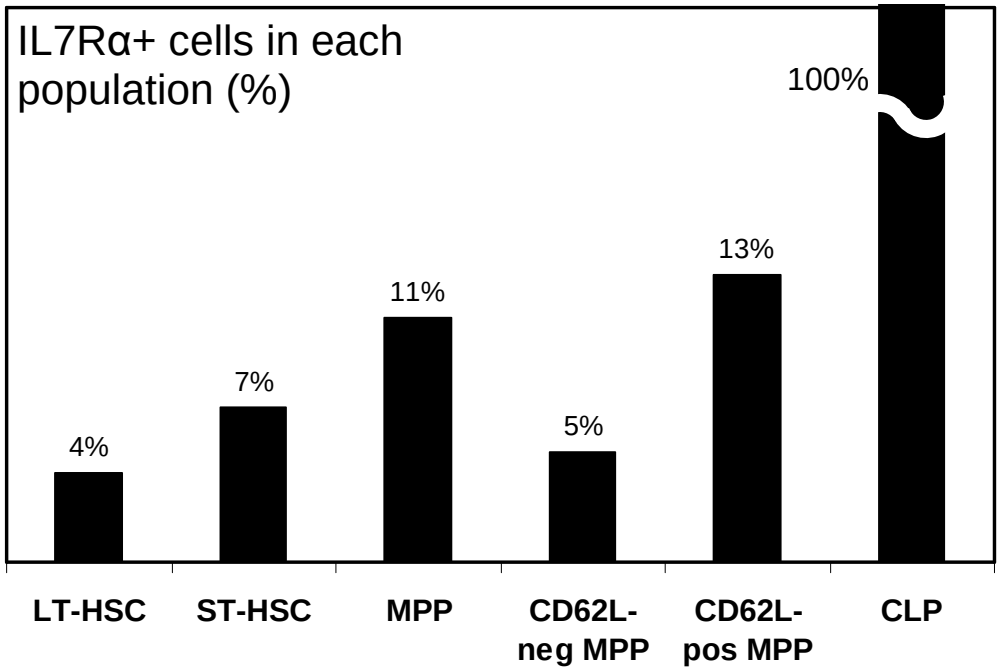
IL7Rα+ cells in each population (%)
4%
7%
11%
5%
13%
100%
LT-HSC
ST-HSC
MPP
CD62L-neg MPP
CD62L-pos MPP
CLP

Figure 3.3 Assessment of myeloid lineage output of transplanted subfractionated MPP populations. MPP of KLS were subfractionated via FACS sorting according to CD62L and Sca-1 levels as indicated in Figure 3.1C and Figure 3.1D. 3000 sorted donor progenitors were transplanted with 250k recipient whole bone marrow cells as competitors into 4 to 5 lethally irradiated recipients, which were periodically analyzed for engraftment via retro-orbital bleeding. Error bars represent SEM. **Panel A** Donor-derived platelets were measured among total platelets in the peripheral blood via flow cytometry. CD62L– Sca-1^{HI} progenitors (triangle) showed the most robust early platelet production compared to CD62L+ Sca-1^{LO} progenitors (square) ($P<0.02$). By week 6, donor platelets were undetectable or nearly undetectable. **Panel B** Donor-derived RBC were measured via HPLC analysis. Consistent with the platelet engraftment data, CD62L– Sca-1^{HI} (triangle) demonstrated the greatest potency for RBC generation. **Panel C** Monocytes and granulocytes were analyzed via flow cytometry and measured as cells of the myeloid lineage among total white blood cells in the peripheral blood. High variations per sample led to statistical insignificance among various donor groups. SEM error bars omitted.

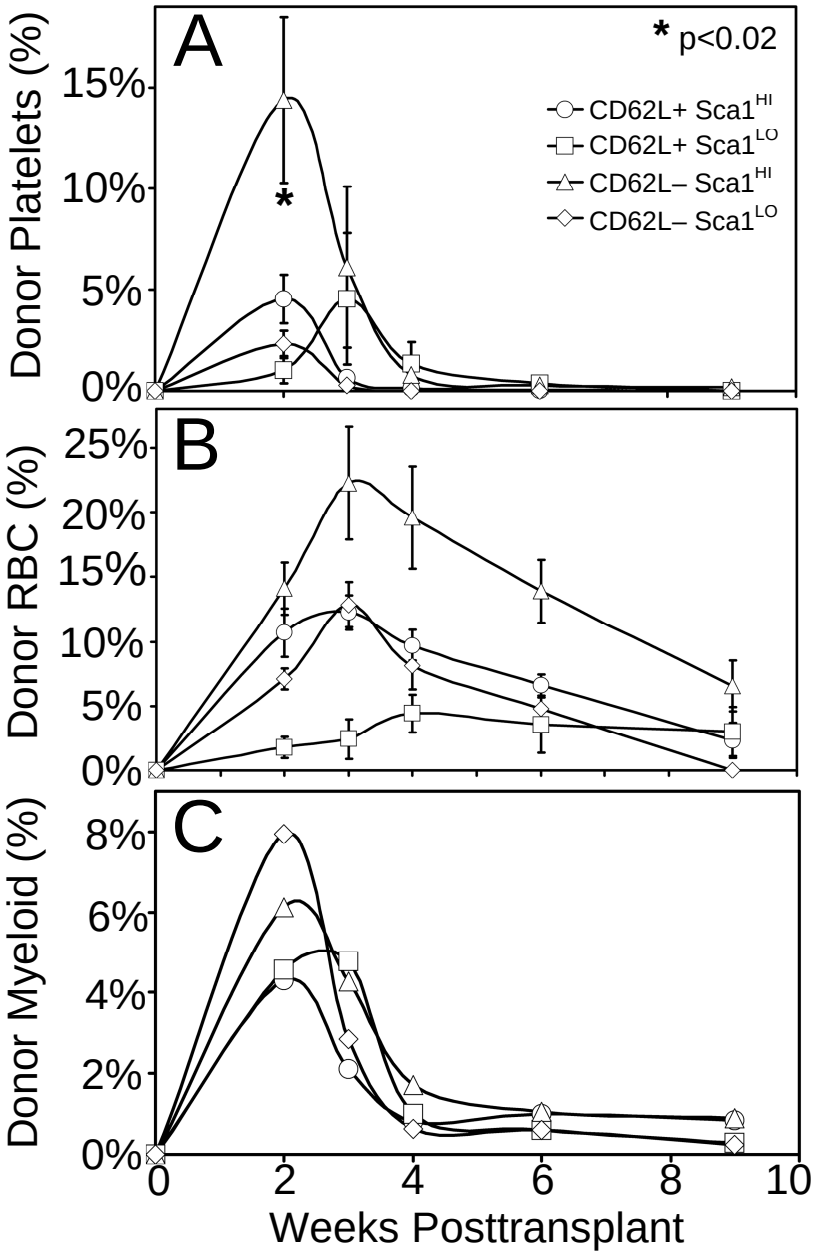
A
* p<0.02
CD62L+ Sca1HI
CD62L+ Sca1LO
CD62L– Sca1HI
CD62L– Sca1LO
Donor Platelets (%)
15%
10%
5%
0%
*
B
Donor RBC (%)
25%
20%
15%
10%
5%
0%
C
Donor Myeloid (%)
8%
6%
4%
2%
0%
0
2
4
6
8
10
Weeks Posttransplant

Figure 3.4 Assessment of lymphoid lineage output of transplanted subfractionated MPP populations. MPP of KLS were subfractionated via FACS sorting according to CD62L and Sca-1 levels as indicated in Figure 3.1C and Figure 3.1D. 3000 sorted progenitors were transplanted into 4 to 5 lethally irradiated recipients with 250k recipient whole bone marrow cells as competitors and periodically analyzed for engraftment via retro-orbital bleeding and FACS analysis. Error bars represent SEM. **Panel A** B cell engraftment was analyzed by quantifying the amount of donor B cells from the total peripheral blood WBC. B cell production peaked early at week 2 and decreased over time, during which CD62L– Sca-1^{HI} progenitors (triangle) maintained the greatest B cell production compared to CD62L+ Sca-1^{LO} progenitors (square) which had the least amount of activity ($p<0.01$). **Panel B** T cell engraftment was quantified from the total peripheral WBC. The amount of T cell production depended on the progenitors separated by Sca-1, regardless of CD62L expression. The greatest difference came from CD62L+ Sca-1^{HI} progenitors (circle) and CD62L– Sca-1^{LO} progenitors (diamond) ($p<0.05$).

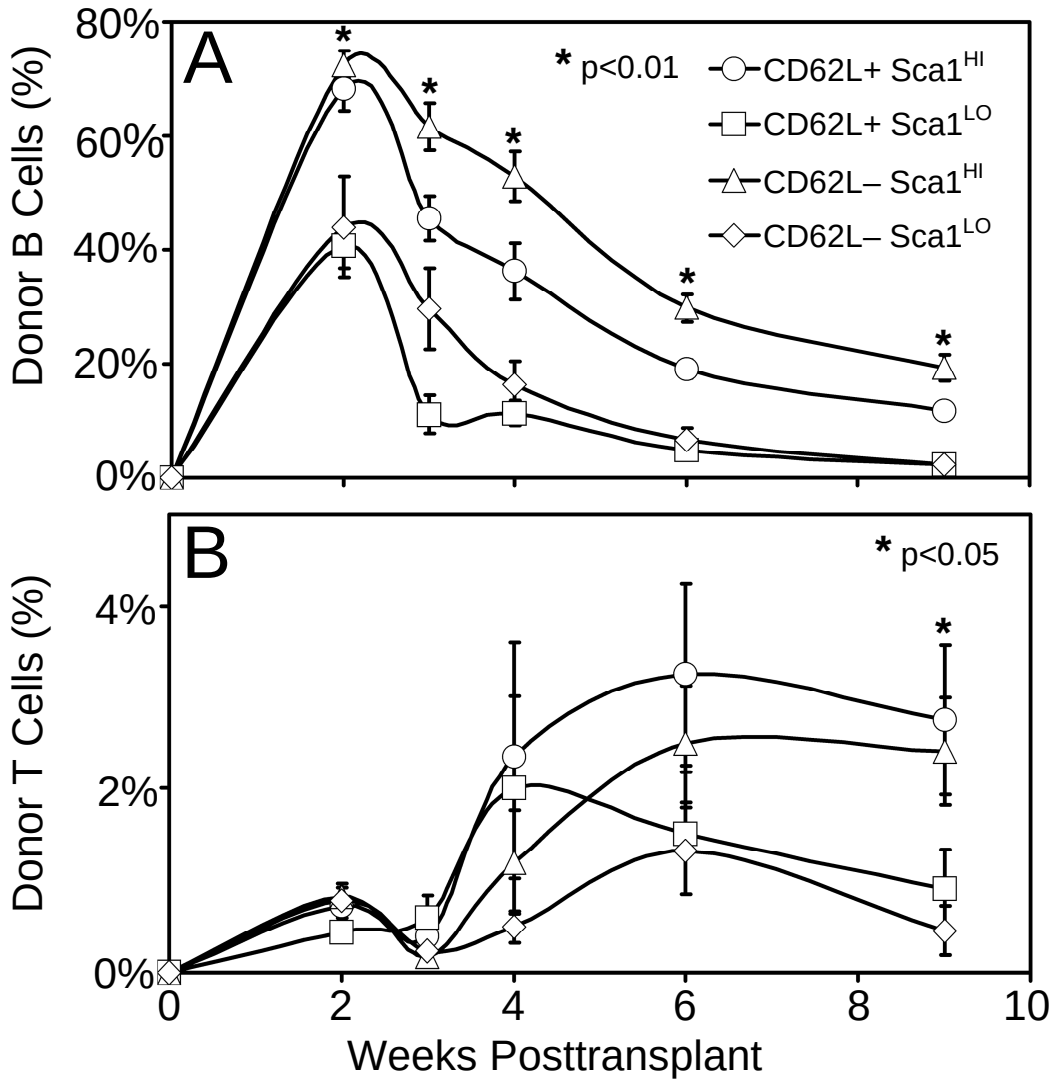
A
B
* p<0.01
* p<0.05
CD62L+ Sca1HI
CD62L+ Sca1LO
CD62L– Sca1HI
CD62L– Sca1LO
Donor B Cells (%)
Donor T Cells (%)
80%
60%
40%
20%
0%
4%
2%
0
2
4
6
8
10
Weeks Posttransplant

Table 3.1 T cell lineage bias among subfractionated MPP populations. **Part A** To detect any lineage bias among MPP populations isolated by CD62L expression, the ratios of mature cells produced by CD62L+ to CD62L– progenitors were determined per lineage. The ratios were determined from the time points that showed the most robust progeny production. CD62L– progenitors had greater number of progenies produced in all lineages compared to CD62L+ progenitors, except in T cell lineage. **Part B** T cell output was compared to B cell output and M cell output per progenitor population by dividing the number of B cells or M cells by the number of T cells per indicated time period. Peak* indicates the analysis of progeny numbers taken from the time points of their greatest production per lineage. The peak times were week 2 for M lineage, week 4 for B lineage, and week 6 for T lineage for all progenitors, except CD62L+ Sca-1^{LO}, for which the peak time for T lineage was week 4. The numbers indicate the number of M cells generated for every 1 T cell generated.

A

Progeny Cell Type	Weeks Posttransplant					Average
	2	3	4	6	9	
	Ratio of CD62L+ to CD62L– progenies					
Platelets	1:3.1	1:1.3				1:2.2
RBC	1:1.7	1:2.4	1:2.0	1:1.8		1:2.0
M Cells	1:1.6	1:1.0				1:1.3
B Cells	1:1.1	1:1.6	1:1.5			1:1.4
T Cells			1:0.4	1:0.8	1:0.8	1:0.7

B

Progenitor	Weeks Posttransplant			
	4	6	9	Peak*
	Number of B cells / 1 T cell generated			
CD62L– Sca1-HI	44	12	8.1	29
CD62L– Sca1-LO	33	5.1	4.9	33
CD62L+ Sca1-HI	15	5.9	4.3	21
CD62L+ Sca1-LO	5.6	3.1	2.4	20
	Number of M cells / 1 T cell generated			
CD62L– Sca1-HI	1.4	0.4	0.4	2.5
CD62L– Sca1-LO	1.3	0.5	0.6	6.0
CD62L+ Sca1-HI	0.3	0.3	0.3	1.3
CD62L+ Sca1-LO	0.5	0.4	0.3	2.4

Figure 3.5 Clonal analysis for erythroid lineage. Clonal RBC potential was determined for each MPP population in vitro. 200 Sorted progenitors per population were grown in methylcellulose and promoted to erythroid development by supplying the cells with stem cell factor (SCF), interleukin-3 (IL-3), and erythropoietin (EPO). Periodically the colonies were stained with benzidine, a highly selective hemoglobin detection agent to identify erythroid activity. HSC indicated as Thy1.1^{LO} were used as a positive control. The error bars are SEM. No statistically significant difference was detected among progenitors.

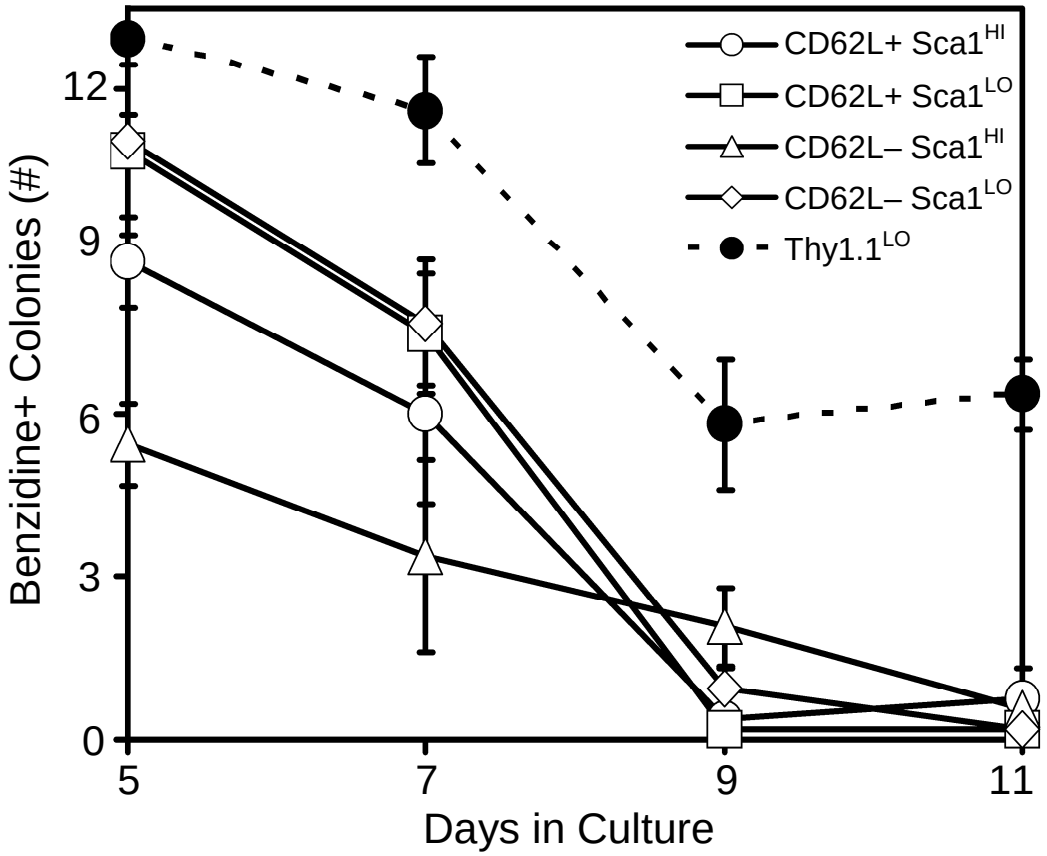
CD62L+ Sca1HI
CD62L+ Sca1LO
CD62L– Sca1HI
CD62L– Sca1LO
Thy1.1LO
Benzidine+ Colonies (#)
0
3
6
9
12
5
7
9
11
Days in Culture

Figure 3.6 Flt3 expression levels in CD62L-subfractionated MPP. Flow cytometric analysis was performed to determine the Flt3 expression levels in CD62L– (black) and CD62L+ (gray) MPPs. Mean fluorescence (MF) for each population is indicated. Similar levels of Flt3 were present in the CD62L subfractionated progenitors.

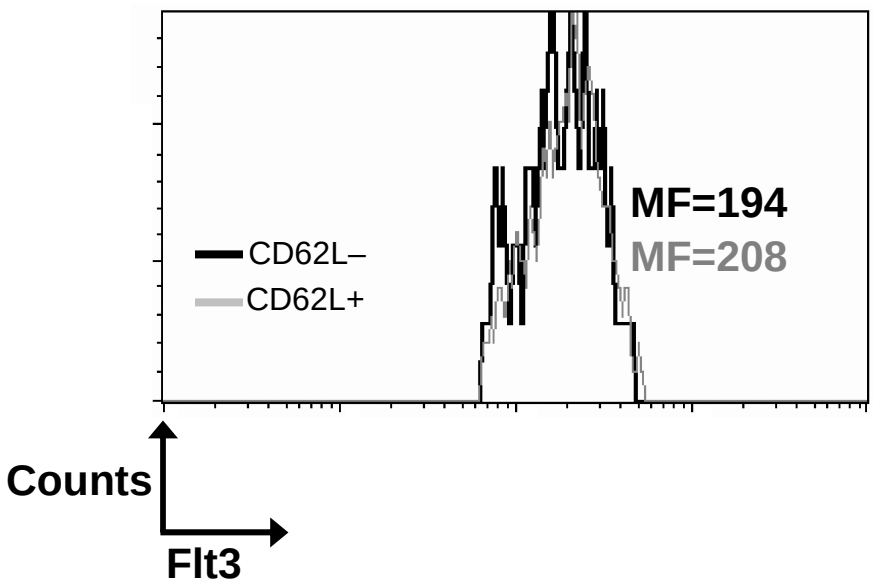
MF=194
MF=208
CD62L–
CD62L+
Counts
Flt3

CHAPTER 4

IDENTIFICATION OF CD62L-EXPRESSING MULTIPOTENT PROGENITORS OUTSIDE THE TRADITIONAL HEMATOPOIETIC STEM CELL COMPARTMENT

Abstract

The end stage progenitor within the hematopoietic stem cell compartment is a multipotent progenitor population that expresses high levels of c-Kit, Sca-1, CD62L and Flt3. We have attempted to identify the next stage progenitor in the previously characterized myeloid progenitor compartment that expresses high level of c-Kit but lacks Sca-1. Within this population we have identified a subset that is phenotypically identical to the multipotent progenitor population of the hematopoietic stem cell compartment with the exception of Sca-1 expression. Transplant experiments demonstrate that this subset within the myeloid progenitor compartment exhibits multipotency, albeit weaker than the multipotent progenitors that express Sca-1. A myeloid committed progenitor population was also identified by the lack of CD62L and Flt3, implicating the loss of CD62L and Flt3 as the marker of progression into the myeloid lineage.

Introduction

All blood cells are generated from hematopoietic stem cells (HSC) in the bone marrow. As the HSC matures, it loses its capacity for self-renewal and passes through a multipotent progenitor stage (MPP). The pool of HSC and MPP cells have been identified to share common expression patterns of Sca-1 and c-Kit, and have been named the hematopoietic stem cell compartment (or KLS) (Spangrude et al., 1988; Ikuta and Weissman, 1992; Christensen and Weissman, 2001).

A traditional model of hematopoietic lineage commitment occurs outside the KLS stage with the bifurcation of lymphoid and myeloid lineages as common lymphoid

progenitors (CLP) (Kondo et al., 1997) and common myeloid progenitors (CMP) (Akashi et al., 2000) are formed. This model was further substantiated with subsequent studies tracing the lymphoid lineage to CLP (Miller et al., 2002; Martin et al., 2003). However, this model has been recently disputed. Recent studies of the MPP of KLS have revealed the formation of lymphoid lineage bias and the significant reduction of erythroid/megakaryocyte lineage (Meg/E) (Adolfsson et al., 2005; Lai et al., 2005; Lai and Kondo, 2006). Our laboratory has also discovered in vitro and in vivo evidence for similar loss of Meg/E potential and lymphoid bias (Chapter 3; Perry et al., 2004; Kwak et al., 2007). Together, the results indicate the shift in lineage potential within the MPP population, prior to the CLP and CMP stages.

To further complicate the model, significant myeloid progenies have been generated from CLP, a population once considered to be composed of pure lymphoid progenitors (Balciunaite et al., 2005; Rumfelt et al., 2006). Previously it was demonstrated that T cell progenitors found in the adult murine thymus lacked B cell potential (Porritt et al., 2004; Lu et al., 2005). Later studies, however, have shown that even these T progenitors maintained some capacity for macrophage production in vitro, indicating that B cell potential may be lost before myeloid potential has been completely lost from the lymphoid lineage (Bell and Bhandoola, 2008; Wada et al., 2008). Additionally, the preservation of macrophage production capability has been observed in what was previously thought as B cell progenitors in the bone marrow (Montecino-Rodriguez et al., 2001).

In 2000, Akashi et al. described the group of cells that exhibited a high level of c-Kit expression and no Sca-1 expression (KLS–) just outside the KLS as the myeloid

progenitor population (Akashi et al., 2000). In that study they further classified three populations out of the myeloid progenitor population according to the surface expression levels of CD34 and FcγR: (1) CD34+FcγR^{LO} as the CMP that gave rise to all myeloid cells, (2) CD34+FcγR^{HI} as the GMP for granulocyte/macrophage restricted progenitors, and (3) CD34–FcγR^{LO} as the MEP for megakaryocyte/erythroid restricted progenitors (Akashi et al., 2000). Another group, however, has demonstrated subsequently that CMP, when transplanted to sublethally irradiated recipients through intrasplenic or intravenous injections, have produced B cells (Yang et al., 2005) and that these B cells were functionally distinct from CLP-derived B cells (Yang et al., 2007). These results show that the commonly described lineage segregation of lymphoid and myeloid lineages through CLP and CMP have been overly simplified and the need for further studies to elucidate the lineage commitment steps.

Previously our laboratory has reported that CD62L is an excellent candidate to study the hematopoietic differentiation process by demonstrating that CD62L-fractionated Thy1.1– fraction of KLS led to the identification T cell-biased MPP (Perry et al., 2004). We have also demonstrated that HSC lacked CD62L expression (Chapter 2). Subsequently we have demonstrated with in vivo evidence that MPP of KLS have lost a significant amount of Meg/E potential, developed T-cell bias, and weakened in overall progeny production as the cells upregulated CD62L and downregulated Sca-1 (Chapter 3). These observations indicate that CD62L is upregulated as hematopoiesis proceeds from HSC, and hence is an excellent marker of early differentiation.

In this report, we have opted to follow the CD62L expression outside KLS in order to study the KLS– fraction of bone marrow that contains myeloid progenitors. By

isolating subpopulations through fluorescence-activated cell sorting, transplant experiments were performed to assess their in vivo lineage potentials. The results demonstrate that CD62L expression is maintained by a subset of myeloid progenitors and that this population exhibits rare lymphoid activity. A minute, but detectable amount of T cell lineage is also shown through in vitro cultures. Together, the results indicate potential lymphoid and myeloid capable multipotent progenitors identifiable by CD62L expression.

Results

KLS– myeloid progenitors include a population phenotypically similar to KLS MPP

Development of the myeloid lineage proceeds from KLS, which contains HSC and MPP, to a Sca-1– c-Kit^{High} population which contains CMP, GMP and MEP (Akashi et al., 2000) as shown in figure 4.1A. Previously we have observed that the most mature population of KLS was the CD62L+Flt3+Sca-1^{Low} MPP that has lost much of Meg/E potential and developed lymphoid bias (Chapter 3). The implication of these three markers regarding to hematopoietic differentiation is that CD62L and Flt3 were upregulated as Sca-1 was downregulated by the early hematopoietic stem cells and progenitors in the KLS compartment as they matured. Therefore, it was reasonable to inquire if this trend continued outside KLS. Following the decreasing trend of Sca-1, we have targeted the KLS– compartment for the identification of the closest progenitor population to KLS MPP.

KLS– cells were stained with antibodies against CD62L and Flt3. We have observed roughly three populations according to the expression profile: CD62L+Flt3+

(++), CD62L+Flt3– (+–), and CD62L–Flt3– (--) (Figure 4.1B). Out of the three populations, CD62L+Flt3+ appeared closest to the MPP of KLS, differing only in Sca-1 expression and sharing the same c-Kit, CD62L and Flt3 expressions, leading to the hypothesis that CD62L+Flt3+ was the most proximal progenitor population to KLS MPP outside KLS.

Multipotent progenitor activity is observed from the pool of myeloid progenitors

In order to assess lineage potentials of the three populations in vivo, a transplant experiment was performed. Sorted 100K cells per population were injected into lethally irradiated recipients. Donor cells in peripheral blood were identified by flow cytometric analysis. RBC analysis was performed through HPLC for the quantification of the Hbb^S hemoglobin variant for the donor RBC and the Hbb^D hemoglobin variant for the recipient RBC. Platelet output was the greatest from the CD62L–Flt3– population, CD62L+Flt3+ population generated a less, but strong, RBC output early on, and CD62L+Flt3– population generated a weak output (Figure 4.2A). Platelet output from all populations diminished over time, however, platelet output from CD62L–Flt3– persisted the most. RBC generation was strong from all three populations, with the output from CD62L+Flt3– being the weakest (Figure 4.2B). The results indicate that CD62L+Flt3+ and CD62L–Flt3– retained a substantial Meg/E potential, while CD62L+Flt3– had nearly lost Meg potential and maintained only erythroid potential.

From the analysis of myeloid leukocytes, we observed that CD62L+Flt3+ had the strongest output, while CD62L–Flt3– generated an intermediate amount with CD62L+Flt3– generating only a weak early burst of activity, similar to its platelet activity

(figure 4.3C). These data demonstrate CMP-like activity from CD62L+Flt3+ and CD62L–Flt3–. The CD62L+Flt3– population appears mostly erythroid-biased in the myeloid lineage.

To assess lymphoid potential, B cell and T cell output was measured. In either case only the CD62L+Flt3+ population generated significant levels of B and T cells with the other two donor populations generating only barely detectable trace amounts of B and T cells (Figure 4.2D and Figure 4.2E). Together, the data indicate that the CD62L–Flt3– population behaves as the CMP population and that the CD62L+Flt3– population as mostly an erythroid progenitor. The CD62L+Flt3+ population, with strong multipotency in all lineages, resembled the KLS MPP. Since the only phenotypic marker difference between CD62L+Flt3+ and KLS MPP is the presence of Sca-1, and since CD62L+Flt3+ exhibited multipotency in vivo, the CD62L+Flt3+ population will hereafter be referred to as KLS– MPP.

The KLS– MPP subset exhibits limited activity compared to the traditional KLS MPP

The multipotent activity of KLS– MPP had not been expected, since the KLS– compartment has been described to be entirely composed of myeloid progenitors and their progenies (Akashi et al., 2000). Therefore, to further characterize the multipotency of KLS– MPP in vivo, a competitive transplant experiment between KLS– MPP and KLS MPP was conducted. Target cells were sorted by fluorescence-activated cell sorting. Sorted 2000 cells of KLS– MPP were injected together with 2000 cells of KLS MPP into sublethally irradiated recipient mice. Lethal irradiation of transplant recipients will cause death if the donor cells do not rescue the recipient's hematopoietic system. Since the

donor cells were composed only of MPP and excluded HSC, we utilized sublethal radiation doses in order to avoid any deaths due to hematopoietic failure. In order to distinguish among KLS– MPP progenies, KLS MPP progenies and the native hematopoietic cells in the peripheral blood, we employed GFP/Ly5.1 donor mice for KLS– MPP, GFP–/Ly5.1 mice for KLS MPP, and GFP–/Ly5.2 mice for recipients. Ly5.1 marker was detected with the anti-Ly5.1-FITC antibody. This allowed for the observation of cells from the three mouse strains in one fluorescence parameter (Figure 4.3A). The native cells would be negative for GFP and Ly5.1 staining. The KLS MPP-derived cells would be in the intermediate Ly5.1 positive only cells. The KLS– MPP-derived cells would express GFP and would appear as the brightest peak; the contribution of Ly5.1-FITC to the bright fluorescence of GFP is minimal. Unfortunately, this experimental design allowed for the observation of white blood cells only, since RBC or platelets do not express Ly5.1 or Ly5.2 (Spangrude et al., 1988).

The transplant results showed that KLS MPP exhibited a strong activity in myeloid leukocytes, B cells and T cells compared to KLS– MPP, which showed only a weak early transient output of B cells with no significant myeloid or T cells (Figure 4.3B~D). The deficiency in MPP activity from KLS– MPP may be due to the fewer number of cells transplanted, since in the previous experiment, 100K cells were used per transplant compared to only 2000 cells in this experiment. The other possibility is that KLS– MPP cells could not compete against KLS MPP cells for engraftment, and were not able to generate enough progenies for detection above the background of the progenies of the KLS MPP population. If there is only a limited space in the bone

marrow for stem cells and progenitors to occupy, then naturally there would be a competition for these niches (Schofield, 1978; reviewed in Yin and Li, 2006).

Multipotent progenitor activity is severely diminished following transplant of low numbers of KLS– MPP

To investigate if competition between KLS– MPP cells and KLS MPP cells resulted in a significant loss of activity, 2000 KLS– MPP cells were transplanted into 3 lethally irradiated hosts with 250K whole bone marrow competitor cells of the recipient-type. In order to minimize any possibility of contamination, the cells were double sorted to achieve >99% purity with 0% contamination from KLS cells. Out of the three recipient mice, only mouse #2 showed a significant activity in all lineages, while the other two mice similarly showed significant output in only RBC and B cells (Figure 4.4A~E).

The presence of RBC and B cell output in all three lineages suggest that KLS– MPP contains at least erythroid/B cell bipotent progenitors. While CMP's capacity to produce B cells (Yang et al., 2005; Yang et al., 2007) and B cell progenitors exhibiting capacity for macrophage production (Montecino-Rodriguez et al., 2001) have been previously described, an erythroid/B cell bipotent progenitor has not been identified and warrants further investigation.

The observation that only one recipient out of the three demonstrated donor-derived cells in all lineages suggest that there is a multipotent progenitor within the KLS– MPP population; however, it may be rare and maintains a limited capacity for progeny production.

In vitro assessment of the KLS– subset suggests a weak T cell potential

The T cell potential demonstrated by the rare MPP of KLS– MPP was not entirely convincing (Figure 4.4E). Hence, an in vitro experiment was conducted to confirm the T cell potential. Sorted progenitor cells from KLS MPP and CLP were also used as positive controls. Sorted 100 cells per progenitor population per well was plated onto multiple wells seeded with OP9-DL1. The culture media was also supplemented with IL-7 and Flt3L to drive T cell development. The cells were cultured for 14 days, and analyzed with flow cytometry. T cell potential was determined using anti-CD44, anti-CD25 and anti-Thy1.1 antibodies to identify cells that have committed to the T cell lineage by progressing to DN2 stage (CD44+ CD25+ Thy1.1+) of thymocyte development as previously shown (Karsunky et al., 2008). The results showed that only a fraction of KLS– MPP seeded wells generated cells of T lineage, and when done so, they did it very poorly (Figure 4.5). The wells seeded with KLS MPP showed a greater fraction of wells generating T lineage cells, and did so most robustly out of the three populations tested. CLP also generated a frequent number of T lineage cells at intermediate level. The results are consistent with the currently accepted model that KLS MPP is the progenitor population of CLP. The weak T cell output seen in KLS– MPP cells confirmed our previous estimate that multipotent progenitor activity within the KLS– MPP fraction is rare and exhibits a limited capacity for multipotency.

Discussion

In this report we have demonstrated that myeloid progenitors in the KLS– compartment include a multipotent progenitor-like population within the CD62L+Flt3+

subset. This subset is phenotypically similar to KLS MPP, with the exception of Sca-1 level, leading us to suspect that it may be the most proximal progeny of KLS MPP. In vivo results have shown that when a large number of the subset was transplanted, they generated a significant amount of progenies in all lineages, prompting us to name them KLS– MPP. Subsequent in vivo and in vitro experiments have suggested that the multipotent progenitors within the KLS– MPP fraction may be rare and of limited capacity.

When a limited number of KLS– MPP were transplanted into lethally irradiated recipients, despite producing only transient, small quantities of platelets, myeloid leukocytes, and T cells, KLS– MPP generated significant amounts of RBC and B cells. The observed RBC and B cell levels were similar to those of the other two recipients with putative erythroid/B cell bipotent progenitors. This may be explained by the possibility that KLS– MPP contains mostly erythroid/B cell bipotent progenitors and much fewer MPP, which were responsible for generating the cells of the other lineage. It is also possible that multipotency observed in KLS– MPP, including the erythroid/B cell bipotency, may be due to individual non-multipotent precursors with already established lineage commitment that are contributing to the apparent multipotency in this subset. Therefore, future experiments examining this subset at clonal level are required to confirm the existence of multipotent progenitors.

Previous studies have reported that there are B220+ B precursors in the c-Kit^{High} Sca-1– compartment, overlapping with the myeloid progenitor population, however, this phenomenon occurs only in juvenile mice and not observed in adult mice as used in our experiments (Ogawa et al., 2000). Since we have observed significant B cell output from

KLS– MPP, finding a B cell precursor that lacks B220 expression from the previously categorized as a pool of myeloid progenitors would be a relevant addition to the field of B cell development.

Interestingly, early T cell potential was observed around week 2 posttransplant event throughout the experiments (Figure 4.2E, 4.3D, 4.4E). These early T cell events may indicate relatively mature bone marrow-derived progenitors that have homed to the thymus, instead of the bone marrow, and initiated T cell generation. The competitive transplant experiment of KLS– MPP versus KLS MPP showed that KLS– MPP did generate a minute but detectable amount of T cells at week 2, however, did not generate T cells at later times (Figure 4.3D). This may indicate the early homing of KLS– MPP to the thymus for T cell generation, only to be overtaken later when KLS MPP generated the primary wave of thymocytes. To verify that early homing takes place, temporal kinetics for thymus seeding by KLS– MPP must be examined directly and compared to the homing kinetics by KLS MPP and HSC.

Also, we have not investigated the expression patterns of CD62L and Flts3 in the previously identified CMP, GMP and MEP populations of the KLS– fraction. Since we have uncovered a potentially most immature population within the KLS– fraction through expressions of CD62L and Flt3, it would be interesting to see if the two markers are also expressed in CMP, the most immature population of the three.

Lastly, the evidence showing that CD62L+ Flt3+ subset of KLS– fraction exhibits multipotency and that CD62L–Flt3– cells have lost lymphoid lineage proposes a new model in which the downregulation of CD62L and Flt3 marks a maturation step from KLS– MPP to myeloid progenitors signified by commitment to the myeloid lineage.

Experimental procedures

Mice

Mice carrying the Thy1.1 and Ly5.1 alleles on the C57BL background were generated in our animal facility by mating the BKa.AK-Thy1^{a}/Ka and B6.SJL-Ptprc^{a} Pep3b/BoyJ strains and selecting for cosegregation of Thy1.1 and Ly5.1 (GFP–Thy1.1+Hbb^{S} mice). GFP transgenic mice, generated by microinjection of C57BL/6 oocytees, were kindly provided by Dr. Masaru Okabe (Osaka University, Osaka, Japan) (Nakanishi et al., 2002). In these mice, the GFP transgene is driven by the chicken β-actin promoter and is expressed in all lineages except in the erythroid lineage. Hence, hemoglobin variant alleles (Hbb^{S} and Hbb^{D}) were used to track erythroid engraftment (see below). In order to generate donor mice for transplant studies, we have crossed the GFP transgenic mice with GFP–Thy1.1+Hbb^{S} mice to generate GFP+Thy1.1+Hbb^{S} mice. B6.Cg-Gpi1^{a} Hbb^{D} H1^{b}/DehJ mice (Harrison et al., 1988) were kindly provided by Dr. David Harrison (Jackson Laboratory, Bar Harbor, ME, USA). These mice are GFP–Thy1.1–Hbb^{D} and were used as transplant recipients. All mice were kept in the animal resources center at the University of Utah under the institutional animal care and use committee approved protocols.

Antibodies

Monoclonal antibodies against CD2 (Rm2.2), CD3 (KT3-1.1), CD5 (53-7.3), CD8 (53-6.7), CD11b (M1/70), Ly-6G (RB6-8C5), TER119, B220 (CD45R; RA3-6B2), and CD19 (1D3) were purified from the media of cultured hybridoma cell lines. PE-conjugated Sca-1 monoclonal antibody was purchased from PharMingen (San Diego, CA,

USA). C-kit (3C11) monoclonal antibody was purified and conjugated to Alexa Fluor 647 in our laboratory. CD4 and CD8 monoclonal antibodies were purified and conjugated to allophycocyanin (APC). Biotinylated Flt3, CD62L APC-AF750, Thy1.1 PerCP-Cy5.5, Mac-1 PE and Gr-1 PE antibodies were purchased from eBioscience (San Diego, CA, USA).

Isolation of hematopoietic progenitors

In order to remove mature cells from the harvested whole bone marrow cells, lineage depletion was performed. The cells were incubated with a cocktail of rat antibodies to mature cell markers (CD2, CD3, CD5, CD8, CD11b, Ly-6G, TER119, B220 and CD19). Secondary labeling of mature cells was performed by two successive incubations with magnetic beads-coupled sheep anti-rat antibodies (Dynal, Oslo, Norway). Each incubation was followed by a depletion step of the labeled cells using a magnetic column (Dynal, Oslo, Norway). The depleted cells were stained with various fluorochrome-conjugated antibodies as indicated in the figures to electronically visualize and sort using FACS Aria instrument (BD Immunocytometry Systems, San Jose, CA, USA). DAPI was used to discriminate dead cells from live cells.

Bone marrow transplantation

The GFP–Thy1.1–Hbb^{D} recipient mice were lethally irradiated (^{137}Cs, 13 Gy delivered in a 3 hour-split dose) or sublethally irradiated (6 Gy, single dose) a day prior to the transplant day. Isolated GFP+Thy1.1+Hbb^{S} donor cells were injected into the

recipients retro-orbitally. The recipient mice were anesthetized with isoflurane using the E-Z Anesthesia system for the injection (Euthanex Corp., Palmer, PA).

Peripheral blood analysis

For the posttransplant analysis, peripheral blood samples were collected from the retro-orbital sinus with heparinized capillary tubes. The mice were anesthetized with isoflurane using the E-Z Anesthesia system (Euthanex Corp., Palmer, PA). Immediately after the collection of blood samples, 10 ul of blood per sample were set aside for platelet analysis. The rest of the samples were mixed with 500ul of 2% Dextran T500 (Amersham Biosciences, Piscataway, NJ) in PBS and incubated at 37 degree C for 30 min for sediment separation of the RBC and WBC fractions. The RBC fraction was processed for HPLC analysis (see below). WBC were stained with PE-conjugated antibodies against Mac-1 and Gr-1 for myeloid WBC detection, Biotinylated B220 or CD19 antibody with a subsequent labeling with Alexa Fluor 750-conjugated avidin for B cell detection, and CD4 and CD8 conjugated with APC for T cell detection. Platelets and WBC were analyzed by FACScan flow cytometer (BD Biosciences, San Jose, CA; modified by Cytek Development, Fremont, CA). Platelet analysis was performed by increasing forward and side scatter parameters until the platelet population could be gated to exclude contaminants.

HPLC analysis of hemoglobin variants

A HPLC cation exchange protocol was developed in our laboratory to discriminate and quantify Hbb^D and Hbb^S in the peripheral blood samples (Spangrude et

al., 2006). A stock solution of 100 mM 5,5'-dithiobis-(2-nitrobenzoic acid) (DTNB) (Sigma-Aldrich, St. Louis, MO) was prepared by dissolving 100 mg of DTNB in 2.5 ml of DMSO and stored at –20 degree C. The RBC fraction was derivatized by adding 5 ul of the RBC fraction into 250ul of 40 mM NaCl and 2 mM DTNB and incubating at room temperature for 30 minutes. Following centrifugation at 12,000 g for 2 minutes, the supernatant were analyzed using a VARIANT hemoglobin testing system (Bio-Rad Laboratories, Hercules, CA) with an optimized β–thalassemia short program.

In vitro T cell potential assay

To assay in vitro T cell potential, OP9-DL1 co-culture system was utilized as previously described (Wang et al., 2005). After the isolation of target populations using FACS, 100 cells per population per well was plated on 24-well plates with the stromal cell line OP9-DL1. The co-cultures were supplemented with Flt3L (10 ng/ml) and IL-7 (10 ng/ml). The co-culture was washed intermittently to discard the old media and replenished with fresh media and cytokines. After 14 days of co-culture, the cells were removed by forceful pipetting and analyzed for T lineage-committed cells using FACScan flow cytometer (BD Biosciences, San Jose, CA).

References

Akashi, K., Traver, D., Miyamoto, T., and Weissman, I.L. (2000). A clonogenic common myeloid progenitor that gives rise to all myeloid lineages. Nature *404*, 193-197.

Balciunaite, G., Ceredig, R., Massa, S. and Rolink, A.G. (2005). A B220+CD117+CD19- hematopoietic progenitor with potent lymphoid and myeloid developmental potential. Eur. J. Immunol. *35*, 2019-2030.

Bell, J.J., and Bhandoola, A. (2008). The earliest thymic progenitors for T cells possess myeloid lineage potential. Nature 452, 764-767.

Christensen, J.L., and Weissman, I.L. (2001). Flk2 is a marker in hematopoietic stem cell differentiation: a simple method to isolate long-term stem cells. Proc. Natl. Acad. Sci. USA *98*, 14541-14546.

Harrison, D.E., Astle, C.M., Lerner, C. (1988) Number and continuous proliferative pattern of transplanted primitive immunohematopoietic stem cells. Proc. Natl. Acad. Sci. USA. *85*, 822-826.

Ikuta, K., and Weissman, I.L. (1992). Evidence that hematopoietic stem cells express mouse c-kit but do not depend on steel factor for their generation. Proc. Natl. Acad. Sci. USA *89*, 1502-1506.

Kondo, M., Weissman, I.L., and Akashi, K. (1997). Identification of clonogenic common lymphoid progenitors in mouse bone marrow. Cell *91*, 661-672.

Kwak, J.Y., Cho, S., and Spangrude, G.J. (2007). Gradients of antigen expression and development potential in hematopoiesis. Ann. N.Y. Acad. Sci. *1106*, 82-88.

Lu, M., Tayu, R., Ikawa, T. et al. (2005). The earliest thymic progenitors in adults are restricted to T, NK, and dendritic cell lineage and have a potential to form more diverse TCRbeta chains than fetal progenitors. J. Immunol. *175*, 5848-5856.

Martin, C. H., Aifantis, I., Scimone, M.L. et al. (2003). Efficient thymic immigration of B220+ lymphoid-restricted bone marrow cells with T precursor potential. Nat. Immunol. *4*, 866-873.

Miller, J.P., Izon, D., DeMuth, W., Gerstein, R., Bhandoola, A. and Allman, D. (2002). The earliest step in B lineage differentiation from common lymphoid progenitors is critically dependent upon interleukin 7. J. Exp. Med. *196*, 705-711.

Montecino-Rodriguez, E., Leathers, H., and Dorshkind, K. (2001) Bipotential B-macrophage progenitors are present in adult bone marrow. Nat. Immunol. *2*, 83-88.

Nakanishi, T., Kuroiwa, A., Yamada, S., Isotani, A., Yamashita, A., Tairaka, A., Hayashi, T., Takagi, T., Ikawa, M., Matsuda, Y., and Okabe, M. (2002). FISH analysis of 142 EGFP transgene integration sites into the mouse genome. Genomics *80*, 564-574.

Ogawa, M., Boekel, E.T., and Melchers, F. (2000) Identification of CD19-B220+c-Kit+Flt3/Flk-2+ cells as early b lymphoid precursors before pre-B-I cells in juvenile mouse bone marrow. International Immunology *12*, 313-324.

Perry, S.S., Wang, H., Pierce, L.J., Yang, A.M., Tsai, S., and Spangrude, G.J. (2004). L-selectin defines a bone marrow analog to the thymic early T-lineage progenitor. Blood *103*, 2990-2996.

Porritt, H.E., Rumfelt, L.L., Tabrizifard, S., Schmitt, T.M., Zuniga-Pflucker, J.C. and Petrie, H.T. (2004). Heterogeneity among DN1 prothymocytes reveals multiple progenitors with different capacities to generate T cell and non-T cell lineages. Immunity *20*, 735-745.

Rumfelt, L.L., Zhou, Y., Rowley, B.M., Shinton, S.A. and Hardy, R.R. (2006). Lineage specification and plasticity in CD19- early B cell precursors. J. Exp. Med. *203*:675-687.

Schofield, R. (1978) The relationship between the spleen colony-forming cell and the haemopoietic stem cell. Blood *4*, 7-25.

Spangrude, G.J., Cho, S., Guedelhoefer, O., VanWoerkom, R.C., and Fleming, W.H. (2006). Mouse models of hematopoietic engraftment: limitations of transgenic green fluorescent protein strains and a high-performance liquid chromatography approach to analysis of erythroid chimerism. Stem Cells *24*, 2045-2051.

Spangrude, G.J., Heimfeld, S., and Weissman, I.L. (1988). Purification and characterization of mouse hematopoietic stem cells. Science *241*, 58-62.

Wada, H., Masuda, K., Satoh, R. Kakugawa, K., Ikawa, T., Katsura, Y., and Kawamoto, H. (2008). Adult T-cell progenitors retain myeloid potential. Nature 452, 768-77.

Yang, G.X., Lian, Z.X., Kikuchi, K., Moritoki, Y., Ansari, A.A., Liu, Y.J., Ikehara, S., and Gershwin, M.E. (2005). Plasmacytoid dendritic cells of different origins have distinct characteristics and functions: studies of lymphoid progenitors versus myeloid progenitors. J. Immunol. *175*, 7281-7287.

Yang, G.X., Lian, Z.X., Chuang, Y.H., Shu, S.A., Moritoki, Y., Lan, R., Wakabayashi, K., Ansari, A.A., Dorshkind, K., Ikehara, S., and Gershwin, M.E. (2007). Generation of functionally distinct B lymphocytes from common myeloid progenitors. Clin. Exp. Immunol. *150*, 349-357.

Yin, T., and Li, L. (2006) The stem cell niches in bone. J. Clin. Invest. *116*, 1195-1201.

Wang, H.F., Pierce, L.J., and Spangrude, G.J. (2005) Lymphoid potential of primitive bone marrow progenitors evaluated in vitro. Ann. N.Y. Acad. Sci. *1044*, 1-10.

Figure 4.1 Flow cytometric analysis of KLS– compartment. Panel A Whole bone marrow depleted of mature cells were analyzed with antibody labeling for c-kit and Sca-1. A typical flow cytometric representation is shown. Separation of c-Kit+Sca-1+ (KLS) and c-Kit+Sca-1– (KLS–) are demonstrated. **Panel B** The cells from panel A were gated for the KLS– population and analyzed for Flt3 and CD62L expressions. The cells were clearly present in three expression patterns: CD62L+Flt3+ (++), CD62L+Flt3– (+-), and CD62L–Flt3– (--). Using FACS sorting, 100K cells from each of the three populations were purified and transplanted through retro-orbital injection into lethally irradiated mice (4 recipients for ++, 5 recipients for +-, 5 recipients for --) with 250K recipient-type whole bone marrow cells as competitors.

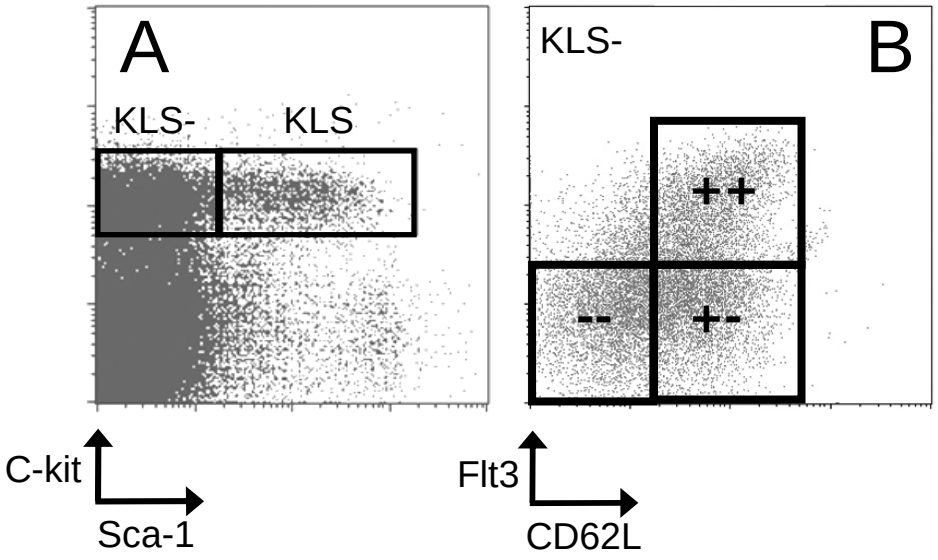
A
KLS-
KLS
C-kit
Sca-1
KLS-
B
++
--
+-
Flt3
CD62L

Figure 4.2 In vivo assessment of lineage potentials via bone marrow transplant. Over a 9 week period, bone marrow transplant recipients were bled with heparinized capillary tubes retro-orbitally to obtain peripheral blood samples. Error bars indicate standard deviation. **Panel A** Platelets were identified by forward and side scatters. Donor-derived platelets were quantified by measuring GFP+ platelets against competitor-derived GFP– platelets. The percentages indicate the donor-derived platelets among total platelets in peripheral blood. **Panel B** Donor-derived RBC's Hbb^S variant was measured against recipient type Hbb^D to quantify donor-derived RBC via HPLC. **Panel C** To determine myeloid potential, the amount of donor-derived leukocytes of myeloid lineage, granulocytes and monocytes, in the blood were measured. The percentages indicate the donor-derived fraction of the total myeloid leukocytes in the blood. **Panel D** To determine lymphoid lineage, donor-derived B cells were identified and quantified. The percentages indicate the donor-derived B cell fraction of the total B cells in the peripheral blood. **Panel E** The other member of the lymphoid lineage, T cells, are quantified here. Donor-derived T cell fraction is indicated by the percentages. Generally, T cell presence in the peripheral blood is detected later than B cell presence, due to T cell's developmental requirement for migration to the thymus.

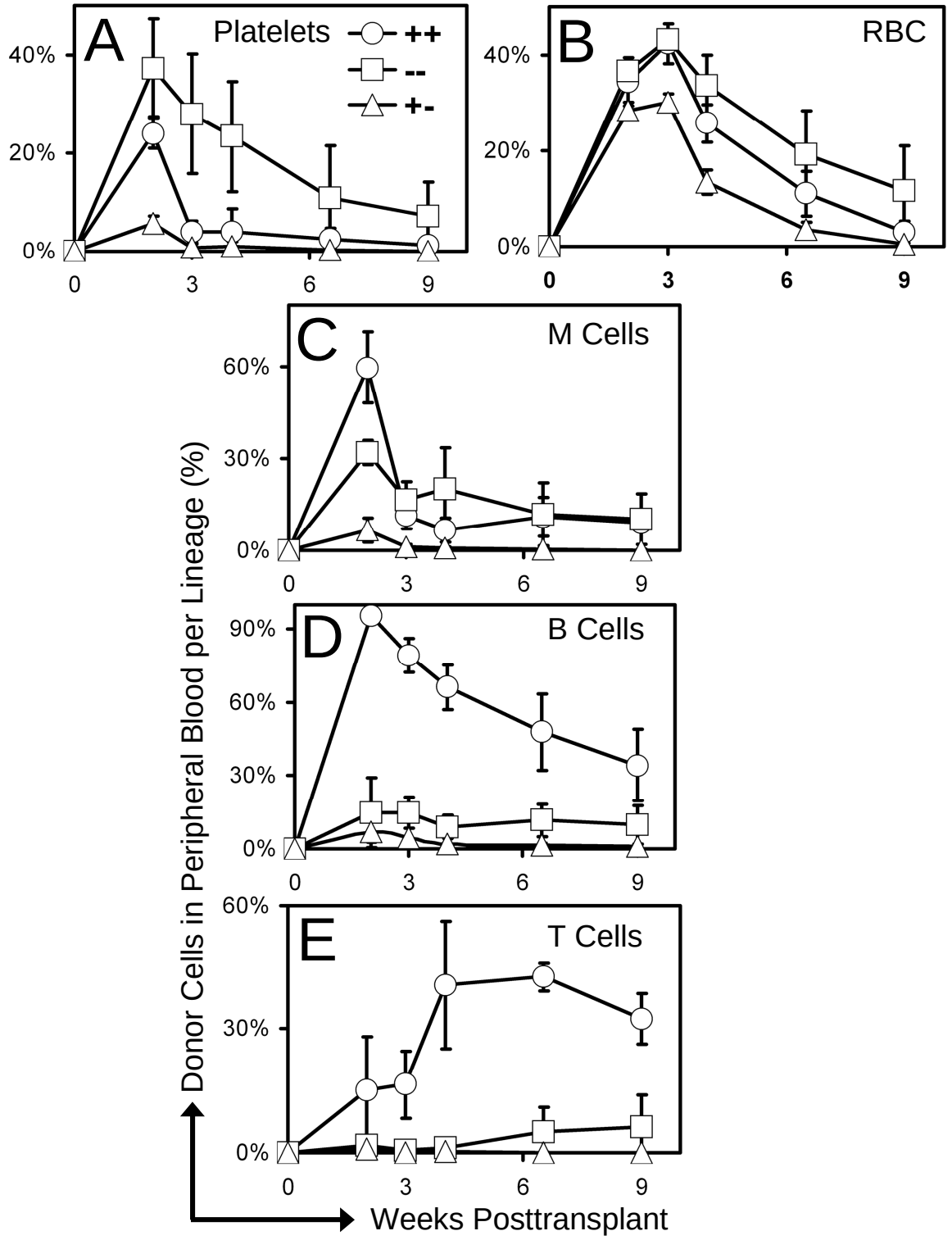
A
Platelets
++
--
+-
40%
20%
0%
0
3
6
9
B
RBC
40%
20%
0%
0
3
6
9
C
M Cells
60%
30%
0%
0
3
6
9
D
B Cells
90%
60%
30%
0%
0
3
6
9
E
T Cells
60%
30%
0%
0
3
6
9
Donor Cells in Peripheral Blood per Lineage (%)
Weeks Posttransplant

Figure 4.3 Competitive bone marrow transplant of Sca-1+ (KLS) MPP and Sca-1– (KLS–) MPP. **Panel A** A histogram schematic for peripheral blood analysis for the detection of the two donor-derived cells are shown. The transplant recipient derived-cells that express Ly5.2 and is not detectable by anti-Ly5.1-FITC antibody labeling or GFP expression is represented as the dotted curve. The Ly5.1-expressing KLS MPP-derived cells are represented as the gray curve. The GFP+ KLS– MPP-derived cells are represented as the black curve. **Panel B** Quantification of donor-derived myeloid leukocytes are shown. KLS MPP-derived granulocytes and monocytes are shown in gray. KLS– MPP-derived cells are shown in black. No myeloid leukocytes from KLS– MPP were detected. **Panel C** Donor-derived B cells are shown as in panel B. A minute but detectable amount of KLS– derived MPP was present. **Panel D** As in panel C, donor-derived T cells are shown to assess lymphoid potential. No significant amount of T cells was detected.

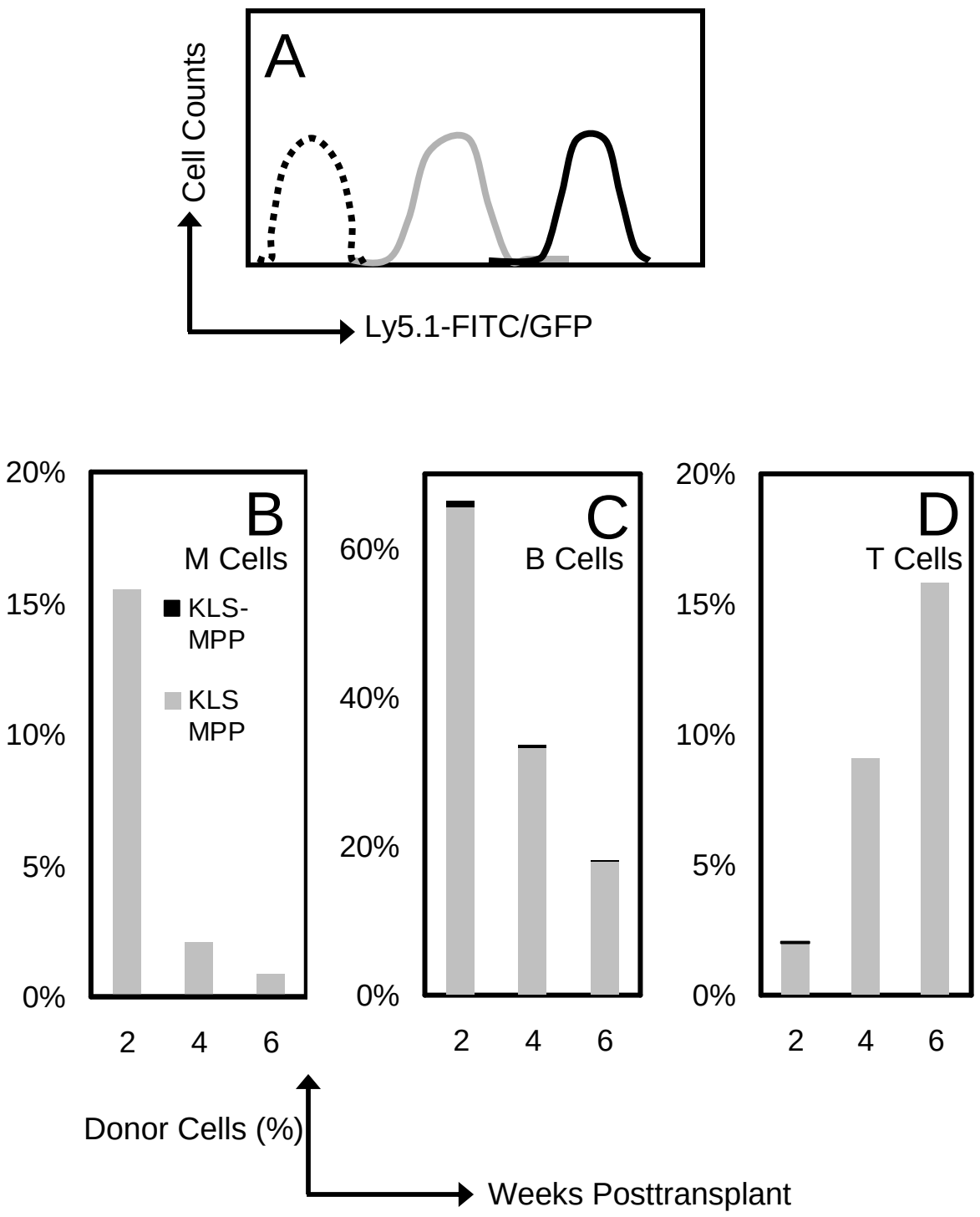
A
Cell Counts
Ly5.1-FITC/GFP
B
M Cells
KLS-
MPP
KLS
MPP
20%
15%
10%
5%
0%
C
B Cells
60%
40%
20%
0%
D
T Cells
20%
15%
10%
5%
0%
2
4
6
Donor Cells (%)
Weeks Posttransplant

Figure 4.4 Double-sorted KLS– MPP output for the assessment of Meg/E, myeloid leukocyte and lymphoid potentials. For the transplant, 2000 double-sorted KLS– MPP cells were injected into three lethally irradiated mice with 250K recipient-type competitor whole bone marrow cells. The average output found among the three recipients is shown as the black line. The percentages indicate the fraction of donor-derived cells from the total cells of the indicated lineage in the peripheral blood. **Panel A** Only a small amount of donor-derived platelets was detected from mouse 2. Mouse 1 and mouse 2 did not show any donor-derived platelet engraftment. **Panel B** All three recipients showed an early burst of RBC activity. **Panel C** All three recipients showed an early production of myeloid leukocytes, however, only one recipient (mouse 2) showed a nominal amount of cells while the other two showed only trace amounts. **Panel D** Strong B cell output was observed in all three recipients. **Panel E** As in panel A and C, only mouse 2 showed some measurable amount of T cells, Other two recipients generated barely detectable trace amounts at week 5.

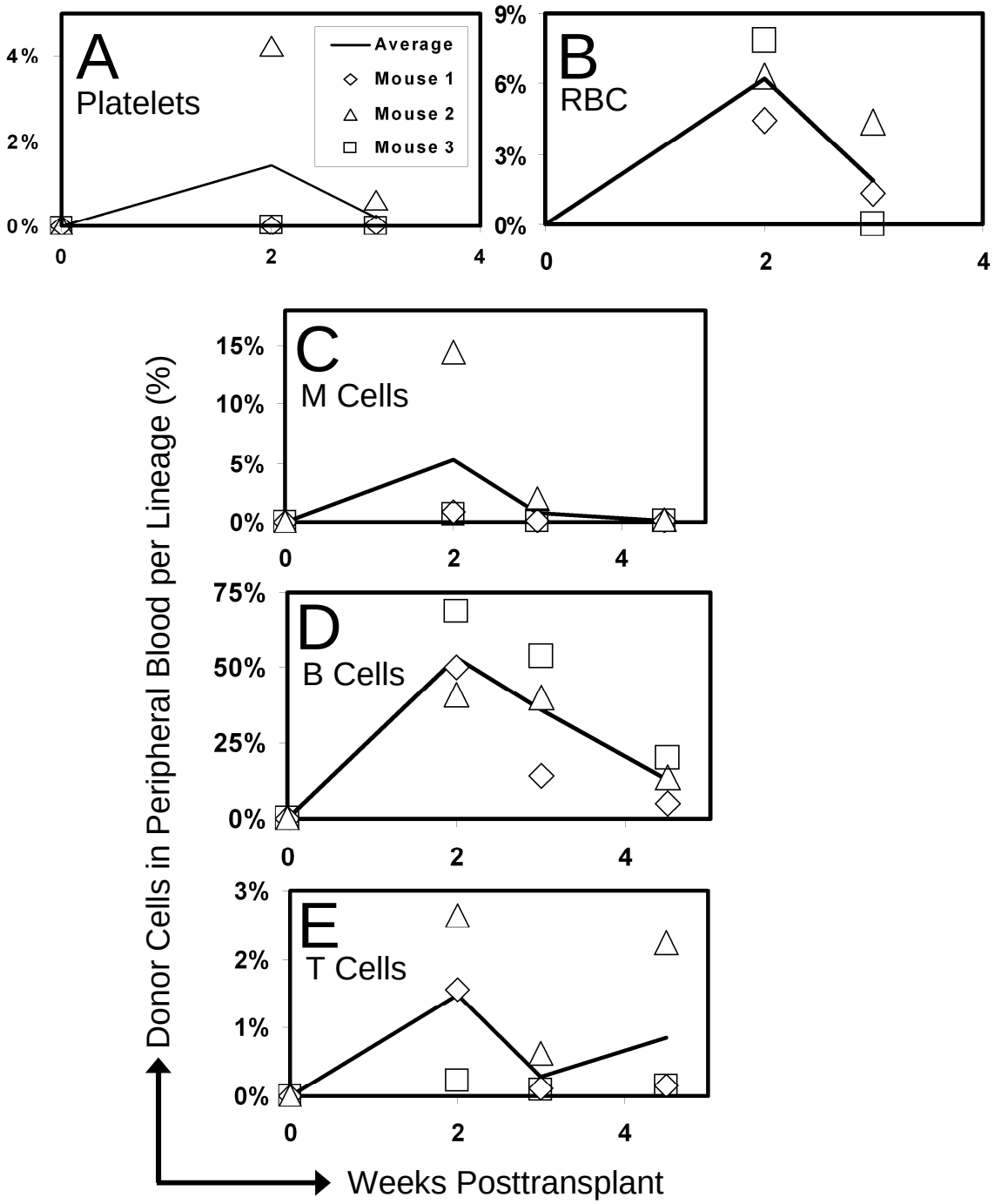
A
Platelets
Average
Mouse 1
Mouse 2
Mouse 3
4%
2%
0%
0
2
4
B
RBC
9%
6%
3%
0%
C
M Cells
15%
10%
5%
D
B Cells
75%
50%
25%
E
T Cells
3%
2%
1%
Donor Cells in Peripheral Blood per Lineage (%)
Weeks Posttransplant

Figure 4.5 In vitro assessment of T cell potential in KLS– MPP versus KLS+ MPP and CLP. In order to assay T cell potential, 100 cells per progenitor population per well were cultured with OP9-DL1 stromal cell line and supplemented with IL-7 and Flt3L cytokines to drive T cell development. The observed T cell output has been standardized to the average T cell output observed from KLS MPP seeded wells. Individual open symbols indicate the degree of T cell output observed per well. The closed symbols indicate the average of T cell output observed in the seeded wells per progenitor population.

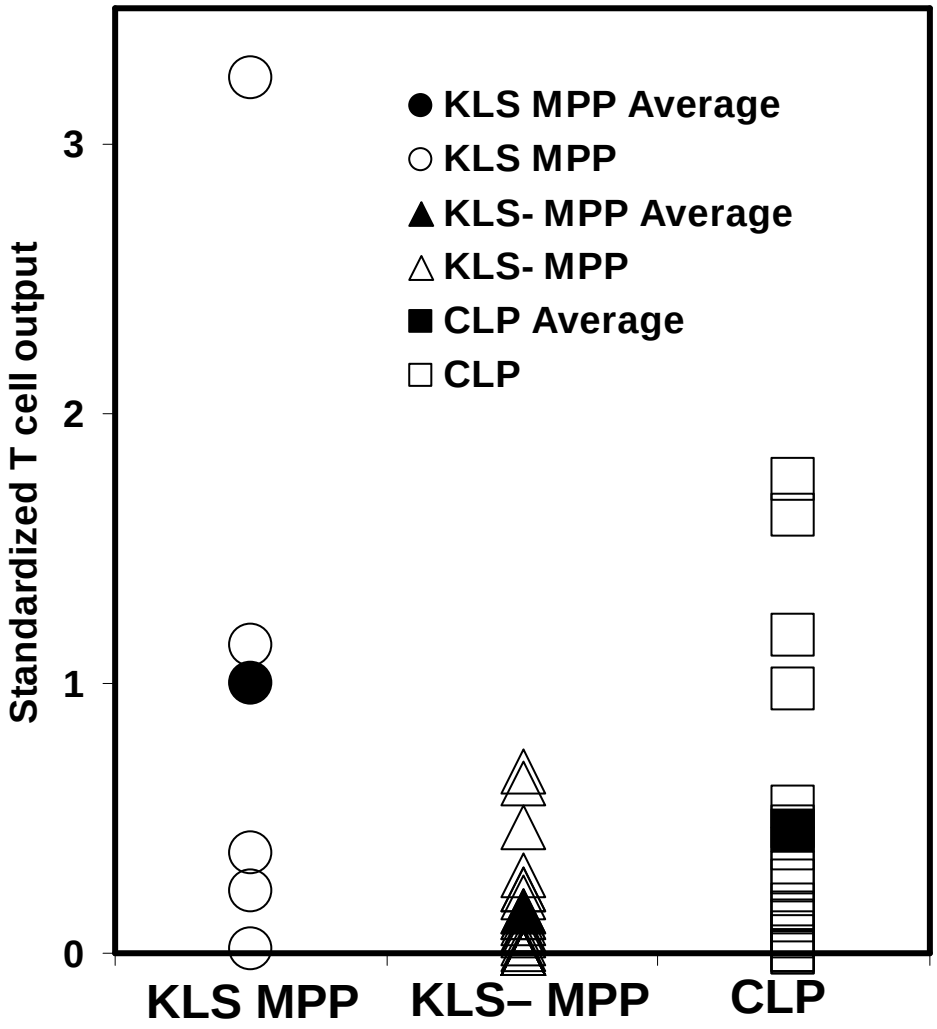
KLS MPP Average
KLS MPP
KLS- MPP Average
KLS- MPP
CLP Average
CLP
Standardized T cell output
0
1
2
3
KLS MPP
KLS– MPP
CLP

CHAPTER 5

SUMMARY

Identification of the CD62L– HSC compartment

Since the initial FACS-mediated enrichment of HSC using the expression patterns of Sca-1 and Thy1.1 (Spangrude et al., 1988), an impressive array of novel markers have been utilized in the quest for the purification of HSC. The current surface marker code for HSC enrichment is Sca-1+C-kit^{BRIGHT}Thy1.1^{LOW}Flt3–CD150+CD48–CD244–CD34–Rh-123$^{–/LOW}$Lin– (Spangurde et al., 1988; Spangrude and Johnson, 1990; Besmer, 1991; Ikuta and Weissman, 1992; Okada et al., 1993; Li and Johnson, 1995; Osawa et al., 1996; Morrison et al., 1997; Rawls et al., 2001; Yang et al., 2005; Kiel et al., 2005; Papathanasiou, 2009) Despite the discovery of numerous markers for HSC enrichment, no group has made the claim of achieving the absolutely pure HSC population, suggesting that the quest for the comprehensive marker set for HSC purification is not yet complete.

We have established the utilization of CD62L as an effective tool for the enrichment of HSC. In vivo evidence demonstrated that the fractionation of the KLS population using CD62L yielded a CD62L+ MPP subset and a CD62L– HSC subset (Figure 2.2 and 2.3). Our data showed that co-staining of KLS cells with CD62L and Thy1.1 resulted in a similar distribution of cells compared to the previously established stem cell markers Flt3 and Thy1.1 (Figure 2.1A and 2.1B). As one might expect from this result, CD62L and Flt3 demonstrated a high frequency of co-expression, approximately 75% of KLS cells (Figure 3.1B). Interestingly, transplanting 500 cells of the CD62L+ fraction successfully rescued lethally irradiated recipients. In contrast, our laboratory has reported previously that 1000 Thy1.1^{LOW} CD62L+ donor cells could not rescue lethally irradiated mice (Perry et al., 2004). The reasons for this discrepancy are

not clear, but may be due to the general health of the irradiated mice in the two experiments, differences in cell preparative methods, or other technical issues. We have also established CD62L as a highly effective tool for the segregation of HSC and MPP as evidenced by the transplant experiment showing a strong HSC activity with 100 CD62L– cells and a complete lack of HSC activity in a population containing 10,000 CD62L+ cells (Figure 2.4A and 2.4B).

In addition, our results establish CD62L as an efficient tool for enriching HSC beyond the capability of the widely used Flt3–Thy1.1^{LOW} strategy. Our CD62L expression analysis showed that there is a significant number of CD62L+ cells within the Flt3–Thy1.1^{LOW} compartment (Figure 2.5D, 2.5E and 2.6C). Subsequent transplant experiments utilizing KLSF– CD62L– and KLSF– CD62L+ cells demonstrated that >99% of HSC activity was localized to the KLSF– CD62L– compartment, while the KLSF– CD62L+ compartment exhibiting only a trace amount of activity (Figure 2.6; see the RU calculations in Chapter 2).

Our experiments have established CD62L as an efficient marker for HSC enrichment within the context of Flt3; however, the same has not been shown within the context of other markers. As discussed above, there are numerous markers that have been shown to also be effective for HSC enrichment. Therefore, future studies are warranted to investigate the co-expression profiles of CD62L with other HSC markers. In addition, it would be interesting to test the overall enhancement of HSC enrichment by utilizing a cocktail of all known HSC markers with or without CD62L.

Evidence for gradual and abrupt population shifts

One of the central debates among early hematopoietic development researchers is regarding the model of HSC differentiation. Recently, the version of the hematopoietic tree established by the Weissman group (Morrison et al., 1997; Kondo et al., 1997; Akashi et al., 2000; Adolfsson et al., 2001; Christensen and Weissman, 2001) has been the subject of intense scrutiny. The tree describes each early hematopoietic population as a stage of hematopoietic differentiation, progressing with abrupt loss of lineage potential and self-renewal capability. While it is now generally accepted that the loss of lineage potential is gradual and not limited to a particular population of cells (Adolfsson et al., 2005; Lai et al., 2005; Forsberg et al., 2006; Lai and Kondo, 2006), there are instances in which abrupt changes are evident. For example, the progression out of the HSC compartment is an abrupt process that is accompanied by changes in several markers. In our own studies, we have demonstrated that the expression of CD62L efficiently marks the end of capacity for continuous self renewal (Chapter 2). Other markers of HSC were established based on similar observations. However, this was not true for every stem cell marker. When we attempted to segregate the Sca-1^{HIGH}CD62L– and Sca-1^{LOW}CD62L– fraction of the KLS population, we observed that there was a greater HSC activity in the Sca-1^{HIGH} fraction, suggesting that it contained a greater number of HSC than the Sca-1^{LOW} fraction (Figure 2.5). Together, our results characterize two stem cell markers that are expressed differentially by HSC: CD62L, expression of which indicates abrupt loss of the stem cell's self-renewal capacity, and Sca-1, the expression of which is gradually lost by HSC as they differentiate.

These observations suggest the need for a comprehensive compilation of known markers and their expression patterns by the cells of early hematopoietic differentiation. This would result in a more accurate depiction of the hematopoietic tree, avoiding overgeneralization and misunderstanding of the events surrounding hematopoiesis.

Heterogeneity of MPP

The traditionally defined Flt3+ Thy1.1^{LOW} MPP population within the KLS subset has been shown to contain heterogeneous progenitor populations. Adolffson et al. have established lymphoid-biased multipotent progenitors (LMPP) as the top 25% of KLS cells for Flt3 expression that overlapped significantly with the traditional MPP but included limited Meg/E potential (Adolffson et al., 2005). More convincing results came from Kondo's group, which demonstrated that the MPP compartment contains two distinct populations according to VCAM-1 expression (Lai et al., 2005; Lai and Kondo, 2006). They reported that the VCAM-1– population was functionally similar to the LMPP, while the VCAM-1+ population contained MPP-like activity. Interestingly, they also reported that the VCAM-1+ population of KLS actually contained Flt3^{HIGH} and Flt3^{LOW} populations. This suggests that the Flt3^{HIGH} population within the VCAM-1+ subset may overlap with the LMPP subset, and that the Meg/E potential of the VCAM-1+ subset may originate from the Flt3^{LOW} subset. These reports indicate the necessity for the utilization of multiple markers to properly identify and subfractionate progenitor populations.

Our findings showed that CD62L is also capable of subfractionating the traditional MPP. We have observed that the MPP population contains CD62L+ and

CD62L– subsets with majority of cells belonging to the CD62L+ subset (Figure 3.1). Furthermore, our data indicated that these subpopulations can be further divided to Sca-1^{HIGh} and Sca-1^{LOW} populations. In vivo engraftment data of the four subpopulations demonstrated a gradual loss of Meg/E potential as the cells of the KLS MPP compartment lost Sca-1 expression without a significant loss in the lymphoid potential (Figure 3.3 and 3.4). In addition, the data showed that with the upregulation of CD62L, the progenitors developed a T cell-lineage bias (Table 3.1). Retrospective analysis of Flt3 levels in the CD62L+ and CD62L– MPP fractions showed the presence of similar expression intensity of Flt3, indicating that Flt3 itself cannot be used to distinguish the CD62L+ and CD62L– populations, despite the high degree of co-expression we have observed previously (Figure 3.1B and 3.6). The detection of a CD62L– fraction within the KLS MPP population also indicated that the CD62L-mediated HSC enrichment in Chapter 2 contains Flt3+ MPP contaminants and that in order to achieve higher purity, we must employ both markers.

Discovery of a rare KLS– MPP population

We have traced CD62L expression into the KLS– compartment to determine if a primitive MPP population resembling the KLS MPP population existed. The surface marker profile of CD62L and Flt3 in KLS– fraction demonstrated that there was a significant number of cells that expressed both markers (Figure 4.1B). Looking at the surface phenotype only, these cells resembled the phenotype of the KLS MPP cells with the sole exception of lacking Sca-1 expression. Therefore, the subset was referred to as KLS– MPP.

In vivo engraftment data showed that the KLS– MPP population does contain MPP activity, however, it was present prominently when a large number of cells were transplanted (Figure 4.2). When a limited number of cells were transplanted, the KLS– MPP subset exhibited MPP activity rarely (Figure 4.4). The in vitro assay also demonstrated that KLS- MPP cells exhibit a minor T-lineage activity (Figure 4.5). The discovery of a rare KLS– MPP subset was unexpected. The KLS– fraction has been previously characterized as a myeloid compartment that contains common myeloid progenitors (CMP) (Akashi et al., 2000). It is possible that the MPP activity we have observed represents a remnant of fading KLS MPP progenitors as they differentiate toward myeloid lineage commitment and downregulate Sca-1. It is also possible that the observed MPP activity represents a conglomeration of progenies generated from multiple types of progenitors with limited lineage potentials. A clonal analysis is required to verify that the multipotency observed is derived from a common progenitor rather than a mixture of unipotent precursor cells.

Evidence for B cell/erythroid bipotent progenitor

During the investigation of the KLS– MPP fraction, we have discovered evidence for a B cell/erythroid bipotent progenitor. Our transplant experiment, using a limited number of donor KLS– MPP cells, generated either MPP-like activity or small but detectable numbers of B cells and RBC (Figure 4.4). The competitive transplant study also revealed that these cells generated B cells, but not myeloid WBC, indicating that the progenitors responsible for B cell output were not CMP (Figure 4.3).

While the capacity of the CMP to produce B cells (Yang et al., 2005; Yang et al., 2007) and the B cell progenitors's capacity for macrophage production (Montecino-Rodriguez et al., 2001) have been previously described, a B cell/erythroid bipotent progenitor has not been identified. It is possible that the previously described CMP's capacity for B cell development may have been the result of B cell/erythroid bipotent progenitors present within the CMP compartment. Again, these issues points to the need for the development of a clonal analysis that is sensitive enough to detect progenitors with limited potential to determine in vivo the source of progenies of unknown origin.

Denouement

In conclusion, this dissertation presents the evidence gathered to test the hypothesis that CD62L can be used as a marker of hematopoietic differentiation. As the origin of hematopoiesis, HSC represents the foremost primitive population. Our demonstration that CD62L is not expressed by HSC establishes CD62L as a marker of HSC enrichment and the expression of CD62L as a marker of hematopoietic differentiation.

The MPP subpopulation with a severely reduced Meg/E potential represents the end stage within the KLS compartment. Our data support the CD62L hypothesis by showing that the majority of MPP in the hematopoietic stem cell compartment expresses CD62L, and that the CD62L+ MPP population exhibited minimal Meg/E potential. Our data also identified a CD62L– Flt3+ population that behaved as a traditionally described MPP and therefore, represents a transitional stage population between the CD62L+Flt3+ MPP and HSC.

Our experiments demonstrated a general trend that as Sca-1 level decreases, the progenitors progress further in their state of maturation. Our data showed that as Sca-1 level decreased in the CD62L– HSC compartment, the frequency of HSC also decreased. We also observed that as the Sca-1 level drops within the MPP population, so does the overall number of progenies produced. Lastly, as Sca-1 expression reached an undetectable level in the KLS– fraction, only a rare MPP activity and severely lineage limited progenitor activity were observed.

These findings suggest the need for the visualization of flow cytometric multiparameter analysis. With a typical dot plot representing only two parameters simultaneously, a biologically significant change in the expression of other parameters may go unnoticed to more casual observers. For instance, we have observed that the changes in CD62L and Sca-1 expressions in early hematopoietic progenitors resulted in the loss or reduction of progenitor activity. However, we have not examined their co-expression relationship in the context of another marker. We were able to take glimpses of their expression relationship as we attempted to subfractionate progenitor populations using three markers, such as in Chapter 2 where we utilized Flt3, CD62L and Sca-1 to obtain KLSF– CD62L–, KLSF– CD62L+, KLF–CD62L–Sca-1^{HIGH} and Sca-1^{LOW} ; however, a comprehensive examination of their expression patterns has not been performed. Therefore, as an example, a semi-three-parameter model using three stem cell markers have been constructed to demonstrate the benefits of examining the relationships of three parameters simultaneously (Figure 5.1).

The three-parameter model was constructed using typical two-parameter dot plots of CD62L versus Thy1.1 at three separate levels of Sca-1 expression (Sca-1^{LOW}, Sca-1^{INT}

and Sca-1^{HIGH}). Thy1.1 is represented on the X-axis, CD62L on the Y-axis, and Sca-1 on the Z-axis. The upper left quadrant of each Z-plane indicates the Thy1.1–CD62L+ cells of KLS. The change in the expression profile of CD62L versus Thy1.1 as Sca-1 level decreases is conspicuously evident. The increase in the number of cells present in the putatively most mature compartment of KLS is dramatic as Sca-1 level progresses from high to intermediate to low, while the number of cells in the immature CD62L–Thy1.1+ compartment decreases. By studying this model and recognizing the change in the CD62L expression pattern in the context of the other two already known stem cell markers, one may suspect that CD62L may mark different stages in hematopoietic differentiation without examining experiment results. An alternative data presentation such as the 3-parameter model provides additional details, and is helpful in enhancing the understanding and interpretation of data. Therefore, as we expand the number of markers available for studying early hematopoietic events, it is practical to utilize other methods such as 3D analysis that may be more appropriate for the execution of experiments and analysis of data to facilitate the progress of research.

References

Adolfsson, J., Borge, O.J., Bryder, D., Theilgaard-Monch, K., Astrand-Grundstrom, I., Sitnicka, E., Sasaki, Y., and Jacobsen, S.E. (2001). Upregulation of Flt3 expression within the bone marrow Lin(–)Sca1(+)c-kit(+) stem cell compartment is accompanied by loss of self-renewal capacity. Immunity *15*, 659-669.

Adolfsson, J., Mansson, R., Buza-Vidas, N., Hultquist, A., Liuba, K., Jensen, C.T., Bryder, D., Yang, L., Borge, O.J., Thoren, L.A., Anderson, K., Sitnicka, E., Sasaki, Y., Sigvardsson, M., and Jacobsen, S.E. (2005). Identification of Flt3+ lympho-myeloid stem cells lacking erythro-megakaryocytic potential: a new road map for blood lineage commitment. Cell *121*, 295-306.

Akashi, K., Traver, D., Miyamoto, T., and Weissman, I.L. (2000). A clonogenic common myeloid progenitor that gives rise to all myeloid lineages. Nature *404*, 193-197.

Besmer, P. (1991) The kit ligand encoded at the murine Steel locus: a pleiotropic growth and differentiation factor. Curr Opin Cell Biol *3*:939-946.

Christensen, J.L., and Weissman, I.L. (2001). Flk2 is a marker in hematopoietic stem cell differentiation: a simple method to isolate long-term stem cells. Proc. Natl. Acad. Sci. USA *98*, 14541-14546.

Forsberg, E.C., Prohaska, S.S., Katzman, S., Heffner, G.C., Stuart, J.M., and Weissman, I.L. (2005). Differential expression of novel potential regulators in hematopoietic stem cells. PLoS Genetics *1*, e28.10.1371/journal.pgen.0010028.

Ikuta, K., and Weissman, I.L. (1992). Evidence that hematopoietic stem cells express mouse c-kit but do not depend on steel factor for their generation. Proc. Natl. Acad. Sci. USA *89*, 1502-1506.

Kiel, M.J., Yilmaz, O.H., Iwashita, T., Yilmaz, O.H., Terhorst, C., and Morrison, s.J. (2005). SLAM family receptors distinguish hematopoietic stem and progenitor cells and reveal endothelial niches for stem cells. Cell *121*, 1109-1121.

Kondo, M., Weissman, I.L., and Akashi, K. (1997). Identification of clonogenic common lymphoid progenitors in mouse bone marrow. Cell *91*, 661-672.

Lai, A.Y., and Kondo, M. (2006). Asymmetrical lymphoid and myeloid lineage commitment in multipotent hematopoietic progenitors. J. Exp. Med. *203*, 1867-1873.

Lai, A.Y., Simon, M.L., Kondo, M. (2005). Heterogeneity of Flt3-expressing multipotent progenitors in mouse bone marrow. J. Immunol. *175*, 5016-5023.

Li, C.L., and Johnson, G.R. Murine hematopoietic stem and progenitor cells: I. enrichment and biologic characterization. Blood *85*, 1472-1479.

Morrison, S.J., Wandycz, A.M., Hemmatic, H.D., Wright, D.E., and Weissman, I.L. (1997). Identification of a lineage of multipotent hematopoietic progenitors. Development *124*, 1929-1939.

Okada, S., Nagayoshi, K., Nakuchi, H., Nishikawa, S.I., Miura, Y., and Suda, T. (1993) Sequential analysis of hematopoietic reconstitution achieved by transplantation of hematopoietic stem cells. Blood *81*, 1720-1725.

Osawa, M., Hanada, K., Hamada, H., and Nakauchi, H. (1996). Long-term lymphohematopoietic reconstitution by a single CD34-low/negative hematopoietic stem cell. Science *273*, 242-245.

Papathanasiou, P., Attema, J.L., Karsunky, H., Xu, J., Smale, S.T., Weissman, I.L. (2009). Evaluation of the long-term reconstituting subset of hematopoietic stem cells with CD150. Stem Cells *27*, 2498-2508.

Perry, S.S., Wang, H., Pierce, L.J., Yang, A.M., Tsai, S., and Spangrude, G.J. (2004). L-selectin defines a bone marrow analog to the thymic early T-lineage progenitor. Blood *103*, 2990-2996.

Rawls, J.F., Mellgren, E.M., and Johnson, S.L. (2001) How the zebrafish gets its stripes. Developmental Biology *240*, 301-314.

Spangurde, G.J., and Johnson, G.R. (1990) Resting and activated subsets of mouse multipotent hematopoietic stem cells. Proc. Natl. Acad. Sci. USA. *87*, 7433-7437.

Spangrude, G.J., Heimfeld, S., and Weissman, I.L. (1988). Purification and characterization of mouse hematopoietic stem cells. Science *241*, 58-62.

Yang, L., Bryder, D., Adolfsson, J., Nygren, J., Mansson, R., Sigvardsson, M., and Jacobsen, S.E. (2005). Identification of Lin(-)Sca1(+)-kit(+)CD34(+)Flt3-short-term hematopoietic stem cells capable of rapidly reconstituting and rescuing myeloablated transplant recipients. Blood *105*, 2717-2723.

Yang, G.X., Lian, Z.X., Chuang, Y.H., Shu, S.A., Moritoki, Y., Lan, R., Wakabayashi, K., Ansari, A.A., Dorshkind, K., Ikehara, S., and Gershwin, M.E. (2007). Generation of functionally distinct B lymphocytes from common myeloid progenitors. Clin. Exp. Immunol. *150*, 349-357.

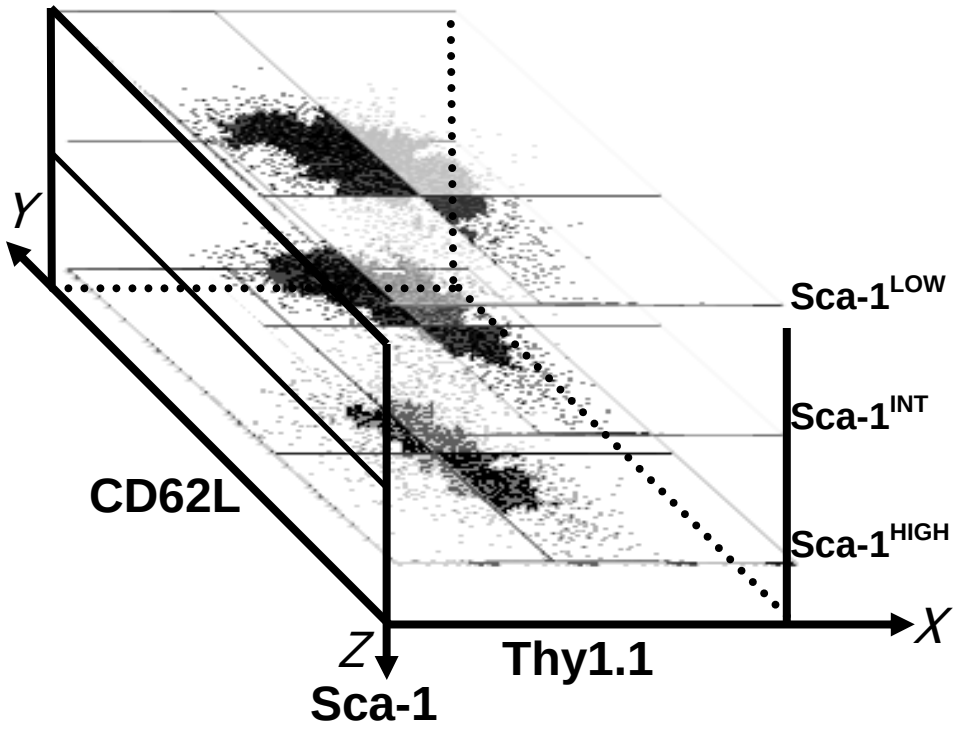

Figure 5.1 Three-parameter analysis of the hematopoietic stem cell compartment

APPENDIX A

MOUSE MODELS OF HEMATOPOIETIC ENGRAFTMENT: LIMITATIONS OF TRANSGENIC GREEN FLUORESCENT PROTEIN STRAINS AND A HIGH-PERFORMANCE LIQUID CHROMATOGRAPHY APPROACH TO ANALYSIS OF ERYTHROID CHIMERISM

Reprinted with permission from Spangrude, G.J., Cho, S., Guedelhoefer, O., VanWoerkom, R.C., and Fleming, W.H. (2006) Mouse models of hematopoietic engraftment: limitations of transgenic green fluorescent protein strains and a HPLC approach to analysis of erythroid chimerism. Stem Cells *24*, 2045-2051.

STEM CELLS®
TECHNOLOGY DEVELOPMENT

Mouse Models of Hematopoietic Engraftment: Limitations of Transgenic Green Fluorescent Protein Strains and a High-Performance Liquid Chromatography Approach to Analysis of Erythroid Chimerism

GERALD J. SPANGRUDE,[a,b] SCOTT CHO,[b] OTTO GUEDELHOEFER,[c] RYAN C. VANWOERKOM,[a] WILLIAM H. FLEMING[d]

[a]Department of Medicine, [b]Department of Pathology, and [c]Department of Neurobiology and Anatomy, University of Utah School of Medicine, Salt Lake City, Utah, USA; [d]Department of Medicine, Division of Hematology and Medical Oncology, Oregon Health & Science University, Portland, Oregon, USA

Key Words. Erythropoiesis • Hematopoietic chimerism • Hematopoietic cell transplantation • Engraftment

ABSTRACT

Transgenic mouse strains ubiquitously expressing green fluorescent protein (GFP) have enabled investigators to develop in vivo transplant models that can detect donor contributions to many different tissues. However, most GFP transgenics lack expression of the reporter in the erythroid lineage. We evaluated expression of GFP in the bone marrow of the OsbY01 transgenic mouse (B6-GFP) in the context of CD71 and TER-119 expression and found that GFP fluorescence is lost prior to the basophilic erythroblast stage of development. However, platelets in B6-GFP mice were found to be uniformly positive for GFP. We therefore used the GFP transgenic model in combination with allelic variants of CD45 and the hemoglobin β (Hbb) chain to develop a model system that allows all blood lineages to be followed in a mouse model of bone marrow transplantation (BMT). To detect Hbb variant molecules, we developed a new protocol based on high-performance liquid chromatography that is sensitive and precise, allowing rapid and quantitative analysis of erythroid chimerism. Platelet and leukocyte engraftment were detected by flow cytometry. BMT into sublethally irradiated (4 Gy) recipients demonstrated the failure of B6-GFP-derived cells to engraft relative to B6-CD45[a]-derived cells, suggesting that an immune barrier may prevent efficient engraftment of the transgenic cells in a setting of minimal ablation. These results establish limitations in the use of transgenic GFP expression as a donor marker in transplantation models. STEM CELLS *2006;24: 2045–2051*

INTRODUCTION

A number of mouse transplant models are available for analysis of engraftment following bone marrow transplantation. Traditionally, erythroid engraftment has been followed using naturally occurring variants of the hemoglobin β (Hbb) chain that have been bred onto a common genetic background [1]. The CD45 allelic model allows flow cytometric analysis of engraftment of the nucleated lineages [2] but is not capable of distinguishing donor-derived erythroid or platelet engraftment. Recently, the use of transgenic mouse strains ubiquitously expressing green fluorescent protein (GFP) as bone marrow donors has been explored as a model system, since donor cells can be readily detected and phenotyped by flow cytometry [3]. However, only one GFP transgenic strain has been reported to express fluorescence in erythrocytes [4], severely limiting simple analysis of erythroid engraftment by this method. Here, we combine CD45 and Hbb alleleic strains with the transgenic GFP model to compare relative efficiencies in detecting engraftment using the different donor markers. To facilitate analysis of erythroid engraftment, we developed a new high-performance liquid chromatography (HPLC) method capable of resolving the Hbb^d and Hbb^s variants.

MATERIALS AND METHODS

Animals

Mice carrying the Thy-1.1 and Ly-5.1 alleles on a C57BL background were generated in our breeding colony by mating the BKa.AK-*Thy1*^{a}/Ka and B6.SJL-*Ptprc*^{a} *Pep3*^{b}/BoyJ strains

Correspondence: Gerald J. Spangrude, Ph.D., University of Utah, Division of Hematology RM 4C416, 30 N 1900 East, Salt Lake City, Utah 84132-2408, USA. Telephone: 801-585-5544; Fax: 801-585-3778; e-mail: gspangrude@mac.com Received January 6, 2006; accepted for publication May 2, 2006; first published online in STEM CELLS *EXPRESS* May 11, 2006.
1066-5099/2006/$20.00/0 doi: 10.1634/stemcells.2006-0013

and selecting for cosegregation of Thy-1.1 (CD90[a]) and Ly-5.1 (CD45[a]). Hereafter, we refer to these mice as B6-CD45[a]. Breeding pairs of B6.Cg-*Gpi1*^{a} *Hbb*^{d} *H1*^{b}/DehJ mice [5] were kindly provided by David Harrison (Jackson Laboratory, Bar Harbor, ME). We refer to these mice as B6-Hbb[d]. C57BL/6CrSlc-Tg(ACTb-EGFP)OsbC14-Y01-FM131 mice were provided by Dr. Masaru Okabe (Osaka University, Osaka, Japan). This transgenic strain was generated by pronuclear injection of fertilized eggs obtained from C57BL/6 matings as previously described [6] and are here referred to as B6-GFP. All animals were maintained in the animal resources center at the University of Utah under protocols approved by the institutional animal care and use committee. All mice were maintained on sterilized food and acidified water to prevent colonization by *Pseudomonas.*

Flow Cytometry

Multiparameter flow cytometric analysis was performed using FACScan and FACSVantage instruments (BD Biosciences, San Jose, CA, http://www.bdbiosciences.com). Bone marrow samples were prepared by flushing isolated femurs with Hanks' balanced salt solution containing 5% newborn calf serum (HyClone, Logan, UT, http://www.hyclone.com). Peripheral blood samples were collected from the retroorbital sinus under isoflurane anesthesia (IsoSol; Vedco Inc., St. Joseph, MO, http://www.vedco.com) delivered using the E-Z Anesthesia system (Euthanex Corp., Palmer, PA, http://www.ezanesthesia.com/index2.htm). Blood was collected in heparinized capillary tubes and mixed with acid citrate dextrose at a 10:1 ratio prior to determination of the complete blood count using a Serono System 9010+CP hematology counter (Serono Diagnostics, Allentown, PA). Samples were then mixed with an equal volume of 2% Dextran T500 (Amersham Biosciences, Piscataway, NJ, http://www.amershambiosciences.com) in phosphate-buffered saline (PBS) and incubated at 37°C for 30 minutes. The upper layer, containing leukocytes, platelets, and residual erythrocytes, was collected for cytometric analysis, whereas the sedimented erythrocytes were washed twice in PBS and stored as a packed cell pellet at –20°C prior to Hbb analysis.

Cell surface antigens were identified using the following antibody conjugates: allophycocyanin-conjugated Ly-5.1; phycoerythrin-conjugated CD4, CD8, CD19, CD117, and Ly-6G (eBiosciences, San Diego, CA, http://www.ebioscience.com); phycoerythrin-conjugated CD11b and biotin-conjugated CD71 (BD Biosciences). TER-119 was purified from conditioned medium in our laboratory and detected using a phycoerythrin-conjugated anti-rat κ light chain reagent (BD Biosciences), followed by blocking with 10 μg of an isotype-matched monoclonal antibody (clone 53-7.3, anti-CD5). Streptavidin-conjugated Alexa Fluor-647-R-phycoerythrin was purchased from Invitrogen (Carlsbad, CA, http://www.invitrogen.com). Dead cells were excluded from analysis using forward and side scatter and propidium iodide gating.

Determination of Hbb Variants by Electrophoresis

Packed erythrocyte samples were lysed by freeze-thaw and clarified by centrifugation at 12,000*g* for 2 minutes. Cystamine derivatization was performed by mixing 20 μl of clarified erythrocyte lysate with 150 μl of a solution containing 67 mM cystamine dihydrochloride, 1.2 mM dithiothreitol, and 100 mM (0.2% wt/vol) ammonium hydroxide [7]. After 20–30 minutes, 5 μl of each sample was electrophoresed under alkaline conditions using the Paragon hemoglobin electrophoresis protocol (Beckman Coulter, Fullerton, CA, http://www.beckmancoulter.com). Dried agarose gels were imaged by scanning (Canon CanoScan LiDE 30 [Canon, Tokyo, http://www.canon.com] controlled by Adobe Photoshop, version 7.0 [Adobe, San Jose, CA, http://www.adobe.com], running on a Macintosh Dual G5 computer, OS X version 10.3.9 [Apple, Cupertino, CA, http://www.apple.com]) and quantitated using ImageJ software, version 1.33u (NIH, Bethesda, MD, http://rsb.info.nih.gov/ij).

Determination of Hbb Variants by HPLC

A cation exchange protocol was developed to separate and quantitate Hbb variant alleles by HPLC. A stock solution of 100 mM 5,5′-dithiobis-(2-nitrobenzoic acid) (DTNB) (Sigma-Aldrich, St. Louis, http://www.sigmaaldrich.com) was prepared by dissolving 10 mg of DTNB in 250 μl of dimethyl sulfoxide and stored at –20°C. Erythrocytes obtained from heparinized blood were washed three times in dextrose-gelatin-veronal buffer and stored as packed pellets at 4°C for up to 2 weeks prior to analysis. Samples were derivatized by adding 5 μl of packed erythrocytes to 100 μl of 40 mM NaCl, 1 mM DTNB and incubating at room temperature for 30 minutes. Following centrifugation (12,000*g* for 2 minutes), samples (20 μl) were injected onto a strong cation exchange column (Shodex IEC SP-825; Phenomenex, Torrance, CA, http://www.phenomenex.com) equilibrated in Buffer A (10 mM citrate, 12.5 mM NaCl, 25 μM thimerosal, pH 5.88), using a Beckman System Gold model 125 solvent module. A convex gradient to Buffer B (10 mM citrate, 30 mM NaCl, 25 μM thimerosal, pH 6.0) was applied over 3.5 minutes at a flow rate of 2 ml/minute and held for 2.9 minutes, followed by a high-salt wash (350 mM NaCl). The column was re-equilibrated in Buffer A between samples for 3 minutes at 2 ml/minute. Protein peaks were detected at 280 and 415 nm after subtraction of background detected at 490 nm, using a Beckman System Gold model 168 diode array detector module. The Hbb[d] variant eluted at 2.9 $\pm$ 0.2 minutes, whereas the Hbb[s] variant eluted at 5.6 $\pm$ 0.1 minutes (mean $\pm$ SD; n = 8). Absorbance data collected at 415 nm were integrated using Beckman System Gold software version 8.1.0 to determine percentage of Hbb[s] and Hbb[d] in experimental samples.

Bone Marrow Transplantation

To directly compare the GFP and CD45 systems in a transplant model, bone marrow cells obtained from B6-CD45[a] and B6-GFP donor animals were mixed at a 50:50 ratio. Radiation was delivered to B6-Hbb[d] recipient mice in a single dose (4 Gy) or in a split dose (2 $\times$ 4 or 2 $\times$ 6 Gy) with a 3-hour interval between doses, using a Shepherd Mark I ^{137}Cs source (JL Shepherd and Associates, Glendale, CA, http://www.jlshepherd.com) at a dose rate of 0.8 Gy/minute. Bone marrow cells were transplanted by the retro-orbital route under isoflurane anesthesia at a dose of 2 $\times$ 10^{6} total cells in 0.2 ml. Peripheral blood samples were collected weekly for analysis of trilineage donor-derived engraftment, as described above and shown in Figure 1.

To confirm the engraftment barrier against B6-GFP bone marrow cells in sublethally irradiated B6-Hbb[d] recipient mice, we transplanted 2 $\times$ 10^{6} bone marrow cells obtained from B6-CD45[a] or B6-GFP donor animals into separate groups of

Table 1. Mouse strains and markers used in transplant experiments

Strain	CD45	Hbb	GFP
B6-CD45^{a}	a	s	negative
B6-Hbb^{d}	b	d	negative
B6-GFP	b	s	positive

Abbreviations: GFP, green fluorescent protein; Hbb, hemoglobin β.

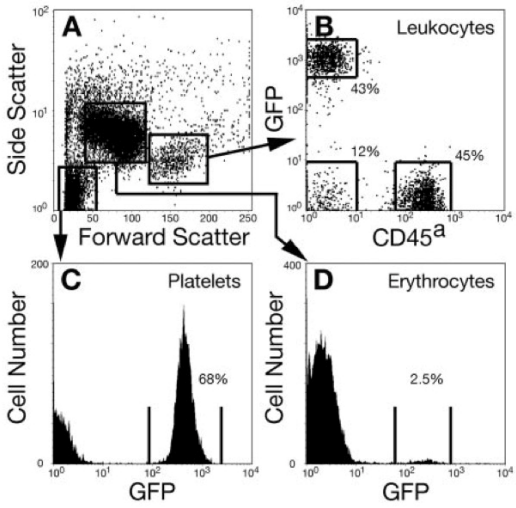

Figure 1. Identification and phenotyping of peripheral blood leukocytes, platelets, and erythrocytes by flow cytometry. Peripheral blood was collected from a supralethally irradiated (2 × 6 Gy) B6-hemoglobin β (Hbb)^{d} recipient 4 weeks after transplantation of bone marrow cells obtained from B6-CD45^{a} and B6-GFP donor animals (1 × 10^{6} from each donor). **(A):** Erythrocyte-depleted peripheral blood was analyzed by forward and side scatter to identify platelets, residual erythrocytes, and leukocytes, as shown by the boxed regions. **(B):** Analysis of cells falling within the leukocyte gate demonstrating three populations, which are derived from the two donor marrow grafts and from endogenous hematopoietic recovery (GFP^{neg}CD45$^{a\text{-}neg}$). **(C):** Analysis of cells falling within the platelet gate, demonstrating expression of GFP by 68% of the platelets. **(D):** Analysis of cells falling within the erythrocyte gate, demonstrating expression of GFP by 2.5% of erythrocytes. Abbreviation: GFP, green fluorescent protein.

irradiated (4 Gy) recipients. Peripheral blood samples were collected weekly for analysis of trilineage donor-derived engraftment, as described above.

Results

Strategy for Comparison of CD45 and GFP as Markers of Donor Engraftment

To directly compare the efficiency of the CD45 and GFP markers in a transplant setting, we designed an experiment in which bone marrow cells obtained from B6-CD45^{a} and B6-GFP donors were mixed and transplanted into irradiated B6-Hbb^{d} recipient mice (Table 1). If the two donor populations function with equal efficiency at engraftment in the recipient animals, we would predict equal representation of cells expressing each marker in all blood lineages. Because CD45 is not expressed by

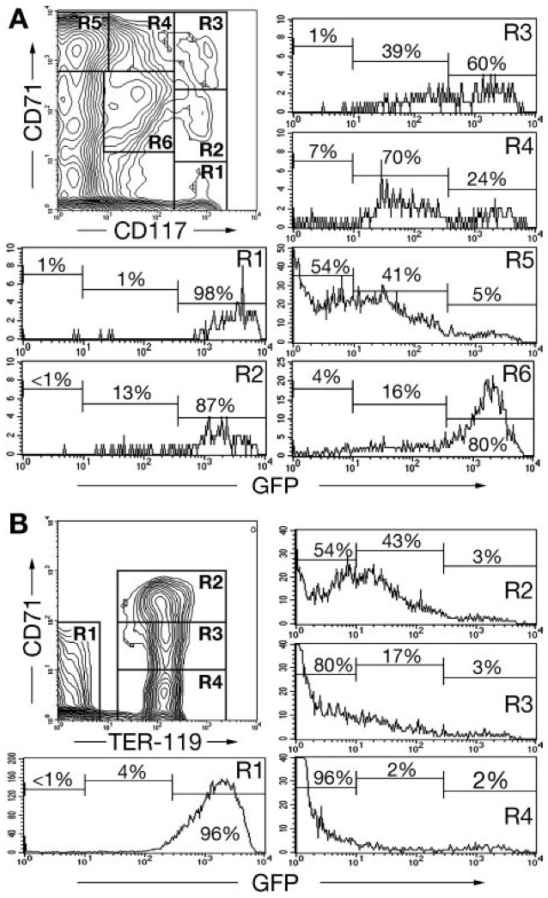

Figure 2. Analysis of GFP expression throughout erythroid lineage development in the bone marrow of B6-GFP mice. **(A):** Bone marrow cells obtained from a B6-GFP donor were stained with allophycocyanin-CD117 and biotin-CD71 antibodies, followed by streptavidin-phycoerythrin-Alexa-Fluor 647. Dead cells were excluded by propidium iodide and scatter gating. The contour plot represents 80% log density. Erythroid development proceeds from a CD117^{high} CD71^{neg} stage (R1) through intermediate stages (R2–R4) to the basophilic erythroblast stage (R5). Lymphoid development proceeds through a CD117^{low} CD71^{low} intermediate (R6). Analysis of GFP expression by the gated populations demonstrates progressive loss of GFP fluorescence during erythroid, but not lymphoid, differentiation. **(B):** Bone marrow cells obtained from a B6-GFP donor were stained with TER-119 followed by phycoerythrin-anti-rat, blocked with an isotype-matched control, and followed with biotin-anti-CD71 and streptavidin-phycoerythrin-Alexa-Fluor 647. Dead cells were excluded by propidium iodide and scatter gating. The contour plot represents 80% log density. Erythroid development proceeds from the basophilic erythroblast stage (R2) to the orthochromatic erythroblast and later stages (R4). GFP expression is already decreased by 100-fold at the basophilic erythroblast stage compared with earlier progenitors (R1) and is progressively lost during maturation. Abbreviation: GFP, green fluorescent protein.

erythrocytes or platelets, however, we were only able to directly compare engraftment of the two bone marrow samples in the leukocyte lineages. We expected to find GFP expression in erythrocyte and platelet lineages, as well as leukocyte lineages. Figure 1 shows a flow cytometry analysis of a 2 × 6 Gy

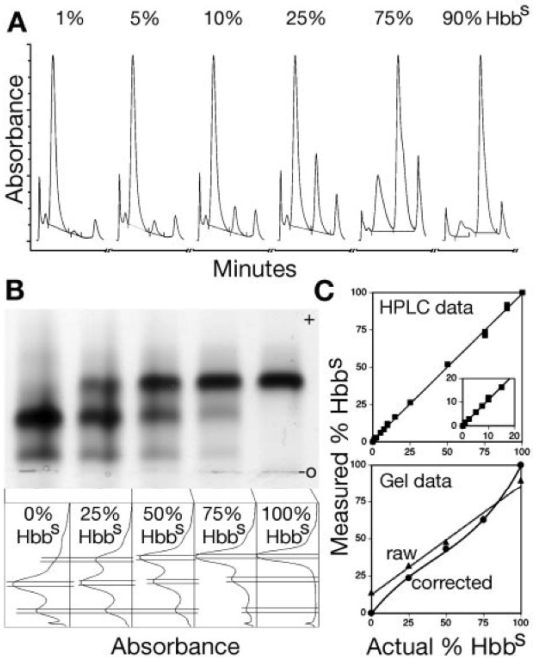

Figure 3. Detection of Hbb allelic variants by HPLC. **(A):** Elution profiles of samples obtained by mixing Hbb^s and Hbb^d blood in defined ratios. The actual percentage of the B6 allelic variant (Hbb^s) is noted above each sample. **(B):** Control mixtures of the indicated percentages of Hbb^s and Hbb^d samples were analyzed by alkaline gel electrophoresis. The origin of application (○) and polarity of the gel (+) are indicated. The dried gel was photographed and analyzed using ImageJ software to integrate the band densities. **(C):** Data obtained by HPLC and gel electrophoresis methods were plotted to demonstrate the relationship between actual and measured percent Hbb^s as determined by the two techniques. HPLC results are linear ($r^2 = .998$) and can accurately detect 1% Hbb^s in a mixture of the two isoforms. To determine the precision of the HPLC method, we evaluated a sample obtained by mixing 5 μl of Hbb^s lysate with 20 μl of Hbb^d lysate in a series of eight sequential HPLC runs and found that the assay detected 21.5 ± 1.8% Hbb^s (mean ± SD; range = 18.5%–24.0%). Raw gel data indicate that the background density in the gel was not subtracted from the peaks, whereas corrected gel data include background subtraction. Raw gel data are linear but have a limit of detection of ~10%. Abbreviations: Hbb, hemoglobin β; HPLC, high-performance liquid chromatography.

irradiated recipient evaluated 4 weeks after transplant. We were able to identify platelet, erythroid, and leukocyte subsets of peripheral blood samples based on forward and side scatter characteristics, as shown in Figure 1A. Gating on the leukocyte subset, we evaluated expression of GFP and $CD45^a$ and found these markers to be present in equal frequencies on mutually exclusive populations, as expected (Fig. 1B). However, although GFP was expressed on approximately 70% of the platelets in this chimeric mouse (Fig. 1C), consistent with the 1:1 transplant of GFP^{pos}:GFP^{neg} bone marrow cells, very little GFP was detected in the erythrocyte lineage (Fig. 1D). This result indicates that although the particular B6-GFP donor mouse strain used in this study allows leukocyte and platelet chimerism to be measured, donor-derived contributions to the erythroid lineage cannot be distinguished from endogenous hematopoietic recovery.

Detection of GFP in Blood Cells Obtained from B6-GFP Transgenic Mice

To determine the stage of erythroid development at which GFP fluorescence is lost, we evaluated the bone marrow of B6-GFP mice with respect to three antigens associated with erythroid differentiation [8]. CD117, the cell surface receptor for steel factor, is expressed early in hematopoiesis and is important for development of the erythroid lineage. CD71, the receptor for transferrin, is expressed at the proerythroblast stage and is maintained at high levels through the basophilic erythroblast stage. CD71 expression is downregulated at the polychromatic erythroblast stage and is absent on reticulocytes and erythrocytes. This developmental sequence can be visualized as gated populations R1–R5, as shown in Figure 2A. The progression of differentiation from early multipotent progenitor cells (Fig. 2A, $CD117^{high}CD71^{neg}$, R1) through several intermediate stages ($CD117^{high}CD71^{low}$, R2; $CD117^{high}CD71^{high}$, R3; $CD117^{low}CD71^{high}$, R4) to the basophilic erythroblast stage ($CD117^{neg}CD71^{high}$, R5) can be visualized using this strategy, as originally described by Socolovsky et al. [8]. Analysis of GFP expression at individual stages of this developmental progression (Fig. 2A) shows decreased fluorescence beginning at the earliest stage of CD71 expression (R2, 87% GFP^{high}) with a transient GFP^{low} phase (Fig. 2A, R3 and R4) followed by the basophilic erythroblast stage ($CD117^{neg}CD71^{high}$), where ~50% of the cells are GFP^{neg} (Fig. 2A, R5). A second developmental pathway, characterized by the phenotype $CD117^{low}CD71^{low}$, correlates with commitment to the lymphoid pathway with concomitant loss of erythroid and megakaryocytic potential [9] and largely retains a GFP^{high} phenotype (Fig. 2A, R6).

GFP Fluorescence Is Lost Prior to the Terminal Stages of Erythroid Development

The lack of GFP fluorescence in the erythroid lineage of B6-GFP mice could be due to degradation of GFP protein over the lifespan of the erythrocyte, decreased synthesis during erythroid development, or both. To further clarify expression of the transgene during erythroid development, we evaluated CD71 expression with respect to TER-119. TER-119 is expressed from the proerythroblast stage of erythroid development and persists through enucleation and throughout the life of the erythrocytes. In contrast, CD71 expression is extinguished at the orthochromatic erythroblast stage of development [8]. As shown in Figure 2B, this analysis revealed rapid loss of GFP fluorescence by $TER\text{-}119^{pos}$ cells during the transition between $CD71^{high}$ (Fig. 2B, R2) to $CD71^{neg}$ (Fig. 2B, R4). These data suggest that GFP expression is lost in the erythroid lineage due to a global repression of nonerythroid genes during development rather than due to fluorescence quenching by hemoglobin or degradation of GFP over the lifespan of the erythrocyte. This interpretation is strengthened by a recent description of a GFP transgenic strain that retains GFP fluorescence in erythrocytes, unlike other transgenic founders harboring the same expression construct [4]. Thus, transgenic GFP expression is likely silenced at the transcriptional level in the erythroid lineage, depending on the site of integration into the genome.

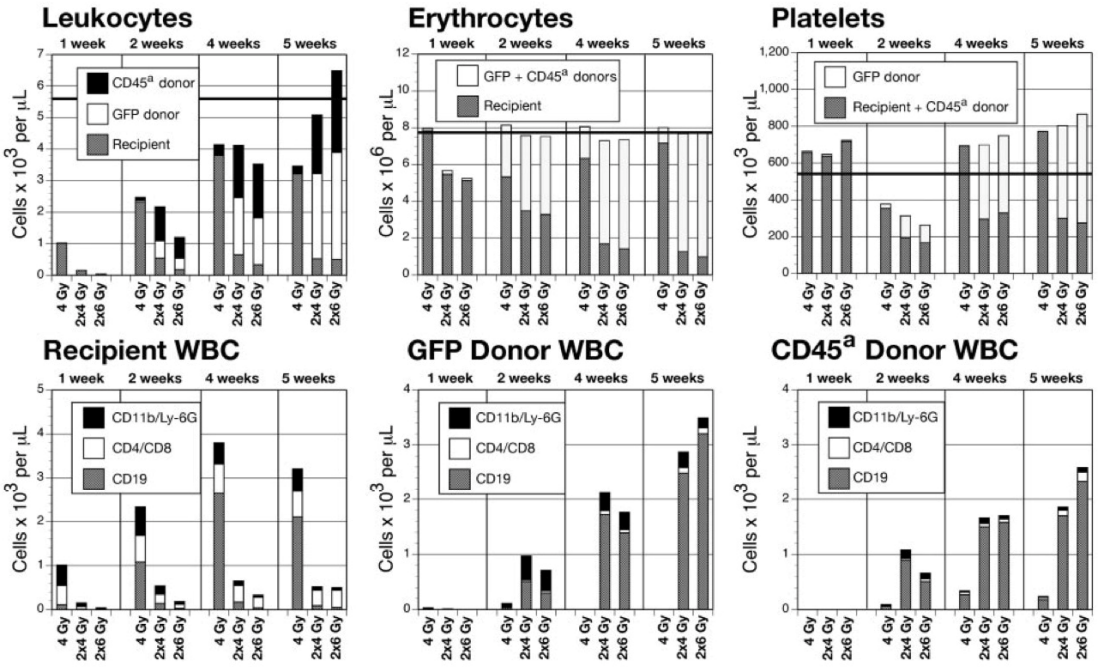

Figure 4. A bone marrow transplant experiment in which equal numbers of bone marrow cells obtained from B6-GFP and B6-CD45^a donors were transplanted into B6-hemoglobin β (Hbb)^d recipients after radiation conditioning at three doses. Top panels: Absolute cell numbers were derived by calculations based on complete blood counts and chimerism analysis for GFP, CD45^a, and Hbb^s. The horizontal lines in each plot indicate the lowest count found for that parameter in a group of 12 normal B6 mice. Normal distributions of each parameter (mean $\pm$ SD) in this group of mice were as follows: leukocytes, 8.8 $\pm$ 2.0 $\times$ 10^3 cells per μl; erythrocytes, 8.5 $\pm$ 0.6 $\times$ 10^6 cells per μl; platelets, 930 $\pm$ 270 $\times$ 10^3 cells per μl. Bottom panels: Peripheral blood leukocytes (WBC) were phenotyped by flow cytometry and are plotted as the number of cells in myeloid (CD11b/Ly-6G), T lymphocyte (CD4/CD8), and B lymphocyte (CD19) lineages that are derived from endogenous recovery or from each of the two donors of bone marrow cells, as indicated. Abbreviations: GFP, green fluorescent protein; WBC, white blood cells.

Detection of Hemoglobin Variants by HPLC

Allelic variants of mouse Hbb can be distinguished by alkaline gel electrophoresis. The Hbb^s variant found in C57BL strain mice differs from the Hbb^d variant by a Cys $\rightarrow$ Gly substitution at position 13. Reduction of thiol groups with cystamine introduces a differential charge due to this allelic variation that allows clear resolution of the two alleles by agarose electrophoresis under alkaline conditions [7]. However, the gel electrophoresis detection system is cumbersome for routine analysis and can present problems of interpretation and quantitation due to irregularities in the gel and underloading or overloading of samples. We therefore developed an automated HPLC method for mouse Hbb analysis (Fig. 3A). Mouse erythrocyte lysates are first reacted with DTNB to reduce free thiols with an acidic moiety. Lysates are then separated by cation exchange chromatography under conditions that resolve Hbb^s from Hbb^d due to the Cys $\rightarrow$ Gly substitution at position 13 in Hbb^s. The acidic charge introduced into Hbb^d by the DTNB derivatization reduces the retention time of Hbb^d to 2.9 minutes, compared with 5.6 minutes for Hbb^s. The two peaks are readily resolved in less than 10 minutes (Fig. 3A). Alkaline gel electrophoresis after reduction with cystamine also resolves the two isoforms (Fig. 3B) but requires quantitation by scanning of the gel. A comparison of artificial mixtures of lysates of the two isoforms showed that although both methods exhibited a linear relationship between measured and actual percent Hbb^s (Fig. 3C), the limit of detection for the gel technique was ~10%, whereas the HPLC technique detected as little as 1% variant Hbb isoform. Correction of the gel data by background subtraction improved resolution at the extremes of the dose-response curve but also led to a nonlinear relationship between measured and actual percent Hbb^s. These data demonstrate that the HPLC method is superior to gel electrophoresis for measuring erythroid chimerism. Since the DTNB-treated lysates are relatively stable, batches of samples can be prepared and run unattended using an HPLC autosampler. Unlike gel electrophoresis, analysis of HPLC data does not require the manual process of quantitation by scanning and integrating the gel bands. Therefore, the HPLC technique represents an automated, rapid throughput approach for routine analysis of mouse Hbb isoforms.

Analysis of Trilineage Engraftment Kinetics in a Mouse Model of Bone Marrow Transplantation

We compared engraftment of B6-CD45^a and B6-GFP bone marrow cells in a competitive setting, where equal numbers of cells from each donor strain were mixed and injected into B6-Hbb^d recipient mice (Fig. 4). Recipients were conditioned with sublethal (4 Gy), lethal (2 $\times$ 4 Gy), and supralethal (2 $\times$ 6 Gy) doses of radiation prior to transplantation. Lethal and supralethal doses of radiation differ in that the latter is fully myeloablative, whereas the former is only partially myeloablative. Sublethal radiation represents a model for nonmyeloabla-

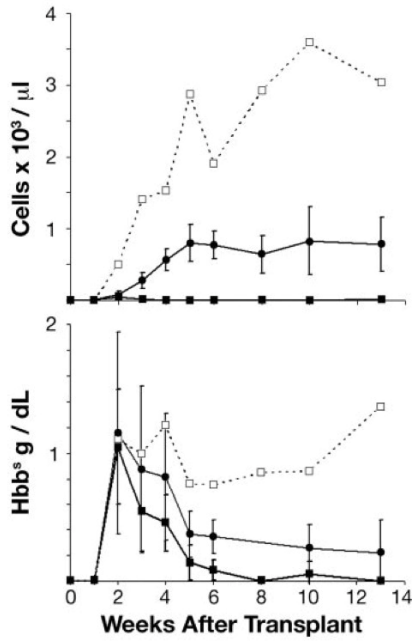

Figure 5. A bone marrow transplant experiment in which bone marrow cells obtained from B6-GFP and B6-CD45^a donors were transplanted separately into B6-Hbb^d recipients after radiation conditioning at a dose of 4 Gy. Top panel: Leukocyte (T cells, B cells, and myeloid cells) engraftment was detected by flow cytometric analysis after antibody staining of CD19, CD4, CD8, Mac-1, and Gr-1 antigens. The cell number was derived from donor contribution fractions from flow cytometric analysis and total leukocyte count. CD45^a donor (circles) engraftment of leukocytes was significantly higher than GFP donor (filled squares) engraftment, excluding the GFP donor outlier (open squares). Bottom panel: Hemoglobin contributions from B6-GFP donor (Hdd^s) and B6-CD45^a Donor (Hdd^s) bone marrow transplants into B6-Hbb^d recipients after sublethal radiation conditioning (4 Gy). Donor-derived hemoglobin concentrations were calculated from total hemoglobin concentrations (g/dl), and the percentages of donor contribution as determined by HPLC analysis. The difference between the engraftment of CD45^a donor (circles) and the engraftment of GFP donor (filled squares) was statistically insignificant, although one outlier from the GFP donor group (open squares) was observed to show a more successful engraftment. Abbreviation: Hbb, hemoglobin β.

tive conditioning regimens. Peripheral blood samples were obtained weekly for analysis of cellularity and for donor contributions to the three major blood lineages (Fig. 4, upper panels). The composition of the leukocyte compartment with respect to T lymphocytes, B lymphocytes, and myeloid cells was also determined for recipient, GFP donor, and CD45^a donor populations (Fig. 4, lower panels).

Sublethal radiation clearly depleted the peripheral blood of leukocytes by 1 week and of platelets by 2 weeks. However, the eventual recovery of these lineages seen between 2 and 5 weeks post-transplantation was predominantly derived from endogenous stem cells rather than by transplanted bone marrow (Fig. 4, leukocytes and platelets). Erythrocyte counts were not affected by sublethal radiation, but Hbb analysis showed a clear contribution of transplanted bone marrow cells to the erythroid compartment at 2 and 4 weeks (Fig. 4, erythrocytes). Interestingly, G6-GFP donor-derived myeloid cells appeared transiently in very small numbers 2 weeks following sublethal radiation but were not detected at later times, and B6-GFP-derived lymphocytes were not detected at any time after transplantation. In contrast, the leukocytes derived from the B6-CD45^a donor, although also present in small numbers, persisted from 2 to 5 weeks and included mostly B lymphocytes (Fig. 4, lower panels). After higher doses of radiation, contributions of the two donor populations to the leukocyte subset were comparable, with a slight predominance of B6-GFP-derived cells seen at 5 weeks post-transplant. Erythrocytes derived from the two bone marrow donors could not be distinguished from each other due to the lack of GFP expression in the erythroid lineage, but Hbb analysis clearly showed a dominance of donor-derived erythrocytes at 2 weeks that increased in number over subsequent weeks (Fig. 4, erythrocytes). Platelets derived from the B6-GFP donor were readily detectable beginning at 2 weeks, and by 5 weeks, over half of the platelets in peripheral blood of the high-dose radiation groups were GFP^{pos}. Although platelets derived from the B6-CD45^a donor could not be distinguished from those derived due to endogenous recovery, we presume that most of the GFP^{neg} platelets seen 5 weeks after myeloablative radiation are derived from the B6-CD45^a donor.

The relative inefficiency of B6-GFP donor cells to engraft in 4-Gy-irradiated recipient mice was confirmed in a second experiment, in which B6-GFP and B6-CD45^a donor cells were independently transplanted into separate groups of sublethally conditioned recipient mice. We observed transient, low-level contributions of both grafts to the erythroid lineage and sustained low-level engraftment of leukocytes in four of four recipients of CD45^a donor cells. In contrast, three of four recipients of B6-GFP donor bone marrow exhibited little if any leukocyte engraftment, whereas one of four recipients engrafted in the leukocyte lineage (Fig. 5). These data demonstrate a lineage-selective effect of relative resistance to leukocyte engraftment by B6-GFP-derived donor cells under conditions of sublethal radiation and limited donor cell transplantation, suggesting that the resistance occurs after megakaryocyte and erythroid lineage divergence from the nucleated cell lineages.

We also evaluated the effect of sex matching in the sublethal radiation setting by transplanting a 50:50 mix of GFP-transgenic and CD45 congenic cells obtained from male donors into two groups of 4-Gy-irradiated recipients, male or female. We observed better engraftment of both B6-CD45^a and B6-GFP cells when donor and host were sex-matched, but even in this case, the engraftment of B6-CD45^a cells was on average 10-fold higher than B6-GFP cells. Furthermore, B6-CD45^a cells engraftment was fivefold higher in the sex-mismatched combination compared with B6-GFP cells in the sex-matched combination ($0.44 \pm 0.15 \times 10^3$ cells per μl vs. $0.09 \pm 0.01 \times 10^3$ cells per μl; $p < .02$). Thus, the GFP transgene induces a more significant immune response than does the combination of the CD45 alloantigen plus the sex-linked differences in the sublethal bone marrow transplant setting.

DISCUSSION

Many of the early studies documenting engraftment kinetics following bone marrow transplantation used Hbb as an indicator of donor-derived hematopoiesis [10, 11]. The introduction of the CD45 allelic system [2] as a means of measuring chimerism of

nucleated blood cells complemented older methods based on chromosomal markers [12], which were cumbersome and allowed evaluation only of dividing cells. However, analysis of engraftment using the CD45 allelic model cannot measure graft contributions to erythroid and platelet lineages, due to the lack of expression of CD45 by these cells. Other methods of chimerism determination, such as Y chromosome-specific sequence detection in a male-to-female transplant system, have demonstrated a biphasic engraftment kinetic, which has been interpreted as representing separate engraftment by hematopoietic progenitor cells versus stem cells [13]. However, the demonstration of highly enriched stem cell populations with rapid engraftment potential [2, 14–16] led to a controversy regarding the ability of such stem cells to mediate radioprotection, which presumably requires rapid engraftment kinetics [17]. This study sheds new light on this old controversy by directly comparing erythroid, platelet, and leukocyte engraftment kinetics in an animal model of transplantation. Our results emphasize the fact that the erythroid lineage displays characteristics of engraftment that are distinct from those of leukocyte and platelet lineages, as shown by transient engraftment of erythrocytes in a sublethally irradiated setting, where little if any engraftment of leukocytes and platelets is seen (Fig. 4, upper panels).

Hbb variants are typically distinguished by gel electrophoresis, but clinical protocols that use HPLC have been introduced in recent years. We developed a protocol to allow distinction of mouse Hbb variants by HPLC as a rapid, sensitive, and quantitative method to measure chimerism in the erythroid lineage. This method uses an acidic derivatization of cysteine residues to introduce a differential charge between Hbb^s and Hbb^d. HPLC allows rapid, reproducible analyses of Hbb isoforms with precise quantitation of isoforms in an automated fashion, which facilitates the determination of graft-derived erythrocytes. Recently, a new transgenic mouse strain has been reported that retains GFP fluorescence in erythrocytes, providing a transplant model in which flow cytometry can be used to determine donor contributions to all blood lineages as well as in many other tissues [4]. Consistent with our results, experiments using the new transgenic strain in a competitive transplant setting demonstrated equivalent contributions of GFP and wild-type bone marrow cells to engraftment after high-dose radiation. Our data using sublethal doses of radiation, however, show that GFP transgenic bone marrow cells are subject to host resistance [11] in nonmyeloablative transplant models (Figs. 4, 5). Therefore, our data support continued application of congenic systems rather than transgenic models in studies that aim to model engraftment in reduced intensity chemotherapy regimens. For routine analysis of Hbb alleles, the HPLC method reported here provides an attractive alternative to traditional gel electrophoresis.

ACKNOWLEDGMENTS

This research was supported by National Institutes of Health Grants HL072026 (G.J.S.), DK57899 (G.J.S.), HL069133 (W.H.F.), HL077818 (W.H.F.), and T32 DK007115 (S.C.).

DISCLOSURES

The authors indicate no potential conflicts of interest.

REFERENCES

1 Harrison DE. Competitive repopulation: A new assay for long-term stem cell functional capacity. Blood 1980;55:77–81.

2 Spangrude GJ, Heimfeld S, Weissman IL. Purification and characterization of mouse hematopoietic stem cells. Science 1988;241:58–62.

3 Anderson DA, Wu Y, Jiang S, et al. Donor marker infidelity in transgenic hematopoietic stem cells. STEM CELLS 2005;23:638–643.

4 Dominici M, Tadjali M, Kepes S et al. Transgenic mice with pancellular enhanced green fluorescent protein expression in primitive hematopoietic cells and all blood cell progeny. Genesis 2005;42:17–22.

5 Harrison DE, Astle CM, Lerner C. Number and continuous proliferative pattern of transplanted primitive immunohematopoietic stem cells. Proc Natl Acad Sci U S A 1988;85:822–826.

6 Nakanishi T, Kuroiwa A, Yamada S et al. FISH analysis of 142 EGFP transgene integration sites into the mouse genome. Genomics 2002;80:564–574.

7 Whitney JB. Simplified typing of mouse hemoglobin (Hbb) phenotypes using cystamine. Biochem Genet 1978;16:667–672.

8 Socolovsky M, Nam H, Fleming MD et al. Ineffective erythropoiesis in Stat5a(–/–)5b(–/–) mice due to decreased survival of early erythroblasts. Blood 2001;98:3261–3273.

9 Kondo M, Weissman IL, Akashi K. Identification of clonogenic common lymphoid progenitors in mouse bone marrow. Cell 1997;91:661–672.

10 Kudisch M, Hamilton BL, Lipton JM. Early detection of hematopoietic engraftment in murine bone marrow transplantation utilizing hemoglobin electrophoretic differences. Transplantation 1983;35:515–518.

11 Down JD, Tarbell NJ, Thames HD et al. Syngeneic and allogeneic bone marrow engraftment after total body irradiation: Dependence on dose, dose rate, and fractionation. Blood 1991;77:661–669.

12 Ford CE, Hamerton JL, Barnes DWH, et al. Cytological identification of radiation-chimaeras. Nature 1956;177:452–454.

13 Jones RJ, Celano P, Sharkis SJ et al. Two phases of engraftment established by serial bone marrow transplantation in mice. Blood 1989;73:397–401.

14 Uchida N, Aguila HL, Fleming WH et al. Rapid and sustained hematopoietic recovery in lethally irradiated mice transplanted with purified Thy-1.1-lo Lin-Sca-1+ hematopoietic stem cells. Blood 1994;83:3758–3779.

15 Spangrude GJ, Brooks DM, Tumas DB. Long-term repopulation of irradiated mice with limiting numbers of purified hematopoietic stem cells: In vivo expansion of stem cell phenotype but not function. Blood 1995;85:1006–1016.

16 Zijlmans JM, Visser JW, Laterveer L et al. The early phase of engraftment after murine blood cell transplantation is mediated by hematopoietic stem cells. Proc Natl Acad Sci U S A 1998;95:725–729.

17 Jones RJ, Collector MI, Barber JP et al. Characterization of mouse lymphohematopoietic stem cells lacking spleen colony-forming activity. Blood 1996;88:487–491.

APPENDIX B

GRADIENTS OF ANTIGEN EXPRESSION AND DEVELOPMENTAL POTENTIAL IN HEMATOPOIESIS

Reprinted with permission from Kwak, J.Y., Cho, S., and Spangrude, G.J. (2007). Gradients of antigen expression and development potential in hematopoiesis. Ann. N.Y. Acad. Sci. *1106,* 82-88.

Gradients of Antigen Expression and Developmental Potential in Hematopoiesis

JAE-YONG KWAK,[a] SCOTT CHO,[b] AND GERALD J. SPANGRUDE[b]

[a]*Division of Hematology/Oncology, Department of Internal Medicine, Chonbuk National University Medical School, Jeonju 561-712, Korea*

[b]*Division of Hematology, Department of Internal Medicine, and Department of Pathology, University of Utah School of Medicine, Salt Lake City, Utah 84132-2408, USA*

ABSTRACT: Prospective isolation of hematopoietic stem and progenitor cell subsets depends upon the premise that expression of combinations of surface antigens reflects developmental potential. During the process of differentiation, however, the loss of antigens associated with stem cells and the concomitant gain of those associated with progenitor cells often occurs as a continuum rather than by discrete binary steps. Coupled with the fact that assay conditions can profoundly influence the developmental fates of prospectively isolated cells, gradients of antigen expression during differentiation have led to a variety of interpretations of lineage commitment in hematopoiesis.

KEYWORDS: fluorescence-activated cell sorting; lymphoid progenitor cells; erythropoiesis; *in vitro* assays

INTRODUCTION

Transcriptional programs that drive hematopoietic differentiation are well described,[1–4] as are the discrete stages of development in the various hematopoietic lineages.[5–7] A number of lines of evidence point to an early segregation of the megakaryocyte and erythroid lineages from the remainder of the myeloid lineages, including targeted mutation studies[8,9] as well as prospective isolation of cell populations representing intermediate stages of hematopoietic development.[10,11] The degree to which megakaryocyte and erythroid lineages segregate from the lymphoid lineage early in development has been controversial, with one group showing near-absolute separation[12] while

Address for correspondence: Gerald J. Spangrude, Ph.D., Division of Hematology, University of Utah, RM4C416, 30 N 1900 East, Salt Lake City, UT 84132-2408. Voice: 801-585-5544; fax: 801-585-3778.
gspangrude@mac.com

Ann. N.Y. Acad. Sci. 1106: 82–88 (2007).
doi: 10.1196/annals.1392.002

another reports much more overlap at the progenitor stage.[13] We show here that at least part of this controversy can be accounted for by a lack of discrete phenotypic stages that correspond to functionally committed progenitor cells. Due in part to a continuum in expression levels of antigens used for prospective isolation, differing arbitrary cut off limits in studies reported by different laboratories have resulted in interpretations that are in disagreement. An additional difference between studies is that unique assays with variable sensitivities are used to detect erythroid and platelet lineage potentials. Using a highly sensitive assay for erythroid lineage development, we show here that residual erythroid potential is maintained even very late during the commitment to lymphoid development. We conclude that in the absence of standardization in the field, differing interpretations of experimental data seem inevitable.

MATERIALS AND METHODS

Isolation of Bone Marrow Cell Populations

Bone marrow cells were isolated from young adult C57BL/Ka-Thy-1.1 mice. After lysis of erythrocytes using ammonium chloride, the cells were incubated in a solution containing monoclonal antibodies specific for lineage-specific antigens followed by depletion using magnetic beads. The lineage-depleted (Lin^{neg}) population was then reacted with labeled monoclonal antibodies specific for Thy-1.1 (fluorescein), Sca-1 (phycoerythrin), Flt3 (biotinylated antibody detected using streptavidin-ECD), and c-kit (allophycocyanin). Dead cells were excluded based on DAPI staining. Cell subsets were isolated by aseptic cell sorting and placed into culture.

Cell Culture Studies

Cell populations isolated by cell sorting were plated in αMEM-based methylcellulose containing 10% fetal calf serum, 10% deionized bovine serum albumen, antibiotics, glutamine, and 2-mercaptoethanol. Colony growth and differentiation were stimulated with recombinant cytokines, including steel factor (100 ng/mL), G-CSF, Flt3L, IL-3, IL-6, IL-7 (all at 10 ng/mL), and erythropoietin (4 U/mL). After the time intervals indicated in the figures, quadruplicate plates were stained using benzidine hydrochloride and scored for total colonies and for colonies containing hemoglobinized erythroid lineage cells colonies based on benzidine staining.[14] Results are reported as mean number of colonies per 100 cells plated, and error bars represent standard error values. Statistical analysis used a one-tailed, unpaired *t*-test with equal variance.

RESULTS AND DISCUSSION

All studies reported here focused on the subset of mouse bone marrow cells characterized by expression of c-kit and Sca-1 in the absence of lineage antigens. This population is referred to as KLS cells. Within this population, progenitor cells biased for lymphoid differentiation can be identified by Flt3 expression, while stem cells and multipotent progenitor (MPP) cells can be identified by Thy-1.1 expression. One report in the literature shows that $Flt3^+$ lymphoid progenitors lack erythroid and platelet potential,[12] while another report demonstrates potential for both lineages.[13] When methylcellulose cultures established with either KLS Thy-1.1^+ MPP or KLS $Flt3^+$ progenitors were evaluated for erythroid lineage potential, we observed the results shown in FIGURE 1. The total colony-forming potential of each population was similar in this experiment, but the proportion of colonies containing erythroid lineage cells was quite distinct. Approximately 50% of the colonies formed by the Thy-1.1^+ MPP population included erythroid lineage cells, and this proportion remained fairly constant throughout the observation period of 6–12 days. In contrast, while a large fraction of colonies formed by $Flt3^+$ progenitors contained erythroid lineage cells at day 6 of culture, this proportion decreased steadily so then by day 12 only about 10% of colonies included hemoglobin as detected by benzidine staining. The experiment shown in FIGURE 1 emphasizes the importance of assay parameters in the interpretation of this experiment, since analysis at early versus late times of culture resulted in profound differences in the frequency of colonies that include erythroid lineage cells.

Several recent publications by Kondo and colleagues have shown that the $Flt3^+$ subset of KLS cells can be further segregated based on co-expression of the VCAM-1 antigen, with the brightest expression of Flt3 correlating with decreased expression of VCAM-1.[15,16] This group has shown that erythroid potential within the Thy-1.1^{neg} KLS population, as detected in a methylcellulose assay, was exclusively associated with cells expressing low, but not high, levels of surface Flt3. To further explore this observation in the context of the data shown in FIGURE 1, we segregated Thy-1.1^{neg} KLS cells into $Flt3^{low}$ and $Flt3^{high}$ subsets as previously described by Lai and Kondo.[16] We also isolated MPP cells as Thy-1.1^+ $Flt3^+$ KLS cells (FIG. 2, top panel). These three populations were cultured in methylcellulose as described for FIGURE 1 and evaluated for erythroid differentiation by benzidine staining. Consistent with the data shown in FIGURE 1, all three populations generated colonies containing erythroid lineage cells when evaluated after 6 days of culture. On subsequent days, however, the frequency of colonies containing benzidine-positive erythroid cells declined dramatically in cultures derived from either the $Flt3^{low}$ or $Flt3^{high}$ subsets. On day 10 of culture, cultures seeded with $Flt3^{high}$ cells contained significantly fewer benzidine-positive colonies relative to either the $Flt3^{low}$ or the MPP cultures (FIG. 2, *lower panel*), and

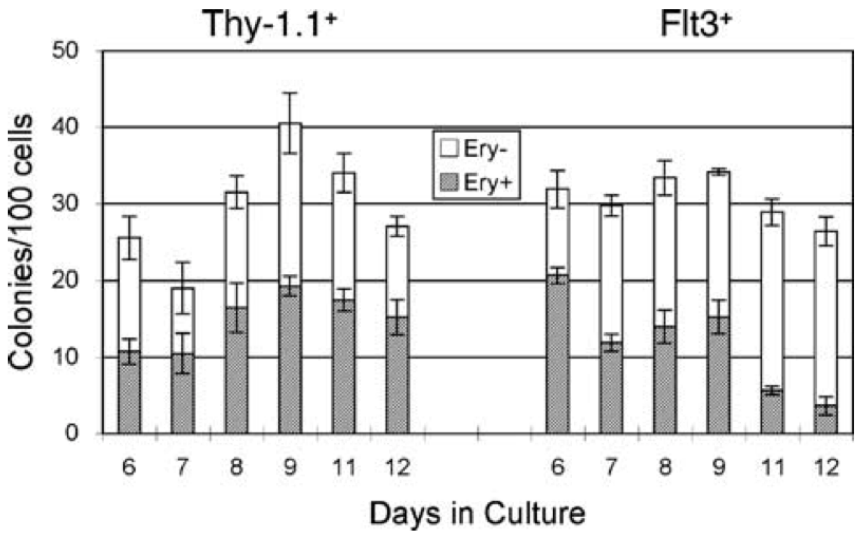

FIGURE 1. KLS cells isolated from mouse bone marrow were separated into Thy-1.1$^+$ and Flt3$^+$ subsets and cultured in methylcellulose in the presence of cytokines as described in "Materials and Methods" section. After the indicated days of culture, replicate cultures were stained with benzidine hydrochloride and colonies were scored as benzidine positive (Ery+) or benzidine negative (Ery–). Data are shown as the mean ± SEM of quadruplicate cultures.

on day 13 both the Flt3^{low} and Flt3^{high} cultures contained significantly fewer benzidine-positive colonies compared to MPP cultures. Apart from quantitative differences that are presumably due to the increased sensitivity of the benzidine detection method for scoring erythroid lineage-containing colonies, the results shown in FIGURE 2 are consistent with the studies reported by Lai and Kondo[16] in that erythroid potential is lost concomitantly with decreasing expression of Thy-1.1 and increasing expression of Flt3. However, discrete expression levels of these two antigens are not observed, and as a result the selection of subsets for functional analysis, as shown in FIGURE 2, is somewhat arbitrary. It is likely that some of the conflicting reports in the literature are due to differences in this arbitrary selection of cell populations. In addition, experimental design and assay sensitivity will have a major impact on the ability to detect differentiation into specific lineages.

FIGURE 3 depicts the general concept that the transitions between some stages of development in early hematopoiesis should be considered as gradients rather than as the discrete steps that are implied by classical tree diagrams of lineage commitment. This view reflects the concept that lineage decisions in early hematopoiesis are likely driven by relative levels of multiple transcriptional regulators and are characterized by quantitative as well as combinatorial aspects. During transitional states, such as the multipotent cell to lymphoid progenitor transition shown in FIGURE 3, extrinsic signals provided by the environment

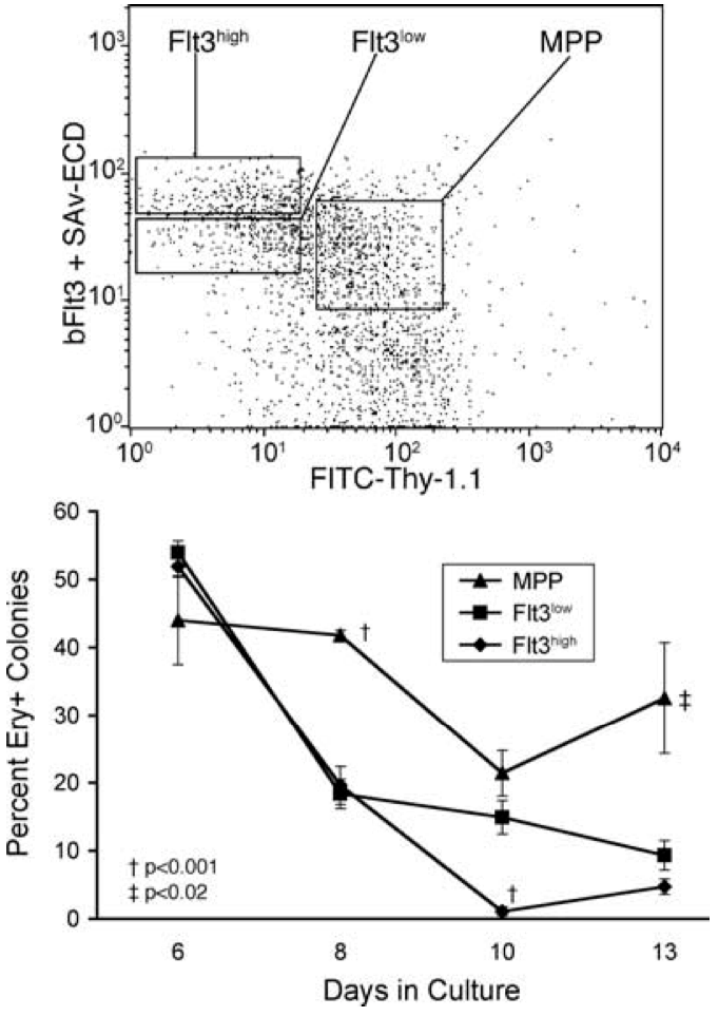

FIGURE 2. KLS cells isolated from mouse bone marrow were separated into three subsets as indicated in the upper panel and cultured in methylcellulose in the presence of cytokines as described in "Materials and Methods" section. After the indicated days of culture, replicate cultures were stained with benzidine hydrochloride and colonies were scored as benzidine positive (Ery+) or benzidine negative (Ery–). Data are shown as the mean percentage of Ery+ colonies ± SEM of quadruplicate cultures. The total number of colonies per 100 cells plated, averaged over the entire experiment ± SEM, was 64 ± 4 (MPP), 44 ± 2 ($Flt3^{low}$), and 26 ± 1 ($Flt3^{high}$) with $n = 16$ in all cases. Symbols adjacent to specific data points indicate the probability that the value is significantly different from the values of the other two groups assayed on the same day.

are likely able to shift developmental decisions in an instructive manner, even though the overall process has stochastic characteristics. The transition between early lymphoid progenitors and the committed precursors for the T and B lymphocyte lineages is thus depicted as a "gray zone" in FIGURE 3, meaning

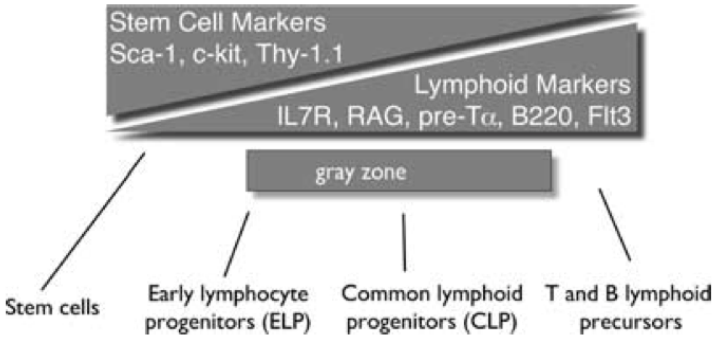

FIGURE 3. Gradients of antigen expression and developmental potential during lymphoid commitment. Mouse stem and progenitor cells can be identified by coexpression of Sca-1, c-kit, and Thy-1.1. These antigens are downregulated and others are upregulated, including IL-7R, RAG (as detected by an eGFP knockin reporter),[7] pre-Tα (as detected by an eGFP transgene reporter),[17] B220, and Flt3, as lymphoid lineage fates are specified. The "gray zone" indicates stages of development that are not resolved well by surface antigen expression and are thus difficult to study by prospective isolation approaches.

that absolute and reproducible physical separations of cells representing the transitional stages in this process of lineage commitment may not be possible. Furthermore, the conditions chosen by experimentalists to evaluate lineage potentials can greatly influence the outcome and interpretation of prospective isolation studies, and lead to conflicting and controversial findings.

While it may be convenient to conceptualize lineage commitments in hematopoietic development as the discrete stages depicted in classical tree diagrams, our efforts to understand mechanistic regulation of hematopoiesis are probably undermined by this notion of binary states. Recognizing that the gradients of antigen expression that are apparent during some lineage transitions in hematopoiesis are likely reflective of similar gradients in developmental potential will likely provide relevant insight into the mechanistic underpinnings of these developmental processes.

REFERENCES

1. Kirito, K. & K. Kaushansky. 2006. Transcriptional regulation of megakaryopoiesis: thrombopoietin signaling and nuclear factors. Curr. Opin. Hematol. **13:** 151–156.
2. Kee, B.L. 2005. Helix-loop-helix proteins in lymphocyte lineage determination. Curr. Top. Microbiol. Immunol. **290:** 15–27.
3. Miyamoto, T. & K. Akashi. 2005. Lineage promiscuous expression of transcription factors in normal hematopoiesis. Int. J. Hematol. **81:** 361–367.
4. Orkin, S.H. 2001. Transcription factors that regulate lineage decisions: the molecular basis of blood diseases. *In* The Molecular Basis of Blood Diseases, 3rd ed. G. Stamatoyannopoulos, P.W. Majerus, R. Perlmutter, H. Varmus, Eds.: 80–102. W.B. Saunders. Philadelphia, PA.

5. SPANGRUDE, G.J., S. HEIMFELD & I.L. WEISSMAN. 1988. Purification and characterization of mouse hematopoietic stem cells. Science **241:** 58–62.
6. MORRISON, S.J. & I.L. WEISSMAN. 1994. The long-term repopulating subset of hematopoietic stem cells is deterministic and isolatable by phenotype. Immunity **1:** 661–673.
7. IGARASHI, H., S.C. GREGORY, T., YOKOTA *et al*. 2002. Transcription from the RAG1 locus marks the earliest lymphocyte progenitors in bone marrow. Immunity **17:** 117–130.
8. SALEQUE, S., S. CAMERON & S.H. ORKIN. 2002. The zinc-finger proto-oncogene Gfi-1b is essential for development of the erythroid and megakaryocytic lineages. Genes Dev. **16:** 301–306.
9. HALL, M.A., D.J. CURTIS, D. METCALF, *et al*. 2003. The critical regulator of embryonic hematopoiesis, SCL, is vital in the adult for megakaryopoiesis, erythropoiesis, and lineage choice in CFU-S12. Proc. Natl. Acad. Sci. USA **100:** 992–997.
10. TRAVER, D., T. MIYAMOTO, J. CHRISTENSEN, *et al*. 2001. Fetal liver myelopoiesis occurs through distinct, prospectively isolatable progenitor subsets. Blood **98:** 627–635.
11. EDVARDSSON, L., J. DYKES & T. OLOFSSON. 2006. Isolation and characterization of human myeloid progenitor populations–TpoR as discriminator between common myeloid and megakaryocyte/erythroid progenitors. Exp. Hematol. **34:** 599–609.
12. ADOLFSSON, J., R. MANSSON, N. BUZA-VIDAS, *et al*. 2005. Identification of Flt3+ lympho-myeloid stem cells lacking erythro-megakaryocytic potential: a revised road map for adult blood lineage commitment. Cell **121:** 295–306.
13. FORSBERG, E.C., T. SERWOLD, S. KOGAN, *et al*. 2006. New evidence supporting megakaryocyte-erythrocyte potential of flk2/flt3+ multipotent hematopoietic progenitors. Cell **126:** 415–426.
14. SLAYTON, W.B., M.P. MOJICA, L.J. PIERCE & G.J. SPANGRUDE. 2001. Observations of residual differentiation potential during lineage commitment. Ann. N. Y. Acad. Sci. **938:** 157–165.
15. LAI, A.Y., S.M. LIN & M. KONDO. 2005. Heterogeneity of Flt3-expressing multipotent progenitors in mouse bone marrow. J. Immunol. **175:** 5016–5023.
16. LAI, A.Y. & M. KONDO. 2006. Asymmetrical lymphoid and myeloid lineage commitment in multipotent hematopoietic progenitors. J. Exp. Med. **203:** 1867–1873.
17. GOUNARI, F., I. AIFANTIS, C. MARTIN, *et al*. 2002. Tracing lymphopoiesis with the aid of a pTalpha-controlled reporter gene. Nat. Immunol. **3:** 489–496.